Stochastic Modeling and Analysis of Power Systems with Intermittent Energy Sources

by

Mehrdad Pirnia

A thesis
presented to the University of Waterloo
in fulfillment of the
thesis requirement for the degree of
Doctor of Philosophy
in
Electrical and Computer Engineering

Waterloo, Ontario, Canada, 2014

I hereby declare that I am the sole author of this thesis. This is a true copy of the thesis, including any required final revisions, as accepted by my examiners.

I understand that my thesis may be made electronically available to the public.

Mehrdad Pirnia

ABSTRACT

Electric power systems continue to increase in complexity because of the deployment of market mechanisms, the integration of renewable generation and distributed energy resources (DER) (e.g., wind and solar), the penetration of electric vehicles and other price sensitive loads. These revolutionary changes and the consequent increase in uncertainty and dynamicity call for significant modifications to power system operation models including unit commitment (UC), economic load dispatch (ELD) and optimal power flow (OPF). Planning and operation of these "smart" electric grids are expected to be impacted significantly, because of the intermittent nature of various supply and demand resources that have penetrated into the system with the recent advances.

The main focus of this thesis is on the application of the Affine Arithmetic (AA) method to power system operational problems. The AA method is a very efficient and accurate tool to incorporate uncertainties, as it takes into account all the information amongst dependent variables, by considering their correlations, and hence provides less conservative bounds compared to the Interval Arithmetic (IA) method. Moreover, the AA method does not require assumptions to approximate the probability distribution function (pdf) of random variables.

In order to take advantage of the AA method in power flow analysis problems, first a novel formulation of the power flow problem within an optimization framework that includes complementarity constraints is proposed. The power flow problem is formulated as a mixed complementarity problem (MCP), which can take advantage of robust and efficient state-of-the-art nonlinear programming (NLP) and complementarity problems solvers. Based on the proposed MCP formulation, it is formally demonstrated that the Newton-Raphson (NR) solution of the power flow problem is essentially a step of the traditional General Reduced Gradient (GRG) algorithm. The solution of the proposed MCP model is compared with the commonly used NR method using a variety of small-, medium-, and large-sized systems in order to examine the flexibility and robustness of this approach.

The MCP-based approach is then used in a power flow problem under uncertainties, in order to obtain the operational ranges for the variables based on the AA method considering active and reactive power demand uncertainties. The proposed approach does not rely on the pdf of the uncertain variables and is therefore shown to be more efficient than the traditional solution

methodologies, such as Monte Carlo Simulation (MCS). Also, because of the characteristics of the MCP-based method, the resulting bounds take into consideration the limits of real and reactive power generation.

The thesis furthermore proposes a novel AA-based method to solve the OPF problem with uncertain generation sources and hence determine the operating margins of the thermal generators in systems under these conditions. In the AA-based OPF problem, all the state and control variables are treated in affine form, comprising a center value and the corresponding noise magnitudes, to represent forecast, model error, and other sources of uncertainty without the need to assume a pdf. The AA-based approach is benchmarked against the MCS-based intervals, and is shown to obtain bounds close to the ones obtained using the MCS method, although they are slightly more conservative. Furthermore, the proposed algorithm to solve the AA-based OPF problem is shown to be efficient as it does not need the pdf approximations of the random variables and does not rely on iterations to converge to a solution. The applicability of the suggested approach is tested on a large real European power system.

Acknowledgments

First, I would like to express my sincere gratitude to my supervisor, Professor Kankar Bhattacharya for his guidance, patience, and trust at every stage of my Ph.D. studies. My decision to start the Ph.D. program in the Electrical Engineering Department was simply because of his encouragement, seemingly boundless patience and fatherly support. While taking a course with him, during my Masters' program in the Management Sciences department, I discovered my interests in the power system engineering area, and after stating my interests to him, I was fortunate to be accepted for the Ph.D. program, under his supervision. Professor Bhattacharya led me patiently through this process. He was always available to address my concerns, continuously kind to forgive my mistakes, and purely devoted to observe my success. I have not only completed this thesis with him, but also learned a lot on how to be a trustworthy scholar bounded with academic values.

I would also like to express my sincere gratitude to Professor Claudio Cañizares for his advice and suggestions, direct guidance and motivations at every stage of this research. His constructive criticisms, insightful interest, and exceptional professionalism and modesty have been a great source of inspiration to me. Not only I dud learn about power systems operation from him, but I also learnt how to maintain a good balance of family time, sport activities and work.

I would like to thank my committee members, Professors David Fuller and Andrew Heunis. I benefited a lot from their constructive feedbacks on my research. I started my Masters' research under Professor Fullers' supervision; he walked me patiently through every stage of my research and taught me how to be a good researcher. His attention to detail and his patience in conducting research have always been admirable for me. Also, Professor Heunis kindly offered me a reading course on stochastic modeling, where I learnt a lot about the subject through many meetings with him. His enthusiasm and willingness to support was exceptional. I would also like to acknowledge the constructive criticisms and useful suggestions from Professor Antonio Gómez Expósito, University of Seville, Spain who served as my Ph.D. external examiner. I also acknowledge Professor Alfredo Vaccaro, University of Sannio, Italy, for the stimulating discussions on Affine Arithmetic (AA) methods and for providing system data which has been used in the studies reported in this thesis.

I wish to acknowledge ABB Corporate Research USA and MITACS Canada for funding the initial stages of this research, Ontario Graduate Scholarship (OGS), and NSERC Strategic Network on Smart Microgrids (NSMG-Net) for funding the latter stages of the research.

Special thanks to Professor Frank Safayeni, who believed in me when I started teaching at university and gave me many opportunities to teach at the Management Sciences Department. Also, many thanks to Professor Jatin Nathwani, Executive Director of the Waterloo Institute for Sustainable Energy (WISE) for his various advice on energy policy and for funding a few of my conference presentations. I also wish to acknowledge Dr. Richard O'Neill for providing me a great opportunity to work under his supervision at Federal Energy Regulatory Commission (FERC), USA in Summer 2012. During that summer internship, I learnt a lot about the AC-Optimal Power Flow and also the industrial applications of my research.

Also, many thanks to my dear friends for their exceptional friendship and support through the happy and sad moments of my life. Thanks to Mostafa Farrokhabadi for being a great friend who brought up engaging conversations on variety of topics, Mariano Arriago for bringing energy and laughter in our gatherings, Hani Alkhouri for being a great roommate, gym partner and a true friend, Andrei and Laura Radulescu, and Ada and Adam Hurst for all the great get-togethers and wonderful humour, Mohammad Farsa Ardalani, Kamyar Rashidi, Mahyar Fotouhi for establishing memorable friendship by being wonderful companies in variety of occasions, Kory Hedman and Anthony Papavasiliou for bringing new insight into my life on how to be a successful scholar and for all the fun moments during conferences. Your presence made this chapter of my life more joyful. I am especially thankful to Siamak Nazari, who was an exceptional friend from the beginning of my studies. I have benefited a lot from his valuable advice and unconditional friendship.

My warm thanks also extends to my past and present officemates Dr. Daniel Olivares, Dr. Mohammad Chehreghani, Dr. Amirhossein Hajimiragha, Behnam Tamimi, Mauricio Restrepo, Dr. Sumit Paudyal, Felipe Ramos, Dr. Edris Pouresmaeil, Adarsh Madhavan, Dr. Juan Carlos Muñoz, Isha Sharma, Indrajit Das, Nafeesa Mehboob, Amir Mosaddegh, and Jose Daniel Lara who supported me generously during our scientific conversations. Their existence provided me with an active, welcoming, safe and scientific work place. I am especially thankful to Ehsan Nasr for sharing his insights on my research, and for being a great partner through our bi-weekly meetings since the start of my Ph.D. program.

Finally I would like to thank my mother Parvaneh, my dad Mohammad, and my brother Shahab for their unconditional love and support through all these years. I am proud to be raised in a family, appraising higher education. Thank you for all the sacrifices you made, the life principles you taught me and the comfort you provided me. Without you and your support I could not have achieved this.

Dedication

This thesis is dedicated to my Mom and Dad,

Parvaneh and Mohammad.

Table of Contents

Nomenclature

Indices and Sets

gen	Set of generator buses
i, j, k	Index of buses
k	Iteration counter, when appearing as a superscript
L	Set of all lines
N	Set of all buses
ND	Set of all buses with uncertain demand
nP	Set of all buses with real power injection uncertainty
nQ	Set of all buses with reactive power injection uncertainty
nPQ	Set of all the PQ buses
rnw	Set of buses with renewable sources of uncertainties
$slack$	Set of slack buses

Variables

δ	Vector of bus voltage angles (radians)
δ_{ij}	Angle difference between bus *i* and *j* (radians)
$\tilde{\delta}_i$	Affine form of bus angle at bus *i* (radians)
$\Delta\delta$	Vector of bus angle mismatch at each NR step (radians)
ε	Vector of mismatch variables (p.u.)
ε_i	Noise representation of an independent source of uncertainty
ε_p	Vector of real power mismatch (p.u.)
$\varepsilon_{P_j^D}$	Noise symbol representing uncertainties of active power injections at bus *j*
ε_q	Vector of reactive power mismatch (p.u.)
$\varepsilon_{Q_j^D}$	Noise symbol representing uncertainties of reactive power injections at bus *j*
ε_{T_i}	Noise symbol representing errors due to the approximations of non-affine operations
$\tilde{e}_i$	Affine form of real component of bus voltage at bus *i* (p.u.)
$\tilde{f}_i$	Affine form of imaginary component of bus voltage at bus *i* (p.u.)
$\tilde{I}_{ij}$	Affine form of line currents at line connecting bus *i* to *j* (p.u.)
$\tilde{I}_{im}$	Vector of the affine imaginary component of bus currents (p.u.)
$\tilde{I}_{im_i}$	Affine imaginary component of currents at bus *i* (p.u.)
$\tilde{I}_r$	Vector of the affine real component of current (p.u.)
$\tilde{I}_{r_i}$	Affine real component of current at bus *i* (p.u.)
λ_i, μ_i	Lagrangian multipliers
$\tilde{P}_i$	Affine representation of real power injection (p.u.)
$\tilde{P}^G$	Vector of affine form of real power generation (p.u.)
$\tilde{P}_i^G$	Affine form of real power generation at bus *i* (p.u.)
P_i	Real power generation at bus *i* (p.u.)
ΔP	Vector of real power injection mismatch variable at each NR step (p.u.)
ΔP_s	Vector of real power generation mismatch variable at slack bus at each NR step (p.u.)

P_s	Real power generation variable at the slack bus (p.u.)
$\tilde{Q}_i$	Affine representation of reactive power injection (p.u.)
$\tilde{Q}_i^G$	Affine form of reactive power generation at bus *i*
Q_G	Reactive power generation at PV buses (p.u.)
Q_i	Reactive power injection at bus *i* (p.u.)
ΔQ	Vector of reactive power mismatch at each NR step (p.u.)
ΔQ_G	Vector of reactive power generation mismatch at PV buses at each NR iteration (p.u.)
u	Vector of control variables in OPF
$\|V_D\|$	Vector of bus voltage magnitude at PQ buses (p.u.)
$\Delta\|V_D\|$	Vector of bus voltage magnitude mismatch at PQ buses at each NR step (p.u.)
$\|V_G\|$	Vector of bus voltage magnitude at PV buses (p.u.)
$\|V_i\|$	Bus voltage magnitude at bus *i* (p.u.)
V_i	Bus voltage at bus *i* (p.u.)
$\tilde{V}_i$	Affine form of bus voltage at bus *i* (p.u.)
V_{Ga}, V_{Gb}	Auxiliary variables to track bus voltage magnitude variation (p.u.)
x	Vector of power flow variables
x_ε	The vector of noises associated with the external uncertainties
$\hat{x}$	Interval representation of variable *x*
$\tilde{x}$	Affine representation of a variable *x*
x_0	Center value of an affine variable *x*
x_i	Partial deviations of an affine variable *x*
x_T	Vector of noise uncertainties for approximation error resulting from non-affine operations
x^{min}	Vector of minimum noise variables
x^{max}	Vector of maximum noise variables
y	Vector of independent auxiliary and $\|V_G\|$variables
z	Vector of optimization variables

Parameters and Functions

A	Matrix of partial deviations for affine form of real and reactive power injection
A_0	Vector of center values for affine form of real and reactive power injection
α	Correction factor in NR method
α_i	Coefficient of real power generation at bus *i* in total generation cost function ($/$MW^2$)
α^k	Step size of the updated NR solution at the k^{th} iteration
B_T	Vector of approximation noise magnitude associated with non-affine operations
$B1$	Vector of center values plus noise magnitudes resulting from non-affine operations approximations
$B2$	Vector of center values minus noise magnitudes resulting from non-affine operations approximations
β	Scalar for step-size adjustment
β_i	Coefficient of real power generation at bus *i* in total generation cost function ($/$MW$)
B_{ij}	Imaginary part of admittance bus matrix (p.u.)
C_i	Fixed parameter in quadratic total generation cost at bus *i* ($)
$\nabla_x f(.)$	Gradient of a function in respect to *x*
δ_{ij}	The angle between bus *i* and *j* (radians)
$\delta_{i,0}$	Center value of bus angles at bus *i* (radians)

$\delta_{i,j}^{P}$	Partial deviations of bus angle at bus *i* due to real power injection at bus *j* (radians)
$\delta_{i,j}^{Q}$	Partial deviations of bus angle at bus *i* due to reactive power injection at bus *j* (radians)
$D_x f(.)$	Differential equations of a function in respect to *x*
$e_{i,0}$	Center value of the real component of bus voltage at bus *i* (p.u.)
e_i^0	Initial values of real components of bus voltages obtained from the deterministic model (p.u.)
e_i^N	New values for real component of bus voltage at bus *i* (p.u.)
$e_{i,j}^{P}$	Partial deviation of real component of bus voltage at bus *i* due to the active power injection uncertainties at bus *j* (p.u.)
$e_{i,j}^{Q}$	Partial deviation of real component of bus voltage at bus *i* due to the reactive power injection at bus *j* (p.u.)
e_i^T	Truncation error for affine real component of bus voltage (p.u.)
φ	Representation of a constant in equations
f_i^N	New values for imaginary component of bus voltage at bus *i* (p.u.)
$f_{i,0}$	Center value of imaginary component of bus voltage at bus *i* (p.u.)
f_i^0	Initial values of imaginary components of bus voltages obtained from deterministic model (p.u.)
$f_{i,j}^{P}$	Partial deviation of imaginary component of bus voltage at bus *i* due to active power injection at bus *j* (p.u.)
$f_{i,j}^{Q}$	Partial deviation of imaginary component of bus voltage at bus *i* due to reactive power injection at bus *j* (p.u.)
f_i^T	Truncation error for affine imaginary component of bus voltage (p.u.)
$\underline{f}(.)$	Lower bound of an affine variable
$\overline{f}(.)$	Upper bound of an affine variable
$\nabla f(x^k)$	Gradient of the function *f(x)* at x^k
G_{ij}	Real part of admittance bus matrix
$H(x^k)$	The Hessian matrix of a function
$I_{im,0}$	Center value for affine imaginary current at bus *i* (p.u.)
I_{ij}^{min}	Minimum limits for line currents (p.u.)
I_{ij}^{max}	Maximum limits for line currents (p.u.)
$I_{im}{}_{i,j}^{P}$	Partial deviation of the imaginary component of current at bus *i* due to the active power injection at bus *j* (p.u.)
$I_{im}{}_{i,j}^{Q}$	Partial deviation of the imaginary component of current at bus *i* due to the reactive power injection at bus *j* (p.u.)
$I_{r}{}_{i,0}$	The center value for affine real current at bus *i* (p.u.)
$I_{r}{}_{i,j}^{P}$	Partial deviation of the real component of current at bus *i* due to the active power injection at bus *j* (p.u.)
$I_{r}{}_{i,j}^{Q}$	Partial deviation of the real component of current at bus *i* due to the reactive power injection at bus *j* (p.u.)
J	Jacobian matrix
M	Matrix used to calculate GRG step
N_G	Number of generators
$P_{i,0}$	Center value for affine real power injection at bus *i* (p.u.)
$\overline{P}_i^D$	Maximum value for real power demand (p.u.)
$\overline{P}_i$	Upper bound of real power injection (p.u.)
$\underline{P}_i^D$	Minimum value for real power demand (p.u.)

$\underline{P_i}$	Lower bound of real power injection (p.u.)
$\tilde{P}_i^D$	Affine real power demand at bus *i* (p.u.)
P_i^{min}	Minimum limit for real power generation at bus *i* (p.u.)
P_i^{max}	Maximum limit for real power generation at bus *i* (p.u.)
$P_{i,j}^P$	Partial deviation of real power at bus *i* due to active power injection variation at bus *j* (p.u.)
$P_{i,j}^Q$	Partial deviation of the real power at bus *i* due to reactive power injection at bus *j* (p.u.)
P_i^T	Noise magnitude associated with approximation error for real power at bus *i* (p.u.)
P_{rated}	Wind turbine rated active power output (p.u.)
P_i^{sp}	Specified real power injection at bus *i* (p.u.)
P^{dem}	Uncertain real power demand (p.u.)
$\bar{P}^{dem}$	Mean value of real power demand (p.u.)
$\Delta P(.)$	Nonlinear function for real power injection mismatch at a bus
$\Delta\tilde{P}_i(.)$	Affine real power mismatch function at bus *i*
ΔP_j^D	Amount of perturbation in real power injections at bus *j*
$Q_{i,0}$	Center value for affine reactive power at bus *i* (p.u.)
$\overline{Q_i}^D$	Maximum value for reactive power demand (p.u.)
$\overline{Q_i}$	Upper bound of reactive power injection (p.u.)
$\underline{Q_i}^D$	Minimum value for reactive power demand (p.u.)
$\underline{Q_i}$	Lower bound of reactive power injection (p.u.)
$\tilde{Q}_i^D$	Affine reactive power demand at bus *i* (p.u.)
Q_i^{min}	Minimum limit for reactive power generation at bus *i* (p.u.)
Q_i^{max}	Maximum limit for reactive power generation at bus *i* (p.u.)
$Q_{i,j}^P$	Partial deviation of reactive power at bus *i* due to active power injection at bus *j* (p.u.)
$Q_{i,j}^Q$	Partial deviation of reactive power at bus *i* due to reactive power injection at bus *j* (p.u.)
Q_i^{sp}	Specified reactive power injection at bus *i* (p.u.)
Q_i^T	Noise magnitude associated with approximation error for reactive power at bus *i* (p.u.)
$\Delta Q(.)$	Nonlinear function for reactive power injection mismatch at a bus
$\Delta\tilde{Q}_i(.)$	Affine reactive power mismatch function at bus *i*
ΔQ_j^D	Perturbation in reactive power injections at bus *j*
Q_G^{max}	Vector of maximum reactive power at generator buses (p.u.)
Q_G^{min}	Vector of minimum reactive power at generator buses (p.u.)
$radP_i(.)$	Function of noise variables, presenting the deviations from center value for real power generation at bus *i*
$radQ_i(.)$	Function of noise variables, presenting the deviations from center value for reactive power generation at bus *i*
σ	Standard deviation of a random variable
σ_i^2	Variance of a random variable x_i
s	GRG step
τ	Tolerance level for the Newton-Raphson method
$V_{i,j}^P$	Partial deviations of bus voltage magnitude at bus *i* due to real power injection at bus *j*
$V_{i,j}^Q$	Partial deviations of bus voltage magnitude at bus *i* due to reactive power injection at

	bus *j*
$V_{i,0}$	Center value for bus voltage magnitude at bus *i*
V_i^{max}	Maximum limit for bus voltage magnitude at bus *i* (p.u.)
V_i^{min}	Minimum limit for bus voltage magnitude at bus *i* (p.u.)
$\|V_{G_{i0}}\|$	Set point value for bus voltage magnitude at PV buses (p.u.)
$\overline{x}$	Upper bound of variable *x*
$\underline{x}$	Lower bound of variable *x*
Δx^{k+1}	The solution update after (*k+1*)th iteration of the Newton-Raphson method.
z_k	Noise magnitude for the approximation error in non-affine operations

GLOSSARY

AA	Affine Arithmetic
cdf	Cumulative Distribution Function
CG	Conjugate Gradient
DG	Distributed Generation
DER	Distributed Energy Sources
DSM	Demand Side Management
EP	Evolutionary Programming
ES	Evolutionary Strategy
FFT	Fast Fourier Transform
FIT	Feed-in Tariff
GA	Genetic Algorithm
GMRES	General Minimal Residual Method
IA	Interval Arithmetic
IESO	Independent Electricity System Operator
IP	Interior Point
IQIP	Improved Quadratic Interior Point
LMP	Locational Marginal Price
LP	Linear Programming
MCC	Multiple Centrally Corrections
MCP	Mixed Complementarity Problem
MPCC	Mathematical Program with Complementarity Constraints
MCS	Monte Carlo Simulation
NLP	Nonlinear Programming
NR	Newton Raphson
ONN	Optimization Neural Network
OPF	Optimal Power Flow
pdf	Probability Distribution Function
PF	Power Flow
P-OPF	Probabilistic Optimal Power Flow
P-PF	Probabilistic Power Flow
PSO	Particle Swarm Optimization
QP	Quadratic Program
QIPM	Quadratic Interior Point Method
ROI	Return on Investment
SCOPF	Security Constraint Optimal Power Flow
SQP	Sequential Quadratic Programming
SR	Spinning Reserve
SVC	Self-Validated Computation
TS	Tabu Search
UC	Unit Commitment

CHAPTER 1

INTRODUCTION

1.1 Motivation

Restructuring of the power sector has motivated new developments in power system operation and planning. Although distributed generation (DG) and demand response programs are not very recent, the current power system operational requirements necessitate that these are looked at more seriously, in order to provide enough supply, in an economical and efficient manner, for the increasing rate of demand growth.

Energy security concerns, environmental issues, transmission line requirements, increasing demand and volatile oil prices have directed lots of attention to renewable DG technologies, specially wind and solar. Wind power penetration has been the highest among all the available DG sources. For instance, in the European Union, 11.6 GW of wind generation capacity was installed in 2012, representing 26% of all new installations, bringing the total wind power capacity to 105.6 GW or 7% of Europe's total electricity demand in that year [1]. Canada had more than 6,400 MW of installed wind energy capacity in 2012, with over 2,000 MW of installation in Ontario and approximately 1,600 MW, and 1,100 MW in Quebec and Alberta, respectively [2]. It is estimated that 2,400 MW of embedded solar and wind capacities will be available in Ontario by 2015 [3]. Ontario's Independent Electricity System Operator (IESO) uses a centralized forecast of all renewable generation output to maintain reliability and efficiency of the system in the presence of uncertainties.

In order to achieve their targets on renewable energy, governments around the world strive to incorporate policy tools such as Feed-in Tariff (FIT) and cap-and-trade mechanisms to incentivize DG investments. For instance, Ontario's targets for renewable energy developments include 5,000 MW of wind energy, 1,500 MW of new hydro capacities and 40 MW of solar by 2025 [4].

Planning and operation of the modern electricity grid is expected to be impacted significantly because of the presence of intermittent renewable sources. The analytical tools used in a traditional grid such as, power flow analysis, optimal power flow (OPF), economic dispatch and unit commitment (UC) will require appropriate modifications to incorporate the variabilities arising from renewable sources. Although local control mechanisms have been developed to

regulate the generation from these renewable sources, they have not been able to accommodate system operators dispatch instructions, and balance the electricity supply and demand.

A wide variety of stochastic methods such as Monte Carlo Simulation (MCS) and Interval Arithmetic (IA) have been exploited in the literature to model and analyze the uncertainties arising from these energy sources. Some of these methods are practically expensive to be developed, while some lack the accuracy required in power system applications. The Affine Arithmetic (AA) method has been demonstrated in [5] to be a highly efficient and accurate technique and provides less conservative bounds than the IA method. This method takes into consideration both the internal and external uncertainties that may arise in the current operation of power systems. However, the AA-based power flow analysis in [5] uses the Newton-Raphson (NR) method of solution which may have convergence problems for large systems when using a flat-start or exceeding the maximum loadability of a system, and require an initial solution which is close to the final solution. Also, the conventional power flow solution methods require iterative PV-PQ bus switching when the reactive power at a generator bus violates the limits.

Therefore there is a need for a more accurate, flexible and robust power flow solution method for undertaking power system analytical studies considering uncertainties. In order to achieve this, an optimization framework is proposed in this thesis that is based on the mixed complementarity problem (MCP)[1] formulation and has the advantage of embedding various power flow solution steps as optimization constraints. The proposed method needs be validated against other established NR-based power flow solution methods, for its computational advantages and accuracy.

Furthermore, there is a need to examine how such a novel power flow solution method can be incorporated within the AA modeling framework, and consequently, to examine how one of the most important power system operational tools - the OPF, can be adopted to the AA-based framework. It is also important to validate the accuracy of the bounds obtained from the AA-based methods with other established methods such as MCS.

1.2 Literature Review

1.2.1 The Power Flow Analysis and Optimal Power Flow (OPF) Problem

The power flow analysis problem is a widely used tool for power system operations and

[1]In mathematical literature the optimization problem which has complementarity constraints is called Mathematical Program with Complementarity Constraints (MPCC). However, in this thesis, such class of optimization problems has been referred to, as MCP. A review of power system literature in this subject reveals a certain degree of ambiguity between these two terminologies.

planning, since it provides network solutions such as bus voltage magnitudes and angles for a given set of operating conditions. It can also serve as a security analysis tool, providing guidelines on acceptable operating conditions in case of sudden disturbances and load changes.

Since the power flow equations are nonlinear, the solution methodologies for these problems have traditionally involved iterative procedures such as the Gauss-Seidel and the NR methods [6] and [7]. In order to address some of the numerical issues in the Gauss-Seidel method, the NR method exploits its "quadratic" convergence characteristics and takes advantage of the admittance matrix sparsity to attain faster convergence [8]. Various improvements to the NR method are reported in the literature involving selection of effective starting point [7], reduction of the number of iterations [9] and [10], and improving the algorithm robustness [11] and [12]. Moreover, in [13] and [14] optimization frameworks are used to solve the power flow analysis problem, however the reported methods do not consider reactive power limits, and therefore rely on PV-PQ bus switching in order to consider the aforementioned limits.

In [15], an approach based on the Krylov subspace methodology is proposed to solve large-scale power flow problems. The method uses an approximation of the Jacobian matrix without explicitly forming this matrix and then eliminates the need for matrix factorizations. The Krylov subspace method uses the Conjugate Gradient (CG) method for linear systems to minimize the residuals in each iteration [16], which is improved in [17] to accommodate other types of matrices such as non-symmetric, non-definite matrices and nonlinear systems. Since the objective of the algorithm is to minimize the residuals, it is also referred to as the Generalized Minimal Residual Method (GMRES) [16]. In order to improve the efficiency of the CG method, a preconditioning technique, based on the Chebyshev pre-conditioner, which does not need matrix ordering, is proposed in [18]. In [19], a fast Newton GMRES algorithm is presented to solve power flow equations using three acceleration schemes: a hybrid scheme, a partial pre-conditioner update scheme, and an adaptive tolerance control scheme. In [20], a novel approach to formulating power flow problems based on the vector continuous Newton's method is presented. The power flow problem is classified into four possible categories: the well-conditioned case in which the solution can be reached from a flat start; the ill-conditioned case wherein the solution cannot be reached from a flat start; the bifurcation point in which a solution exists, which can be either the saddle-node bifurcation or a limit induced bifurcation; and finally the unsolvable case.

All existing iterative algorithms need an initial solution such as a "flat-start", i.e. setting the bus voltage angles to zero radian and load bus voltage magnitudes to 1 p.u. However, most of the solution methods encounter convergence problems from flat-start initialization when the size of

the system is large (typically, more than 1000 buses) [7].

The OPF problem is to optimize the steady state performance of a system, by minimizing an objective function such as loss or cost and satisfying some equality and inequality constraints. The OPF problem has received lots of attention from utilities in the past three decades. It was first introduced in [21], aiming to optimize different objective functions such as fuel cost and system loss, subject to power flow and other operating constraints, such as real power control, generator bus voltage magnitude limit, reactive power control of switchable VAR sources and transformer tap setting [22]. Depending on the system size and operating conditions, these problems can be large scale, nonlinear and non-convex. A vast body of literature, proposing different solution methods to the OPF problem using Nonlinear Programming (NLP) algorithms, Quadratic Programming (QP), Linear Programming (LP), Interior point methods (IP) and heuristics has evolved.

Most of the proposed NLP methods are based on the NR method, relying on Lagrange multipliers and Kurush-Kuhn-Tucker (KKT) conditions. In [23], the OPF problem, dispatching real power is formulated based on Lagrange multipliers, where all the Lagrange multipliers associated with the equality constraints are obtained using an iterative method, while the Lagrange multipliers associated with the binding inequality constraints are calculated once the optimal solution is obtained. In [24], the Powell and Fletcher-Powell methods are used to find an accurate and efficient direction for an optimal solution to the OPF problem. This method ensures that the minimum point is obtained when the Hessian is constructed, does not need to evaluate the inverse of the Jacobian directly, and demonstrates quadratic convergence. Furthermore, in [25] the Powell method is used to solve the constrained OPF problem while the Fletcher-Powell method solves the unconstrained problem. This method depicts a substantially better performance than the Hessian approach. In [26] an optimization method is proposed to solve the OPF problem, based on the reduced gradient method. In this approach the load flow solution is obtained by a very efficient NR method, using a proper weighting factor and incorporating the gradient directly from the reduced Jacobian, and there is no need to solve the load flow problem repeatedly. In order to reduce the computation time and simplify the OPF problem, decomposition-based methods have been proposed. In [27], the OPF problem is decomposed into a P-optimization problem, solving for real power dispatch and angles and a Q-optimization problem, solving for reactive power and bus voltage magnitudes. In [28] the OPF problem is decomposed into active power and reactive power sub-problems, which are solved by the Newton’s approach using KKT

conditions, and an advanced sparsity technique. The method uses a heuristic to find the binding inequality constraints.

Another nonlinear method that has been vastly used in solving the OPF problem is sequential quadratic programming (SQP), where an NLP is approximated by a quadratic program (QP), and then the solution to this intermediary QP is obtained by solving a sequence of LPs. In [29] the economic dispatch problem is formulated as a QP, using Wolfe's algorithm to handle equality and non-equality constraints. The main advantage of the method is that it does not need any penalty factors or determination of gradient step size. A quadratic nonlinear optimization approach is proposed in [30], that uses the exact second derivative solution for the OPF problem. The method creates a sequence of QP sub-problems, quadratically converging to the optimal solution of the original non-linear problem. It can also handle non-convergent problems, by adding shunt capacitors when the problem is ill-conditioned or infeasible. In [31] the constrained load flow problem is solved by a sequence of QP sub-problems, where only one control variable is adjusted at a time, till a solution to the problem is obtained. The priority order for adjustment of control variables is reactive power, followed by bus voltage magnitude, and then transformer tap ratios. However, using the SQP method the reduced Hessian is built iteratively, which renders these methods slow as there are larger number of control variables. To overcome the drawbacks of the Newton's method for its reliance on good initial solutions points, an improved quadratic interior point (IQIP) method is proposed in [32] that has the advantage of using a general starting point and fast convergence for OPF problems.

In order to overcome the deficiencies of NLP algorithms, such as convergence and choosing initial solutions, linearization techniques are used to solve the OPF problems. The major modelling challenge with these approaches is linearizing the power flow equations. The dual simplex method is widely used to solve the linearized OPF problem as it has a simpler initialization and also less storage needs than the primal problem. In [33], a linear programming (LP) model, using fast decoupled technique is proposed to determine the reactive power dispatch in an OPF framework, in which the active power dispatch is fixed. A linearization technique based on Newton's method is proposed in [34], that uses quadratic penalties to enforce inequality constraints. The emergence of the Interior Point (IP) method is a major breakthrough in solving the OPF problems. This method can easily handle the inequalities by using logarithmic barrier functions in the Lagrangian expression and also does not need a strictly feasible initial solution [35]. However it requires a heuristic to decrease the barrier parameter and also a positive slack variable for inequality constraints. To overcome these problems, extensions to the IP method such

as the primal-dual IP and higher-order IP methods (e.g., the predictor-corrector, multiple predictor-corrector and multiple centrally corrections) are used to solve OPF problems [36]. Since the solution to the large sparse matrix in primal-dual IP is a significant task, the number of matrix factorizations is reduced to a necessary minimum in the predictor-corrector algorithm and is found to be faster than primal-dual IP method. Furthermore, to improve the predictor-corrector IP method, in [37] an efficient multiple centrally correction (MCC) technique is introduced to solve the OPF problem. It uses the same predictor direction as the predictor-corrector method, but looks at more corrector terms to improve the centrality of the next iterate and to increase the step length in order to converge faster. Testing this method on a large test system, MCC is proved to be fast and robust.

Since most of the NLP and LP methods are based on assumptions of smoothness and convexity of the optimization models, the role of heuristic methods has become more significant in the literature. In [38] and [39], genetic algorithm (GA) is used to solve the OPF problem, while in [40] a particle swarm optimization (PSO) technique is employed, wherein the assumption on the differentiability of the optimization problem is no longer necessary since it is a derivative free technique.

1.2.2 Probabilistic Power Flow and OPF

Since deterministic power flow models ignore the uncertainties associated with load and generation, a wide variety of probabilistic approaches have been reported in the literature to incorporate these uncertainties in power flow models. The main idea behind probabilistic power flow is to model the statistical characteristics of the state variables, e.g., bus voltage magnitude and angles. Three main approaches are suggested in the literature to solve these problems: 1) numerical approach, using MCS; 2) analytical approach, using convolution methods; and 3) alternative approaches such as IA, AA and fuzzy arithmetic methods. Numerical approaches are very time consuming since they require a large number of simulations; therefore the main focus in the literature has been on analytical and alternative approaches.

Methods to solve the probabilistic power flow problems, using analytical approaches, first introduced in [41] and [42], considered a dc model of the network, and loads as independent random variables with a probability distribution function (pdf). Thus the results are obtained in the form of power flow pdfs after using convolution methods. Since demand is assumed to have a normal pdf, the output random variables are also assumed to be normally distributed (central limit theorem) [43]. However this assumption is proven to be unreliable in [44], as the output variables can have different pdfs, regardless of the size of the system. The probabilistic approach proposed

in [42] is improved in [44] by considering correlation amongst demand variables. All the dependent variables are converted to a single variable by considering their net arithmetic sum and the resulting independent variable is convoluted with the rest of the independent variables. In [45], the generation system is classified as dependent (e.g., peak and intermittent generators) and independent generators (e.g., base generators), and hence a "requested dependent generation" factor is defined which is convoluted with the rest of the independent generators. Two linearization techniques are proposed in [46] to improve the pdf of the state variables in an ac power flow. Both dc power flow and independency assumptions are removed by suggesting a linear dependence between input values in an AC power system in [47] and [48].

In [48], the power flow equations are linearized around their expected value and then a Fast Fourier Transform (FFT) convolution based technique is proposed to transform the input data, e.g., load and generation into output information. This technique shows a better precision and speed than other convolution methods, e.g., Laplace transformation, as it takes advantage of the properties of exponential functions. A multi-linearization technique is proposed in [49], that reduces the inaccuracy resulting from power flow linearization only around the expected value of the input data, especially around the tail region as it is furthest from the point of linearization. In this paper instead of one linearization around the expected value, different points based on the maximum and minimum values of input data are linearized. A convolution process is then used to find the pdf of each of these linearized points. In order to improve the linear approximations of the power flow equations, a second order probabilistic load flow method, based on the expansion of the power flow equations around a solution point using Taylor series is used in [50], and then the technique of moments is applied to the second order approximations to obtain the statistical characteristics of the output variables. In a different approach, [51] uses a linearized power flow model around a deterministic point, but solves the probabilistic power flow by the cumulants method instead of convolution techniques suggested in previous literature. This technique has the advantage of easier implementation by using the same subroutines, employed in the deterministic power flow. Enhancing the cumulants method, [52] proposed a method combining the concept of cumulants and Gram-Charlier expansion theory to estimate the pdf of line flow. This method is substantially faster than the other method and is able to obtain the Cumulative Distribution Function (cdf) and pdf of line flow in one run. In [53] a hybrid approach using the convolution method and MCS is suggested which incorporates the statistical nature and characterization of wind generation. This method is proven to have better efficiency than MCS and better accuracy than convolution methods.

Although MCS is a very popular method for its simple implementation, it suffers from large execution time, on the other hand convolution methods suffer from lack of accuracy and for the complexity of their mathematical developments. Therefore, other methods are suggested in the literature as alternatives to analytical and numerical approaches. In [54] the IA method is used to determine strict bounds to the solution of the power flow problem with uncertainties, where the interval linear power flow equations are solved by using iterative methods or by employing explicit inverse of matrices to obtain the hull of the solution set. One of the main advantages of IA is its ability to consider internal errors related to roundoff during computational process. In [55], the statistical moments of the solution quantities are obtained using a two-point estimate method, taking into account the uncertainties of the network parameters (e.g., line parameters changing due to temperature variations) and power injections. Uncertainties in power flow problems are also modeled as fuzzy sets in [56] and [57], where the fuzzy generations and loads values are defined using different membership functions with a certain degree of possibility. In [58] an optimization algorithm based on the worst case scenario is proposed to estimate the boundaries of the power flow variables.

In [5], a new solution methodology based on a self-validated approach is proposed, where uncertain variables are presented in affine form, representing uncertainties in data and calculation. The AA-based method is shown to provide more conservative bounds since it considers all sources of internal and external uncertainties. The AA-based intervals associated with the power flow variables are compared with the MCS intervals.

Since the development of the probabilistic load flow models, significant emphasis has been placed on their applications to large and real power systems for both short-term operations and long-term planning. In [59], probabilistic power flow is applied to a Brazilian North/north-eastern system to study network expansion planning, considering problems such as overload on transmission equipment, overload or under-voltage at bus bars and insufficient active/reactive power injections. In [60], probabilistic power flow is used to consider network topology uncertainties. The distribution probability of the power flow variables are calculated for every possible network topology and the weighted sum of the pdfs from each solution is used to find the pdf of the final solution. Furthermore, in [61] MCS is used to capture the load and generation variations in the power flow problem based on their expected mean and standard deviation, which are used to find the impact of wind generation on grid voltage profile.

Moreover, in order to incorporate uncertainties associated with the OPF problem, probabilistic approaches are suggested in the literature. One of the first attempts in solving the P-OPF problem

is proposed in [62] where the multivariate Gram-Charlier method is employed to model the pdf of uncertain variables. Furthermore, in [63] the error between the forecast and the actual demand is assumed to have a Gaussian probability function. The model is solved using MCS and then the statistical characteristics (e.g., mean and variance) of the system variables such as active power generation and system losses are calculated, so that the dispatcher can allocate enough spinning reserve capacity for a certain time interval, knowing uncertainties associated with optimal values. A different approach, based on sensitivity analysis technique is proposed in [64] wherein operating constraint violations and their probabilities are determined for the whole planning horizon and then an iterative approach is used to adjust the control variables while satisfying their limits.

In order to improve the computational efficiency of OPF solution methods, analytical methods are proposed as well. For instance, in [65] the Cumulant method is suggested to simplify the convolution of independent random variables, and then Gram-Charlier/Edgeworth Expansion theory is used to reconstruct the pdfs from the cumulants. Furthermore, [66] uses the Cumulant method to solve the P-OPF problem using logarithmic barrier IP method. The proposed method compares the results for load variables using the Gaussian distribution and Gamma distribution.

Since some of these approaches require derivatives of nonlinear functions, the functions are assumed to be differentiable. Another method to solve the P-OPF problem based on the two-point estimate method is proposed in [67] which alleviates the calculation of derivatives and thus improves the computational efficiency of the solution process. Finally, in [68], a Chance Constrained Programming (CPP) method is used to solve an OPF problem with uncertain demand variables; in order to enhance the execution time, the OPF problem is linearized and a back-mapping approach is implemented to compute the probabilities of satisfying the inequality constraints.

A security assessment approach is proposed in [69] to measure the trade-off between economy and system security in power system operation. This optimal probabilistic security analysis method uses the P-OPF framework to assess the probability of outage of generators and transmission facilities by employing an improved PSO method.

1.2.3 Distributed Generation (DG)

In [70], DG is described as “an electric power source connected directly to the distribution network or on the consumer site of the meter”. This definition does not consider the size of DG, the area of power delivery, DG technology, and its environmental impacts. In [71], DG is defined

under a wider category: distributed energy resources (DER), where, besides generation capacities, it also includes mechanisms to reduce demand (e.g., demand side management (DSM), and storage capacities. Other literature define DG based on using renewables, congestion, and dispatchability [72].

In [73] the barriers of DG integration are categorized as technical, institutional practices and regulatory policies. The benefits from DG [71] are identified as combined heat and power plants, standby/emergency generation, peak shaving, grid loss reduction, generation and transmission expansion deferral, renewable energy production. Its technical and financial barriers are categorized as islanding, voltage regulation, harmonics, reverse power flow, over voltage conditions, metering and system losses.

In [74] appropriate policy mechanisms to encourage the deployment of DG resources are studied. Although these mechanisms, especially FIT, have proven to be significant incentives for DG investors, a study reported in [75] concludes that this mechanism reduces the social welfare in Ontario's electricity market, even though it increases producers' welfare or basically the investors' profit.

In [76] a SQP algorithm is proposed to achieve minimum cost while satisfying demand and system constraints. The SQP program evaluates different DG sources, in regards to their contribution in network loss and also their associated cost. Since DGs are located in the distribution networks, their impacts on transmission networks are not studied much in literature. However, DGs can have significant impacts on transmission lines when DG operators participate in spot market and need to trade electricity with remote areas. In [77] a multi-objective model given the uncertainties in load and generation is presented. This paper uses two stochastic processes, geometric Brownian and a mean reverting process to estimate the system load and market price in order to measure the values of different DG investments. Then the proposed transmission expansion planning multi-objective model simulates the transmission companies' behaviour.

1.2.3.1 DG Impact on System Operation

Because of the large-scale penetration of wind generation sources into the grid, most of the literature on system impacts of DG are focused on this aspect. Their analysis includes stochastic wind dispatch in short-term, reserve requirements, and wind operation, in coordination with other sources of energy such as thermal generators.

In [78] a stochastic day-ahead UC model is presented for power systems with wind penetration;

and then a real-time UC model uses the output to re-dispatch generation based on wind power availability. In [79], an approach referred to as the “risk limiting dispatch” is introduced, in which risks are managed by considering generation as a heterogeneous commodity of probabilistic power in an optimization framework, maximizing operators’ profit subject to constraints on loss of load risk.

Since wind power is unpredictable, varies randomly over time and has inverse correlation with demand, its scheduling and dispatch models are quite different than traditional generation scheduling problems. Many probabilistic-based decision making approaches are suggested in the literature to incorporate this variability. One of the major issues in wind dispatch is the associated reserve requirements, to keep track of the stochastic wind generation and assuring the adequacy of generation capacity to meet the demand.

In [80], a UC model considering stochastic nature of wind generation and demand, and ramp rate limitations of generating capacities for the Swedish wind-hydro-thermal power system is proposed. Since the model fixes the spinning reserve requirements at all time periods, therefore the trade-off between the cost of providing reserve capacities and reduction in the cost of interruptions is ignored. A stochastic security constrained UC model is presented in [81] and [82], in which the reserve requirements are scheduled in an implicit manner, and reserve capacities are determined at each time period and for each generating unit. In [83], another technique to calculate reserve requirements, while minimizing the total system operating cost is suggested. In this model, the optimal amount of reserve capacity is included in the UC model as a constraint based on the estimations of demand and wind generation. Contradictory to other literature, authors in this paper conclude that increasing amount of wind power does not require more reserve capacity. In [84] a security based UC model is proposed to schedule the flexible reserve requirements that are deployed due to the intra-hour variability of wind generation. In this paper, the variability of wind generation is detected by its power spectral density and then the flexibility of reserve capacities is modeled in frequency domain. Finally, a new set of constraints are introduced that can be added to the original UC models.

1.3 Research Objectives

As previously discussed, the existing NR-based power flow solution methods have convergence problems for large systems when using a flat-start or exceeding the maximum loadability of a system, and require an initial solution which is close to the final solution. This

research proposes an MCP optimization framework to address this issue and properly represent reactive power generation limits and the voltage recovery process of voltage regulators.

Also, integration of DG sources into the electricity grid has introduced significant levels of uncertainties in power system operations, including power flow analysis, OPF, UC and ELD models. Since many of the approaches, addressing these uncertainties suffer from large computation time, lack of accuracy and difficulties in pdf approximations, this thesis attempts to exploit the AA method, in order to accommodate these uncertainties. The main objectives of this research are as follows:

- Develop an optimization based model of the classical power flow problem using complementarity conditions, to properly represent generator bus voltage control, including reactive power limits and voltage recovery processes.
- Establish the mathematical proof that the NR solution method for solving the power flow problem is basically a step of the Generalized Reduced Gradient (GRG) algorithm, applied to solve the proposed same problem.
- Validate the proposed MCP based power flow solution method against other NR based methods to ensure its accuracy, computational advantages and flexibility, considering a range of test systems, including real and large-scale systems.
- Develop the complete mathematical formulation for the AA-based power flow analysis problem, incorporating uncertainties arising from both external (e.g., weather forecast and measurement errors) and internal sources (e.g., truncation and roundoff errors), where the power flow problem is solved using the previously proposed MCP formulation.
- Validate the outcomes of the AA model with the ones from other robust stochastic methods such as the MCS.
- Develop a novel AA-OPF formulation and its solution methodology for analysis and determination of optimal operational bounds for dispatchable generators in a power system with uncertainties arising from the presence of intermittent generation sources.
- Validate the AA-OPF model considering both, a small test system and a large-scale real power system, to compare and contrast the accuracy of operational margins vis-à-vis those obtained from MCS.

1.4 Thesis Outline

The rest of the thesis is outlined as follows:

Chapter-2 presents a background review on uncertainty analysis tools, such as IA, AA and MCS; and also NLP solution methods such as NR and gradient methods. In addition, DG technologies, their benefits and shortcomings are briefly discussed. Finally the chapter presents a review of power flow analysis techniques, including deterministic and stochastic methods, i.e., NR method and AA, respectively.

Chapter-3 discusses the proposed MCP formulation for an optimization based power flow model and examines its robustness and flexibility by providing a benchmark against other classical methods, such as the NR method. In Chapter-4, the probabilistic power flow model is solved using the AA method. A thorough comparison of the solution of the power flow uncertain variables, using the AA and MCS methods is presented. Chapter-5 presents a novel AA-based formulation of the OPF problem with uncertain variables. The accuracy of the proposed model is tested by comparing the obtained bounds from the AA method with those from MCS.

Finally, Chapter-6 summarizes the thesis and discusses the contributions of this research, and outlines the scope for future.

CHAPTER 2

BACKGROUND REVIEW

2.1 Introduction

This Chapter provides a background to the tools and methodologies used in the research presented in this thesis. First the deterministic and probabilistic power flow and the OPF problems are discussed and then a brief background to the NLP and its solution approaches is presented. Furthermore, the tools for uncertainty analysis, such as IA, AA and MCS are discussed. And finally a brief review of DGs, including their advantages and barriers are discussed.

2.2 Power Flow Analysis Problem

2.2.1 Power Flow Analysis Problem

The power flow analysis problem is formulated as a set of simultaneous nonlinear equations for real and reactive power injection mismatch functions $\Delta P(\,.\,)$ and $\Delta Q(\,.\,)$, respectively, as follows:

$$\Delta P(\delta, P_s, |V_D|, Q_G) = \; P_i^{sp} - |V_i| \sum_{j=1}^{n} |V_j| \left(G_{ij} \cos\delta_{ij} + B_{ij} \sin\delta_{ij}\right) = 0 \qquad \begin{matrix} \forall i \in N \\ i \neq slack \end{matrix} \tag{1}$$

$$\Delta Q(\delta, P_s, |V_D|, Q_G) = Q_i^{sp} - |V_i| \sum_{j=1}^{n} |V_j| \left(G_{ij} \sin\delta_{ij} - B_{ij} \cos\delta_{ij}\right) = 0 \qquad \forall i \in nPQ \tag{2}$$

where all the variables are defined in the nomenclature. Equations (1) and (2) can be expressed in vector form as:

$$f(x) = \begin{bmatrix} \Delta P(\delta, P_s, |V_D|, Q_G) \\ \Delta Q(\delta, P_s, |V_D|, Q_G) \end{bmatrix} = 0 \tag{3}$$

Since the solution to (3) cannot be expressed in closed form [85], these equations are solved iteratively, in which an initial guess $\left(\delta^0, {P_s}^0, \left|V_D^0\right|, {Q_G}^0\right)$ is selected close to the "desired" solution $(\delta^*, {P_s}^*, |V_D^*|, {Q_G}^*)$, and it is iteratively updated to obtain a solution x^* such that $f(x^*) \approx 0$.

The NR method applied to the solution of the power flow equations (1) and (2), yields the following linear equations:

$$\begin{bmatrix}\Delta P\\ \Delta Q\end{bmatrix} = [\,J\,]\begin{bmatrix}\Delta\delta\\ \Delta P_s\\ |\Delta V_D|\\ \Delta Q_G\end{bmatrix} \tag{4}$$

In this process, at the end of each iteration, the reactive power generation Q_G from each generator is calculated. If Q_G violates either of its limits at a bus, it is fixed at the corresponding limiting value and the particular "generator" bus (PV bus) is switched to a "load" bus (PQ bus). The bus is switched back to a PV bus when $|V_G|$ returns to its set-point value.

The NR method is much faster than other iterative methods since it converges quadratically when starting from an initial point "close" to the observed solution [15]. One of the main disadvantages of this method is that, when the initial solution is "too far" from the final solution, it has difficulties to converge. In such a case, the assumption that higher order terms of the Taylor series can be ignored is no longer valid, since these terms have a significant effect on the convergence of the solution.

Although the NR method has a fast convergence with less iterations, each iteration is computationally heavy, since the computational burden of the full Jacobian matrix is a function of N^2 [85]. In [86], a method is proposed to update the Jacobian matrix whenever the rate of convergence slows down, which is referred to as the "dishonest" Newton method.

2.2.2 Probabilistic Power Flow Analysis

Because of the existence of uncertainties in power systems, probabilistic approaches to power flow analysis problems have been proposed. These uncertainties arise from either approximation errors or external sources such as generation intermittency, demand fluctuation, weather forecast, random outage, gas price and energy policies.

Probabilistic approaches try to capture these uncertainties by approximating or linearizing the power flow equations (3) and using the pdf of the input data (demand and generation) to directly obtain probabilistic characteristics, e.g., pdf of the power flow variables. In order to use convolution methods for probabilistic power flow calculations, nodal power injections need be independent. For instance, if A and B are two independent random variables with pdfs $f_A(a)$ and $f_B(b)$, using convolution method, random variable C and its pdf is obtained as follows:

$$C = A + B \tag{5}$$

$$f_C(c) = \int_{-\infty}^{\infty} f_A(a)\, f_B(c-a)\, da \tag{6}$$

On the other hand, numerical methods, such as MCS can be used to solve probabilistic power flows. Although MCS has a high computation cost, it is one of the most popular methods for power system uncertainty analysis because of its simple implementation. For instance, in the context of the probabilistic power flow problem, generation and demand are uncertain and can be associated with an appropriate pdf, especially when there is large-scale integration of non-dispatchable renewable energy sources (e.g., wind and solar). The pdf for load is usually assumed to be normal, as follows [87]:

$$pdf\left(P^{dem}\right) = \frac{1}{\sigma\sqrt{2\pi}}\, e^{\frac{-(P^{dem}-\bar{P}^{dem})^2}{2\sigma^2}} \tag{7}$$

where $\bar{P}^{dem}$ is the mean value and σ is the standard deviation. As a result, the standard deviation and the average of historical data determine the load at each time period.

Employment of self-validated computation (SVC) methods such as AA, are also gaining popularity in solving probabilistic power flow models because of the accuracy and efficiency of their solution algorithm [5]. In this method, the power flow state variables are represented in affine form as follows:

$$\tilde{V}_i = V_{i,0} + \sum_{j\epsilon N} V_{i,j}^P\, \varepsilon_{P_j^D} + \sum_{j\epsilon N} V_{i,j}^Q\, \varepsilon_{Q_j^D} \qquad \forall i \in N \tag{8}$$

$$\tilde{\delta}_i = \delta_{i,0} + \sum_{j\epsilon N} \delta_{i,j}^P\, \varepsilon_{P_j^D} + \sum_{j\epsilon N} \delta_{i,j}^Q\, \varepsilon_{Q_j^D} \qquad \forall i \in N \tag{9}$$

where $\varepsilon_{P_j^D}$ and $\varepsilon_{Q_j^D}$ are the noises representing the uncertainties of the active power and reactive power injections at the jth bus respectively, while $V_{i,0}$ and $\delta_{i,0}$ are the center values for voltage magnitudes and bus angles at bus i. $V_{i,j}^P$ and $\delta_{i,j}^P$ are partial deviations of the ith bus voltage magnitudes and bus angles due to changes in real power injection at bus j, and $V_{i,j}^Q$ and $\delta_{i,j}^Q$ are partial deviations of the ith bus voltage magnitudes and bus angles due to changes in reactive power injection at bus j.

Using the affine equations (8)-(9) and affine operations (discussed later), the real and reactive power injections at a bus can be easily represented in affine forms $\tilde{P}_i$ and $\tilde{Q}_i$ as follows:

$$\tilde{P}_i = P_{i,0} + \sum_{j \epsilon N} P_{i,j}^P \, \varepsilon_{P_j^D} + \sum_{j \epsilon N} P_{i,j}^Q \, \varepsilon_{Q_j^D} + P_i^T \varepsilon_{T_i} \qquad \forall i \in N \quad (10)$$

$$\tilde{Q}_i = Q_{i,0} + \sum_{j \epsilon N} Q_{i,j}^P \, \varepsilon_{P_j^D} + \sum_{j \epsilon N} Q_{i,j}^Q \, \varepsilon_{Q_j^D} + Q_i^T \varepsilon_{T_i} \qquad \forall i \in N \quad (11)$$

where ε_{T_i} is the new noise variable representing approximation errors due to the presence of non-affine operations. All the other variables and parameters are explained in the Nomenclature. Having the affine forms of (10)-(11), real and reactive powers can be easily represented in interval forms.

2.3 The Optimal Power Flow Problem

The OPF problem [22] is an optimization problem, that seeks to find the optimal setting of control variables in order to minimize or maximize an objective function such as total generation cost, real power losses, bus voltage deviations or emissions, while satisfying various operating constraints such as power flow equations, bus voltage magnitude and angle limits, and real and reactive power generation limits. The general form of an OPF problem is as follows:

$$\min \quad F(x,u) \qquad (12)$$

$$\text{s.t.} \quad g(x,u) = 0 \qquad (13)$$

$$h(x,u) \leq 0 \qquad (14)$$

where $g(x,u)$ represents the nonlinear power flow equations (1) and (2) and $h(x,u)$ is the set of nonlinear inequality constraints on the vectors x (vector of state variables, e.g., bus voltage magnitudes, angles and reactive power output of generators) and u (vector of control variables). Depending on the objective function, the control variables in an OPF framework can be as follows:

- Active and reactive power generation
- Phase-shifter angles
- Net interchange
- Active and reactive power load (load shedding)
- Transmission line flows

- Control voltage setting
- LTC transformer tap setting
- Line switching

For example, in the fuel cost minimization OPF problem, the only control variable is active power generation, and the other variables are held at their nominal values. Depending on the objective function and constraints, the OPF problem can be categorized as follows [88]:

1- Linear problem (LP): when the objective function and constraints are linear (e.g., dc power flow)

2- Nonlinear problem (NLP): when the objective function or constraints are nonlinear (e.g., ac power flow)

3- Mixed-integer linear (nonlinear) problem: when the control variables are both discrete and continuous.

The basic mathematical formulation of the OPF problem for an active power loss minimization objective is as follows:

$$\min \quad \frac{1}{2}\sum_{i=1}^{N}\sum_{j=1}^{N} G_{ij}\left(V_i^2 + V_j^2 - 2V_iV_j\cos(\delta_j - \delta_i)\right) \tag{15}$$

$$\text{s.t.} \quad \Delta P(\delta, P_s, |V_D|, Q_G) = P_i^{sp} - |V_i|\sum_{j=1}^{n}|V_j|\left(G_{ij}\cos\delta_{ij} + B_{ij}\sin\delta_{ij}\right) = 0 \qquad \forall i \in N \tag{16}$$

$$\Delta Q(\delta, P_s, |V_D|, Q_G) = Q_i^{sp} - |V_i|\sum_{j=1}^{n}|V_j|\left(G_{ij}\sin\delta_{ij} - B_{ij}\cos\delta_{ij}\right) = 0 \qquad \forall i \in N \tag{17}$$

$$P_i^{Min} \le P_i \le P_i^{Max} \qquad \forall i \in gen \tag{18}$$

$$Q_i^{Min} \le Q_i \le Q_i^{Max} \qquad \forall i \in gen \tag{19}$$

$$V_i^{Min} \le |V_i| \le V_i^{Max} \qquad \forall i \in N \tag{20}$$

In the above optimization problem, (15) is a quadratic objective function minimizing the total active power loss, (16)-(17) are nonlinear power flow constraints, representing real and reactive power mismatch at a bus, and (18)-(22) represent the limits associated with real and reactive

power generation, bus voltage magnitudes and phasor angles at each bus, and line current at each line respectively.

An extension to the OPF problem is the Security Constrained OPF (SCOPF), in which the objective is to minimize the total generation cost, subject to constraints (16)-(20) and additional security constraints such as limits on bus voltage magnitudes, thermal limits determined by the lines' current carrying capacity, and line power flow limits [89], as written below:

$$-\pi \leq \delta_i \leq \pi \qquad \forall i \in N \quad (21)$$

$$I_{ij}^{min} \leq I_{ij} \leq I_{ij}^{max} \quad \text{and} \quad P_{ij} \leq P_{ij}^{Max} \qquad \forall ij \in L \quad (22)$$

There are many LP and NLP-based methods, suggested in the literature to solve OPF problems. Since these problems are usually applied to large systems, in real time, they are required to be reliable, fast, flexible and maintainable [89]. For instance, in a cost minimizing OPF problem, the nonlinear cost curve is linearized by piecewise linearization technique, in which the cost curve is segmented into smaller units and where adjacent points are connected by straight lines, and then the LP problem is solved using simplex method.

Interior point (IP) is another technique which can either solve the linearized OPF from within the feasible interior region or directly solve the non-linear OPF problem. The IP method starts the search from inside the polytope and moves towards the direction of the optimal point, choosing a proper step length. In the IP algorithm, an elimination procedure is applied on the linearized load flow around the base load flow solution considering small perturbations in order to apply the Improved Quadratic Interior Point Method (QIPM). The modified model has a quadratic objective function subject to the linear constraints.

2.4 Nonlinear Programming (NLP)

An NLP problem can either be an unconstrained optimization problem or a constrained one. It is an unconstrained problem, when there are no additional constraints on x except that it is a vector defined over a feasible set. On the other hand, a general constrained NLP problem is represented as follows [90]:

$$\min \ z = f(x) \qquad (23)$$

$$\text{s.t.} \quad h_i(x) = 0 \qquad (24)$$

$$g_i(x) \leq 0 \tag{25}$$

where $f(x)$, $h(x)$ and $g(x)$ are the objective function, and the set of equality and inequality constraints, respectively, in which at least one is nonlinear. They are also continuously differentiable in the feasible region. The feasible region for an NLP problem is a convex set, meaning that any line connecting two-points in the region, lies entirely in the feasible region.

The Lagrangian of the above NLP problem (23)-(25) is as follows:

$$L(x, \lambda, \mu) = f(x) + \sum_i \lambda_i^T h_i(x) + \sum_i \mu_i^T g_i(x) \tag{26}$$

where λ_i and μ_i are the dual variables of the constraints (24)-(25). The Lagrangian plays an important role in NLP algorithms as it combines the objective function and all the constraints into a single unconstrained function.

Karush-Kuhn-Tucker (KKT) conditions are necessary but not sufficient conditions for a point x to be a local optimal point. KKT conditions for a local optimal point x^*, for a minimization NLP, in which all the constraints are converted into the form of less than or equality (e.g., $g_i(x) \leq 0$) with the Lagrangian multiplier λ_i are as follows [90]:

$$\nabla_x L(x, \lambda, \mu) = 0 \tag{27}$$

$$h(x) = 0 \tag{28}$$

$$g(x) \leq 0 \tag{29}$$

$$\mu^T g(x) = 0 \tag{30}$$

$$\mu \geq 0 \tag{31}$$

where ∇_x denotes the gradient of a function in respect to x, and $h(x)$, $g(x)$ and μ are vectors with components $h_i(x)$, $g_i(x)$ and μ_i, as their components respectively. Constraint (27) states that the gradient of the Lagrangian with respect to x at an optimal solution is zero. Constraints (28) and (29) are to enforce the equality and inequality constraints.

Constraint (30) is referenced to as the complementarity constraint, denoted by "$\perp$". For a continuously differentiable function $g(x)$, the complementarity condition is defined as follows:

$$\mu \perp g(x) \tag{32}$$

for all μ and $g(x)$, there would be three situations in which (32) is satisfied:

$$\mu_i = 0 \text{ and } g_i(x) \neq 0 \tag{33}$$

$$\mu_i \neq 0 \text{ and } g_i(x) = 0 \tag{34}$$

$$\mu_i = 0 \text{ and } g_i(x) = 0 \tag{35}$$

Among the above three equations, conditions (33) and (34) (strict complementarity conditions) are the most desirable situations in the application of engineering and economics, while the last condition (35) (non-strict complementarity) is not desirable. Available solvers such as PATH [91] introduce mechanisms to avoid such a condition.

2.4.1 Solution Methods

There are many algorithms, proposed in the literature to solve NLP problems. The major classical approaches use the gradient method, line search, Lagrange multiplier method, NR method, trust region optimization, quasi-Newton method, double dogleg optimization and conjugate gradient optimization [88]. Besides the classical approaches, problem specific heuristic methods such as neural network, evolutionary algorithm (e.g., evolutionary programming, evolutionary strategy and genetic algorithms), tabu search and PSO have been used to solve large-scale NLP problems. All the available algorithms are categorized into two groups [90]:

1- Direct algorithms in which a finite number of operations result in the final solution.

2- Iterative algorithms in which a sequence of iterations converge to a solution that is very close to the optimal and satisfies the termination criterion.

In general the iterative methods for solving NLP problems adopt the following solution step [90]:

$$x^{k+1} = x^k + \alpha^k \, \Delta x^k \tag{36}$$

where x^0 is the initial solution, k is the number of the iteration, x^k is the value of the solution at the kth iteration, α^k is the step size which is usually between 0 and 1; and Δx^k is the step direction in the kth iteration. The step direction ensures that the algorithm is moving in a direction to improve the solution which the step size ensures a sufficient improvement from the solution in the previous iterate.

2.4.1.1 The Newton-Raphson Method (NR)

Using the KKT conditions, the NLP problem can be converted to a system of nonlinear equations. Since 1980, significant research has been carried out on the development of solution methods for nonlinear simultaneous equations, including pivoting and iterative methods. One of the well-established iterative methods, the NR method, has been found most suitable because of its fast convergence properties [92].

The NR method relies on nonlinear approximation obtained from a Taylor series [93]. Expanding the nonlinear function $f(x) = 0$ around a nominal value of $x = x^k$ results in the following expression for an iteration $k + 1$:

$$f(x) \approx f\left(x^k\right) + \frac{df(x^k)}{dx}\left(x^{k+1} - x^k\right) \approx f\left(x^k\right) + \frac{df(x^k)}{dx}\Delta x^{k+1} = 0 \tag{37}$$

Therefore, the solution update from the previous iteration can be expressed as follows, if the initial guess for the solution at $k = 0$ (x^0) is very close to the final solution x^*:

$$\Delta x^{k+1} = -\alpha\left[\frac{df\left(x^k\right)}{dx}\right]^{-1} f\left(x^k\right) \tag{38}$$

$$x^{k+1} = x^k - \alpha\left[\frac{df\left(x^k\right)}{dx}\right]^{-1} f\left(x^k\right) \tag{39}$$

where the scalar $\alpha > 0$ is a "correction" factor to control the NR convergence [94]. This method, typically referred as "robust" NR, converges when $\left|f\left(x^{k+1}\right) - f\left(x^k\right)\right| < \tau$, where τ is the convergence tolerance.

2.4.1.2 Gradient Method

The gradient method [90] maintains the feasibility of solution in each iteration; and therefore the algorithm can be terminated before it converges while the approximate solution is still useful. However, this method suffers from heavy computation time, as it should ensure that all the linear and nonlinear constraints are satisfied in each iteration.

This method relies on the gradient of the function in order to find the direction of the search as given below:

$$S^k = -\nabla f(x^k) \tag{40}$$

$$S^k = \nabla f(x^k) \tag{41}$$

where $\nabla f(x^k)$ is the gradient of the function $f(x)$ at x^k. The simplest gradient method is based on the direction of the steepest descent (40) for minimization problems and steepest ascent (41) for maximization problems. The optimum search step can be computed as follows:

$$\alpha^{*k} = \frac{[\nabla f(x^k)]^T \nabla f(x^k)}{[\nabla f(x^k)]^T H(x^k)\, \nabla f(x^k)} \tag{42}$$

where *T* denotes transpose and $H(x^k)$ is the Hessian matrix of the objective function.

2.5 Tools for Uncertainty Analysis

Numerical calculations are prone to errors in obtaining the exact values of the mathematical computations, because of the existence of uncertainties. Most of the uncertainty analysis techniques, such as MCS try to capture the external uncertainties, affecting the input data; and neglect the impact of the internal errors, caused by approximation and truncation. To resolve this issue SVC or "automatic result verification" such as IA, and AA methods are proposed, which keep track of internal errors inherently. In the next three subsections, the two most popular SVC methods, i.e., IA and AA and subsequently the MCS method are discussed.

2.5.1 Interval Arithmetic (IA)

The IA method [95], is the simplest self-validated range analysis technique, providing the most conservative bounds where the value of $\hat{x}$ lies between an upper bound $\bar{x}$ and lower bound $\underline{x}$. Basic IA operations between two quantities $\hat{x}$ and $\hat{y}$ return the following intervals, assuming two conditions: 1) None of the intervals are empty; 2) The upper and lower bounds of each interval are finite real numbers. These assumptions prevent certain operations such as $0 \times \infty$ and $(-\infty) \times (+\infty)$:

$$\hat{x} + \hat{y} = [\, \underline{x} + \underline{y}\,, \bar{x} + \bar{y}\,] \tag{43}$$

$$\hat{x} - \hat{y} = [\, \underline{x} - \bar{y}\,, \bar{x} - \underline{y}\,] \tag{44}$$

$$\hat{x}\,.\,\hat{y} = [\, \underline{z}_{prod}\,, \overline{z}_{prod}\,] \tag{45}$$

$$\hat{x}\ /\ \hat{y} = [\, \underline{z}_{div}\,, \overline{z}_{div}\,] \tag{46}$$

where:

$$\underline{z}_{prod} = \min\{\, \underline{x}.\underline{y}\,, \underline{x}.\bar{y}, \bar{x}.\underline{y}\,, \bar{x}.\bar{y}\,\}$$

$$\overline{z}_{prod} = \max\{\, \underline{x}.\underline{y}\,, \underline{x}.\bar{y}, \bar{x}.\underline{y}\,, \bar{x}.\bar{y}\,\}$$

where:

$$\underline{z}_{div} = \min\{\, \underline{x} \,/\, \underline{y}\,,\ \underline{x} \,/\, \bar{y},\ \bar{x} \,/\, \underline{y}\,,\ \bar{x} \,/\, \bar{y}\,\}, \text{ assuming } \ \bar{y} \neq 0 \text{ and } \underline{y} \neq 0$$

$$\overline{z}_{div} = \max\{\, \underline{x} \,/\, \underline{y}\,,\ \underline{x} \,/\, \bar{y},\ \bar{x} \,/\, \underline{y}\,,\ \bar{x} \,/\, \bar{y}\,\}, \text{ assuming } \ \bar{y} \neq 0 \text{ and } \underline{y} \neq 0$$

IA functional relations for other operations such as logarithm, square root, exponential, sine and cosine are given in [95]. More complicated functions can be implemented using the elementary ones. In all the above operations, it is recommended to widen the bounds by rounding them in the most conservative direction to handle round-off errors. Moreover one should be careful of the overflow problem in which the result is greater than allocated memory space, and the domain violation problem, in which the argument interval of an IA operation is outside the domain of the corresponding function.

One of the main disadvantages of IA is error explosion, resulting in very conservative final bounds, which are too wide to be useful. Error explosion usually occurs in long chains of computation, where the input of one operation is the output of another, which is typical in power system analysis problems. The main reason for the wider bounds in IA calculations is the independency problem, in which the correlation between IA values are neglected and are therefore considered independent, e.g., $\hat{x}$ and $\hat{y}$ are independent values in (43)-(46).

To overcome the error explosion problem, the IA arguments can be split into smaller sub-domains and then the limits are obtained using the small ranges which can be combined to form a final, single interval. Other techniques to overcome the error explosion problem depending on the function and the input intervals, have been suggested in [95].

2.5.2 Affine Arithmetic (AA)

The AA method is a range analysis technique, which not only handles external uncertainties such as weather forecast errors but also internal errors such as arithmetic roundoff, series truncation and function approximation [95]. Although AA is computationally more expensive than the IA method, it provides narrower intervals, thus justifying the extra cost.

An affine value $\tilde{x}$ of a value (either a variable or a parameter) x, is represented in the following form:

$$\tilde{x} = x_0 + x_1\varepsilon_1 + x_2\varepsilon_2 + \cdots + x_n\varepsilon_n \quad (47)$$

where:

$\tilde{x}$ The representation of a value in affine form

x_0 The central value of the affine form

x_i Partial deviations of the affine form or the coefficient of the noise variable ε_i

ε_i Noise variables which are in the interval [-1,+1]

Each noise variable ε_i represents an independent source of uncertainty and each coefficient x_i states the magnitude of that uncertainty. Each affine form can be converted to an interval form by adding or subtracting the summation of the absolute values of all noise magnitudes to or from the central value x_0 in order to find the upper and lower bounds, as follows:

$$[\hat{x}] = \left[x_0 - \sum_i |x_i| \ , x_0 + \sum_i |x_i|\right] \quad (48)$$

In (48), $\sum_i |x_i|$ is called the total deviation of the affine form $\tilde{x}$.

On the other hand, knowing the interval $[a, b]$ for x, an equivalent affine form for $\tilde{x}$ can be obtained as follows:

$$x_0 = \frac{b + a}{2} \quad (49)$$

$$x_1 = \frac{b - a}{2} \quad (50)$$

$$\tilde{x} = x_0 + x_1\varepsilon_1 \quad (51)$$

As shown in (49)-(51), x_0 is the midpoint and x_1 is half of the interval width.

2.5.2.1 Affine Operations

Each affine operation $\tilde{f}(.)$ computes an affine form $\tilde{z}$, which is consistent with the affine input values as follows:

$$\tilde{f}(\tilde{x}, \tilde{y}) \rightarrow \tilde{z} \quad (52)$$

Let consider $\hat{x}$ and $\hat{y}$ as follows:

$$\tilde{x} = x_0 + x_1\varepsilon_1 + x_2\varepsilon_2 + \cdots + x_n\varepsilon_n = x_0 + \sum_{i=1}^{n} x_i\varepsilon_i \tag{53}$$

$$\tilde{y} = y_0 + y_1\varepsilon_1 + y_2\varepsilon_2 + \cdots + y_n\varepsilon_n = y_0 + \sum_{i=1}^{n} y_i\varepsilon_i \tag{54}$$

Then the affine elementary operations in order to find $\hat{z}$ are as follows:

$$\tilde{x} \pm \tilde{y} = (x_0 \pm y_0) + (x_1 \pm y_1)\varepsilon_1 + (x_2 \pm y_2)\varepsilon_2 + \cdots + (x_n \pm y_n)\varepsilon_n \tag{55}$$

$$\varphi\tilde{x} = (\varphi x_0) + (\varphi x_1)\varepsilon_1 + (\varphi x_2)\varepsilon_2 + \cdots + (\varphi x_n)\varepsilon_n \tag{56}$$

$$\tilde{x} \pm \varphi = (x_0 \pm \varphi) + x_1\varepsilon_1 + x_2\varepsilon_2 + \cdots + x_n\varepsilon_n \tag{57}$$

where φ is a constant in (56) and (57).

From (53)-(54) it is noted that each noise variable ε_i shows a partial dependency between the two values $\tilde{x}$ and $\tilde{y}$. Therefore, in (55), ε_i contributes to the same uncertainty in the resulting affine form $\tilde{z}$ with the noise magnitudes corresponding to the coefficients of ε_i in affine input values.

2.5.2.2 Non-Affine Operations

Non-affine operations require a good affine approximation and an extra term, called approximation error, to represent internal errors such as the roundoff error. For instance, a non-affine multiplication operation between the two affine values $\tilde{x}$ and $\tilde{y}$ are given as follows:

$$\tilde{x}.\tilde{y} = x_0\, y_0 + \sum_{i=1}^{n} (x_0\, y_i + y_0\, x_i)\, \varepsilon_i + z_k\, \varepsilon_k \tag{58}$$

The result of the above non-affine function is an affine value containing the information provided by $\tilde{x}$ and $\tilde{y}$; and the approximation error represented by $z_k\varepsilon_k$, where $|z_k|$ must be an upper bound on the absolute magnitude of the approximation error, as follows:

$$\left(\sum_{i=1}^{n} |x_i\, \varepsilon_i|\right)\left(\sum_{i=1}^{n} |y_i\, \varepsilon_i|\right) \leq |z_k| \tag{59}$$

The simplest and most conservative affine approximation (e.g., trivial affine approximation) is calculated as follows:

$$z_k = \sum_{i=1}^{n} |x_i| \sum_{i=1}^{n} |y_i| \tag{60}$$

Therefore after substituting (60) in (58) the product function can be represented as follows:

$$\tilde{x}.\tilde{y} = x_0\, y_0 + \sum_{i=1}^{n} (x_0\, y_i + y_0\, x_i)\, \varepsilon_i + \left(\sum_{i=1}^{n} |x_i| \sum_{i=1}^{n} |y_i| \right) \varepsilon_k \tag{61}$$

The affine approximation presented in (61) is computationally efficient, but not the most accurate one. The error of this approximation is at most four times the error reported by the most accurate method, Chebyshev approximation [95]. Furthermore, ε_k is assumed to be 1 throughout this thesis. Even though this simplification may result in wider intervals, it reduces the number of noise symbols for each non-affine operation, and since there are many non-affine operations in power system models, this would significantly reduce the number of noise symbols in realistic applications.

2.5.3 Monte Carlo Simulation (MCS)

MCS is the process of generating a set of deterministic solutions to a stochastic problem, wherein each solution is obtained by random input values based on their corresponding pdf [96]. In order to obtain valid simulation results, the process is repeated many times and then the statistical characteristics of the simulation such as min, max, average, median and variance of the sample are calculated.

The main concerns in MCS are:

- Choosing the appropriate pdf to generate random input values
- Number of the iterations to obtain the convergence of the expected values

Usually thousands of simulations are required, thus the computation cost of this approach and resource requirement is very high when the size of the problem is large.

After obtaining the simulation results on a random variable X, its statistical characteristics are calculated using the following equations:

$$\mu_i = E(X_i) = \int_{-\infty}^{\infty} x f_{X_i}(x)\, dx \tag{62}$$

$$\sigma_i^2 = E[(X_i - \mu_i)^2] = E\left(X_i^2\right) - \mu_i^2 \tag{63}$$

where $f_{X_i}(x)$ is the pdf that the continuous variable X takes the value x_i and μ_i and σ_i^2 are the mean (expected value) and the variance of the random variable x_i.

2.6 Distributed Generation (DG)

Although the concept of DG is not new, there has been more attention on DG developments in recent years, because of the advances in renewable energy technologies, government incentives such as FIT and Renewable Portfolio Standards, energy security concerns, environmental issues, transmission line requirements and increased demand. The main drivers for such investments around the globe are as follows [97]:

- Environmental drivers: These drivers include limiting greenhouse gas (GHG) emissions and avoidance of the construction of the new transmission circuits and large generating units.
- Commercial drivers: DG investments are predicted to lower electricity prices in the long run, also they help in deferring the construction of large generation capacities. Furthermore, building DGs close to load centers helps alleviate investments in long transmission lines. Besides, combined heat and power (CHP) units help in utilizing the system (60% to 70% efficiency) in industrial sites where there is a continuous need for power and heat.
- Technical drivers: Voltage drop and line losses in distribution networks are high, since resistance becomes significant in distribution feeders [98]. DGs can assist in improving the voltage profiles and hence improve the power quality. It can also help in load factor correction.

DG sources may be categorized as follows [99]:

- Renewable sources: wind power, solar photovoltaic, small hydro, biomass, tidal energy, wave energy and geothermal.
- Non-renewables: reciprocating engine, micro-turbine and fuel cell

- Storage devices: super conducting magnetic energy storage (SMES), battery energy storage system (BESS), flywheel, ultra capacitors and modular pumped hydro.

All the above renewable sources except biomass generation are not dispatchable and therefore integrating them to the grid causes a great deal of uncertainty due to the stochastic nature of their availability. Wind power is the most mature technology among all the available renewable sources. The average cost of wind power generation is projected to be as low as 3 cents per KWh by 2020 [100].

Introducing high penetration of DG can impact power system operations, such as system security, voltage regulation and power flow. Some of the DG integration issues, mentioned in the literature are as follows [101]:

- In contrast to transmission networks, distribution networks provide one-directional power flow, while DG integration requires networks accommodating bi-directional power flow [102], since they generate active power and sometimes generate or absorb reactive power. Therefore distribution systems with DG integration are active, not passive networks.
- DG units use asynchronous generators versus large central capacities which use synchronous generators. Synchronous machines help in reactive power support while asynchronous machines not only do not provide reactive power, but also need reactive power for their operation. Thus, induction based DGs may cause voltage drop in the system [103].
- Transmission expansion planning is more complicated in the presence of DG penetration, as the planner should consider the objectives of all the DG investors, facilitate market competition, provide non-discriminating network access for all DGs, and enhance reliability and security of the system [77].

2.7 Summary

In this Chapter a background on deterministic and stochastic power flow and OPF problems is presented. Also, the mathematical tools for uncertainty analysis, including MCS and SVC such as AA and IA are discussed. It is concluded that AA is one of the superior SVC-based sensitivity analysis tools, since it considers all the information amongst dependent variables and also provides less conservative bounds compared to IA.

Furthermore, a brief review of NLP and complementarity conditions, and their formulation and solution methodologies are presented. Among all the solution methodologies, the main focus is on optimality conditions (e.g., KT conditions), NR and gradient method.

Finally a brief review of DG technologies, their advantages and shortcomings, and their system operation and planning issues are presented.

CHAPTER 3

REVISITING THE POWER FLOW PROBLEM BASED ON A MIXED COMPEMENTARITY FORMULATION APPROACH

3.1 Introduction

In order to formulate the power flow problem under uncertainty, an optimization framework is needed to assure the flexibility, accuracy and robustness of the solution methodology. Hence, in this Chapter, a novel formulation of the power flow problem is proposed within an optimization framework that includes complementarity constraints. Accordingly, the power flow problem is formulated as a MCP, which can take advantage of state-of-the-art NLP and complementarity problems using solvers such as COINIPOPT [104], MINOS [105] and PATHNLP [16]. The proposed method properly represents reactive power generation limits and the voltage recovery process of voltage regulators. Furthermore, the MCP-based power flow model, which by design always has a theoretical solution, is shown to have increased robustness and flexibility with respect to the existent power flow methods, which have convergence problems for large systems when using a flat-start and cannot yield solutions when the maximum loadability of the system is exceeded. Based on the proposed MCP formulation, it is also formally demonstrated that the NR solution of the power flow problem is essentially a step of the traditional GRG algorithm. Finally, the solution of the proposed MCP model is compared with the "standard" NR solution approach for a variety of small-, medium-, large-sized systems in order to examine the flexibility and robustness of this approach.

3.2 Optimization Formulation of the Power Flow Problem

Based on [106], the power flow analysis problem can be represented, as an MCP problem as follows:

$$\min \quad F(\varepsilon_p, \varepsilon_q) = \sum_i \left\{ {\varepsilon_p}_i^{\,2} + {\varepsilon_q}_i^{\,2} \right\} \tag{64}$$

$$\text{s.t.} \quad \Delta P_i(\delta, P_s, |V_D|, |V_G|, Q_G) - \varepsilon_{p_i} = 0 \qquad \forall i \in N \tag{65}$$

$$\Delta Q_i(\delta, P_s, |V_D|, |V_G|, Q_G) - \varepsilon_{q_i} = 0 \qquad \forall i \in N \quad (66)$$

$$|V_{G_i}| = |V_{Gi_0}| + V_{Ga_i} - V_{Gb_i} \qquad \forall i \in gen \quad (67)$$

$$0 \leq \left(Q_{G_i} - Q_{G_i}^{min}\right) \perp V_{Ga_i} \geq 0 \qquad \forall i \in gen \quad (68)$$

$$0 \leq \left(Q_{G_i}^{max} - Q_{G_i}\right) \perp V_{Gb_i} \geq 0 \qquad \forall i \in gen \quad (69)$$

$$|V_{G_i}|, V_{Ga_i}, V_{Gb_i} \geq 0 \qquad \forall i \in gen \quad (70)$$

where $\perp$ represents a complementarity condition, i.e., for $0 \leq a \perp b \geq 0, a = 0,$ if $b \geq 0,$ and $b = 0,$ if $a \geq 0$, which can be presented by: $ab = 0, a \geq 0, b \geq 0$. This optimization formulation comprises the set of nonlinear constraints (65) and (66) representing the power flow equations, where $|V_G|$ is treated as a variable, and a set of complementarity constraints given by (68) and (69), and associated constraints (67) and (70). This model includes the auxiliary variables V_{Ga} and V_{Gb} to track bus voltage magnitude variations, at generator and slack buses, when reactive power generation reaches limits as explained in more detail in Section 3.2.1. The objective is to minimize the total active and reactive power mismatches at all buses.

There may be multiple feasible solutions to the proposed optimization model (64)-(70), as there are up to 2^N solutions to a power flow problem [107], which may be found by varying the initial guess and utilizing different solution algorithms. All optimal solutions are mathematically acceptable, because they satisfy all the complementarity and power flow constraints imposed in the model; however, only one is typically adequate in practice.

Expressing the power flow problem as an optimization model presents greater flexibility, because it allows finding "partial" solutions and other types of constraints, such as voltage limits at buses, can be included to help find solutions to "non-converging" power flows. Furthermore, this formulation allows finding "critical" buses in the system, based on Lagrangian multipliers, for compensation purposes. Finally, the proposed MCP model always has a theoretically feasible solution since ε may not necessarily be zero, which could be useful for studying non-convergent power flow problems.

3.2.1 Complementarity Conditions to Model Reactive Power Limits

In [106], the following set of complementarity conditions is proposed in an OPF framework, to model the relationship between the reactive power generation Q_G and bus voltage magnitude $|V_G|$ at each "generator" bus, representing the effect of maximum and minimum limits on voltage control:

$$0 \leq \left(Q_{G_i} - Q_{G_i}^{min}\right) \perp V_{Ga_i} \geq 0 \qquad \forall i \in gen \quad (71)$$

$$0 \leq \left(Q_{G_i}^{max} - Q_{G_i}\right) \perp V_{Gb_i} \geq 0 \qquad \forall i \in gen \quad (72)$$

Here, the operator ⊥ denotes the following:

$$\left(Q_{G_i} - Q_{G_i}^{min}\right) V_{Ga_i} = 0 \qquad \forall i \in gen \quad (73)$$

$$\left(Q_{G_i} - Q_{G_i}^{min}\right) \geq 0 \qquad \forall i \in gen \quad (74)$$

$$V_{Ga_i} \geq 0 \qquad \forall i \in gen \quad (75)$$

$$\left(Q_{G_i}^{max} - Q_{G_i}\right) V_{Gb_i} = 0 \qquad \forall i \in gen \quad (76)$$

$$\left(Q_{G_i}^{max} - Q_{G_i}\right) \geq 0 \qquad \forall i \in gen \quad (77)$$

$$V_{Gb_i} \geq 0 \qquad \forall i \in gen \quad (78)$$

Equations (73)-(75) state that when Q_G is at its minimum limit, V_{Ga} can take a positive value, and similarly for (76)-(78), so that when Q_G is at its maximum limit, V_{Gb} can take a positive value. It is to be noted that (73) and (76) are complementarity conditions, and hence are not "active" simultaneously; therefore, it is not possible for both V_{Ga} and V_{Gb} to have positive values at the same time. The auxiliary variables V_{Ga} and V_{Gb} are, accordingly, used to affect the changes of the bus voltage magnitudes at the generator buses as follows:

$$|V_{G_i}| = |V_{Gi_0}| + V_{Ga_i} - V_{Gb_i} \qquad \forall i \in gen \quad (79)$$

This complementarity model properly represents a generator's voltage control system, since if V_{Ga_i} is positive and $V_{Gb_i} = 0$ for $Q_{G_i} = Q_{G_i}^{min}$, the corresponding bus voltage increases; on the other hand, if V_{Gb_i} is positive and $V_{Ga_i} = 0$ for $Q_{G_i} = Q_{G_i}^{max}$, the corresponding bus voltage decreases. In (73)-(79), the Q_G variables are independent of the auxiliary variables V_{Ga} and V_{Gb}.

Based on equations (73)-(79), the proposed MCP model (64)-(70) can be represented as follows:

$$\min \quad F(\varepsilon_p, \varepsilon_q) = \sum_i \left\{ {\varepsilon_p}_i^{\,2} + {\varepsilon_q}_i^{\,2} \right\} \tag{80}$$

$$\text{s.t.} \quad \Delta P_i(\delta, P_s, |V_D|, |V_G|, Q_G) - \varepsilon_{p_i} = 0 \qquad \forall i \in N \tag{81}$$

$$\Delta Q_i(\delta, P_s, |V_D|, |V_G|, Q_G) - \varepsilon_{q_i} = 0 \qquad \forall i \in N \tag{82}$$

$$|V_{G_i}| - |V_{Gi_0}| - V_{Ga_i} + V_{Gb_i} = 0 \qquad \forall i \in gen \tag{83}$$

$$\left(Q_{G_i} - Q_{G_i}^{min}\right) V_{Ga_i} = 0 \qquad \forall i \in gen \tag{84}$$

$$\left(Q_{G_i}^{max} - Q_{G_i}\right) V_{Gb_i} = 0 \qquad \forall i \in gen \tag{85}$$

$$\left(Q_{G_i} - Q_{G_i}^{min}\right) \geq 0 \qquad \forall i \in gen \tag{86}$$

$$\left(Q_{G_i}^{max} - Q_{G_i}\right) \geq 0 \qquad \forall i \in gen \tag{87}$$

$$|V_{G_i}|, V_{Ga_i}, V_{Gb_i} \geq 0 \qquad \forall i \in gen \tag{88}$$

3.3 Newton-Raphson as an MCP Solution Step

This section presents an in-depth explanation of the differences between the proposed optimization-based power flow method and the standard NR-based power flow solution approach. In [24], Carpentier discusses the use of NR to solve the corrector step equations of the GRG method applied to the "classical" OPF problem. A similar approach is used here in order to demonstrate that the solution of the MCP power flow model (64)-(70), which is *not* a standard OPF problem, basically corresponds to the NR solution of the power flow equations (65) and (66) for $\varepsilon_p = \varepsilon_q = 0$. Thus, this section explains why the power flow solvers do not converge in some cases. To demonstrate this, first the GRG method is applied to the power flow problem where the generator bus voltage magnitudes are fixed and the complementarity constraints are ignored, demonstrating that the standard NR-based power flow solution method is just a particular step of the GRG approach applied to a simplified version of the proposed optimization method. The complementarity constraints are subsequently included in the analysis to properly represent generator voltage controls and reactive power limits, proposing a possible extension to the existing NR-based approach to better compare the power flow solution process for practical

applications. Observe that such a perspective on power flow problems is not available in the power system literature to the best of our knowledge.

First, the GRG method of solution of the optimization model considering only constraints (65) and (66) is compared with the NR method. Thus, Let the proposed MCP model be written as follows, for $|V_G| = |V_{G_0}|$:

$$\min F(\varepsilon) \tag{89}$$

$$\text{s.t. } f(x,\varepsilon) = f\,(z) = \begin{bmatrix}\Delta P(\delta, P_s, |V_D|, Q_G, \varepsilon)\\ \Delta Q(\delta, P_s, |V_D|, Q_G, \varepsilon)\end{bmatrix} = 0 \tag{90}$$

where the optimization variables z are divided into power flow variables x and mismatch variables ε, as follows:

$$x = \begin{bmatrix}\delta\\ P_S\\ |V_D|\\ Q_G\end{bmatrix},\ \varepsilon = \begin{bmatrix}\varepsilon_p\\ \varepsilon_q\end{bmatrix} \tag{91}$$

Then, in order to solve (89)-(90) using the GRG method, the following two steps are required [108]:

1. *Predictor Step*: Assuming that there is a set of values for z satisfying the constraints $f(z) = 0$, say $z^m = (x^m, \varepsilon^m)$, this "guess" can be improved by moving in the direction of the steepest descent, resulting in $z^{m+1} = (x^{m+1}, \varepsilon^{m+1})$ as follows:

$$z^{m+1} = z^m + \beta s^m \tag{92}$$

where s^m is the step calculated by the gradient of $F(\varepsilon)$ as follows:

$$s^m = -MM^T \nabla_z F(\varepsilon^m) \tag{93}$$

$$M = \begin{bmatrix}-[D_x f(z^m)]^{-1}\, D_\varepsilon f(z^m)\\ I_{2N}\end{bmatrix}_{(2N+2N)\times 2N} \tag{94}$$

and $\beta > 0$ is a scalar for step-size adjustment such that $F(\varepsilon^{m+1}) < F(\varepsilon^m)$.

2. *Corrector Step:* The predicted value of z^{m+1} should then be corrected to ensure it satisfies the constraints $f\,(z) = 0$. This can be done by the following robust NR procedure to obtain a $z^* = (x^*, \varepsilon^{m+1})$ such that $f\,(z^*) = 0$:

$$x^{k+1} = x^k - \alpha[D_x f(x^k, \varepsilon^{m+1})]^{-1} f(x^k, \varepsilon^{m+1}) \tag{95}$$

where $x^k = x^{m+1}$ obtained from (92), and the scalar $\alpha > 0$ is used to ensure convergence. The iteration k is repeated until convergence is obtained, i.e., until z^* is found. These predictor and corrector steps are repeated until $F(\varepsilon)$ is "close" to zero.

Observe that (95) is exactly the same as (39) for $\varepsilon = 0$. Thus, it can be readily concluded that the NR method applied to the solution of power flow equations (1) and (2), basically corresponds to the corrector step of the GRG method applied to the solution of the optimization model (89)-(90).

Now, let rewrite the proposed MCP model as follows:

$$\min \quad F(\varepsilon) \tag{96}$$

$$\text{s.t} \quad g(\hat{x}, \varepsilon) = \begin{bmatrix} f(x, y, \varepsilon) \\ h(x, y, \varepsilon) \end{bmatrix} = 0 \tag{97}$$

$$\hat{g}(x, y) \geq 0 \tag{98}$$

where $f(x, y, \varepsilon)$ represents the equality constraints (81) and (82); $h(x, y, \varepsilon)$ represents the equality constraints (83)-(85); $\hat{g}(x, y)$ corresponds to the inequality constraints (86)-(88); and $\hat{x}$ is a vector of dependent variables defined as:

$$\hat{x} = \begin{bmatrix} x \\ - \\ y \end{bmatrix} = \begin{bmatrix} \delta \\ P_S \\ |V_D| \\ Q_G \\ \hline |V_G| \\ V_{Ga} \\ V_{Gb} \end{bmatrix} \tag{99}$$

Therefore, the predictor and corrector steps of the GRG method can be stated as follows, considering that ε is a set of independent variables:

1. Predictor Step:

$$z^{m+1} = z^m + \beta s^m \tag{100}$$

$$s^m = -MM^T \nabla_z F(\varepsilon^m) \tag{101}$$

$$\begin{bmatrix} -[D_{\hat{x}}\, g(z^m)]^{-1}\, D_\varepsilon g(z^m) \\ I_{2N} \end{bmatrix}_{(2N+2N+3N_G)\times(2N+3N_G)} \tag{102}$$

where $z = (x, y, \varepsilon)$, and β is a scalar chosen so that $F(\varepsilon^{m+1}) < F(\varepsilon^m)$ and $\hat{g}(\hat{x}^{m+1}) = \hat{g}(x^{m+1}, y^{m+1}) \geq 0$.

2. *Corrector Step*:

$$\hat{x}^{k+1} = \hat{x}^k - \alpha[D_{\hat{x}} g(\hat{x}^k, \varepsilon^{m+1})]^{-1} g(\hat{x}^k, \varepsilon^{m+1}) \tag{103}$$

where α is chosen to ensure convergence, and guarantee that $\hat{g}\left(\hat{x}^{k+1}\right) = \hat{g}(x^{k+1}, y^{k+1}) \geq 0$.

Note that (103), for $\varepsilon = 0$, can be considered basically a "new" NR solution procedure to solve the power flow problem that properly models the generator voltage controls, since it accounts for the generator reactive power limits and its terminal voltage recovery. Some commercially available solvers that use a variety of numerical techniques to solve optimization problems, such as the NLP formulation (64)-(70), including the aforementioned GRG method, and their performance for various test-systems are discussed in the next section.

3.4 Results and Discussions

3.4.1 Base Model

The proposed mathematical model (64)-(70) is coded in the General Algebraic Modeling System (GAMS) programming platform [109]. The model is tested considering the IEEE 14-bus, 30-bus, 57-bus, 118-bus and 300-bus test systems and real 1211-bus and 2975-bus systems using the power flow optimization model (80)-(88). The 1211-bus system has 312 generators and 447 loads, 1143 lines, 622 fixed transformers; and the 2975-bus system has 374 generators, 874 loads, 273 shunts, 2146 lines and 1411 transformers. A flat start is used in all cases since this is known to yield convergence problems in "standard" NR-based power flow solvers as the system size increases. This was indeed the case when using the robust NR-based power flow program UWPFLOW [110] DSAT [111] to solve the large practical systems from a flat start.

The solvers used for the studies shown here are: (1) MINOS [105], which is a GRG-based solver; (2) PATH-NLP, a PATH-based solver; and (3) COINIPOPT, an interior-point solver. All solvers have their parameters set at their respective default, off-the-shelf settings, so as not to bias their "standard" performance. Major settings such as tolerance level or maximum number of iterations of the solver are by default the same for all solvers (e.g., feasibility tolerance is 10^{-6}). The large execution times for the large systems in Tables I to III can be attributed in part to the overhead and non-optimality of the code used to solve the MCP model using GAMS.

The results presented in Table I show the total execution time required to solve each test-system with various solvers in GAMS. Observe that for the small 14-bus, 30-bus and the 57-bus systems, and medium 118-bus and 300-bus systems, feasible and locally optimal solutions are attained in a few seconds, with all the different methods considered. However, the larger 1211-bus and 2975-bus systems are only solved by the IP method, which is a barrier method that generates a sequence of strictly feasible iterates lying in the interior of the feasible region. The GRG-based solver is only able to solve the test systems up to the 300-bus system, and does not converge for larger systems as expected, given the well-known poor convergence characteristics of this method. The PATH-based method shows reasonably good convergence for systems up to 1211-bus; however, it fails to arrive at an optimal solution for the 2975-bus system. In all the convergent cases, the objective function $F(\varepsilon)$ did not exceed a value of 10^{-7},thus showing that a

Table I
EXECUTION TIME FOR POLAR FORM MCP POWER FLOW MODEL

System	Interior-point Method (s)	Path Method(s)	GRG-Based Method(s)
14-bus	0.125	0.083	0.078
30-bus	0.063	0.145	0.188
57- bus	0.275	0.109	0.516
118-bus	0.615	0.625	8.02
300-bus	5.187	5.5	4.047
1211-bus	23.297	71.265	Non-convergent
2975-bus	162.301	Non-convergent	Non-convergent

proper solution of the power flow equations was obtained.

Some of the NLP methods and associated solvers failed to yield a solution in some cases. This is due to the non-convex characteristics of the MCP model, as well as possible non-strict solutions of the complementarity constraints, which makes the problem numerically hard to solve.

The MCP solutions obtained for the IEEE test systems match closely the power flow solutions reported by the standard NR-based power flow solution approach, and the solutions for the real systems are basically the same as those obtained with commercial-grade power flow solvers, UWPFLOW and DSAT. Hence, these solutions can be considered to be “adequate in practice”.

Table II

EXECUTION TIME FOR RECTANGULAR FORM MCP POWER FLOW MODEL

System	Interior-point Method(s)	Path-Based Method(s)	GRG-Based Method(s)
14-bus	0.156	0.078	0.047
30-bus	0.392	0.039	0.141
57- bus	1.296	0.078	0.344
118-bus	10.665	0.39	1.359
300-bus	8.812	3.687	Non-convergent
1211-bus	94.907	28.39	Non-convergent
2975-bus	381.025	Non-convergent	Non-convergent

Table III

CONVERGENCE TIME WITH DIFFERENT BUS VOLTAGE LIMITS, USING INTERIOR-POINT METHOD IN POLAR FORM

System	Bus voltage limits [0.8, 1.2] (s)	Bus voltage limits [0.9, 1.1] (s)
14-bus	0.156	0.109
30-bus	0.079	0.074
57- bus	2.301	0.625
118-bus	4.451	1.764
300-bus	17.547	5.797
1211-bus	644.761	44.172
2975-bus	225.016	419.922

3.4.2 Flexibility of the Proposed Model

It is important to highlight the flexibility and adaptability of the proposed model, which easily accommodates other forms of power flow representations. For example, power flow analysis in rectangular coordinates, where the voltage phasor is represented as a complex number, can be carried out without the need for extensive software coding. Thus, Table II summarizes the results of representing the power flow equations in rectangular coordinates. Observe the faster convergence for the GRG-based and PATH-based solvers. For instance, for the IEEE 118-bus system, the GRG-based solver converges after 1.359 seconds, while it takes 8.02 seconds for the polar form model (Table I). Furthermore, the PATH-based solver now converges for larger test systems, such as the 1211-bus system in 28.39 seconds, while it takes 71.265 seconds to converge in polar form. On the other hand, the interior-point-based solver shows worse performance with the rectangular form model, with a significant increase in the execution time.

Other advantage of the proposed MCP optimization formulation of the power flow problem is its ability to incorporate system constraints such as bus voltage limits to guarantee the quality of the solution. Thus, observe in Table III, that imposing voltage limits [0.8,1.2] and [0.9,1.1] allows the solver to attain a feasible solution with the polar form. Considering the limits for the voltages reduces the feasible search area, resulting in a better search direction to find a feasible solution.

Finally, different loading conditions have been tested to demonstrate the flexibility of the model. For instance, when real power demand is increased to 91.6 MW from 21.7 MW at Bus 2 for the 30-bus test system, the standard NR method fails to obtain a solution, while the MCP model yields a power flow solution under the same loading conditions while maintaining bus voltages within 0.95 and 1.05 at all buses, thus meeting the voltage constraints considered in this case. On another test for the same system, the standard NR solution approach fails to obtain a solution when reactive power demand is increased to 150 MVAR at Bus 21, whereas the MCP model yields a solution with a reactive power mismatch at this bus of ε_q=0.059, being the largest mismatch of all power flow mismatch equations, which signals to the operator that reactive power support is needed at that bus. These types of analyses are not feasible with a standard power flow formulation.

In order to test the quality of the final converged solutions for bus voltage magnitudes, a parameter, “Voltage Quality Index” (VQI) is defined for each test system as follows:

$$VQI = \frac{1}{N}\sum_{i=1}^{N}\left||V_i| - V_0\right| \tag{104}$$

where V_0 is the desired bus voltage magnitude of 1.0 p.u. and $|V_i|$ is the converged bus voltage magnitude, using either the proposed MCP formulation or the standard NR-based power flow solution approach. Note that a better value of this index means less loss and reactive power flows in the system, thus it is an adequate means for judging the quality of the solution. Table IV depicts the *VQI* values for all test systems; observe that *VQI* is very small in all cases, but this index is smaller for large systems when using the proposed MCP method than when using the standard NR-based power flow solution approach. Thus, it can be argued that the quality of the solutions obtained by the MCP formulation is somewhat superior to the standard NR-based approach for large systems.

Table IV
COMPARISON OF VOLTAGE QUALITY INDEX USING DIFFERENT METHODS

System	Proposed MCP based Power Flow, using IP	NR Power Flow solution approach
14-bus	0.04847	0.04864
30-bus	0.02986	0.02983
57-bus	0.02395	0.02370
118-bus	0.02268	0.02277
300-bus	0.02713	0.02555
1211-bus	0.03597	0.03685
2975-bus	0.00751	0.05981

3.4.3 Robustness

The proposed model is said to be robust when a feasible and practical solution is obtained, regardless of the choice of initial guess. The robustness of the model is based on the premise that the proposed MCP formulation leads to converged power flow solutions with flat-starts, when standard power flow solution methods are not able to do so. Therefore, since the proposed MCP leads to a converged solution with flat-starts for the large, real 1211-bus and 2975-bus systems, it is argued that the proposed method is robust.

In order to evaluate the convergence performance of the proposed MCP model in terms of iterations, a comparison is made between the PATH-based solver using the proposed MCP model and the robust NR-based power flow solvers. As shown in Table V, the performance of the MCP solver for small and medium sized systems is very close to the performance of the power flow solvers. However, as shown in this table and Figure 1, the proposed method converges to the solution from a flat start for large systems, while the power flow solvers do not converge in these cases.

It should be mentioned that restating the power flow problem as the proposed optimization model, allows the use of more sophisticated and robust optimization solution approaches. For example, trust-region methods, which are shown to be quite robust for the solution of a variety of OPF-based problems can be used to obtain solutions of non-converging power flow cases.

Table V
ITERATION COMPARISON OF THE PROPOSED MCP MODEL

System	Proposed MCP based Power Flow	NR Power Flow
IEEE 14-bus	3	3
IEEE 30-bus	3	4
IEEE 57-bus	6	5
IEEE 118-bus	9	5
IEEE 300-bus	12	10
1200-bus	12	Non-convergent
Real 2975-bus	147	Non-convergent

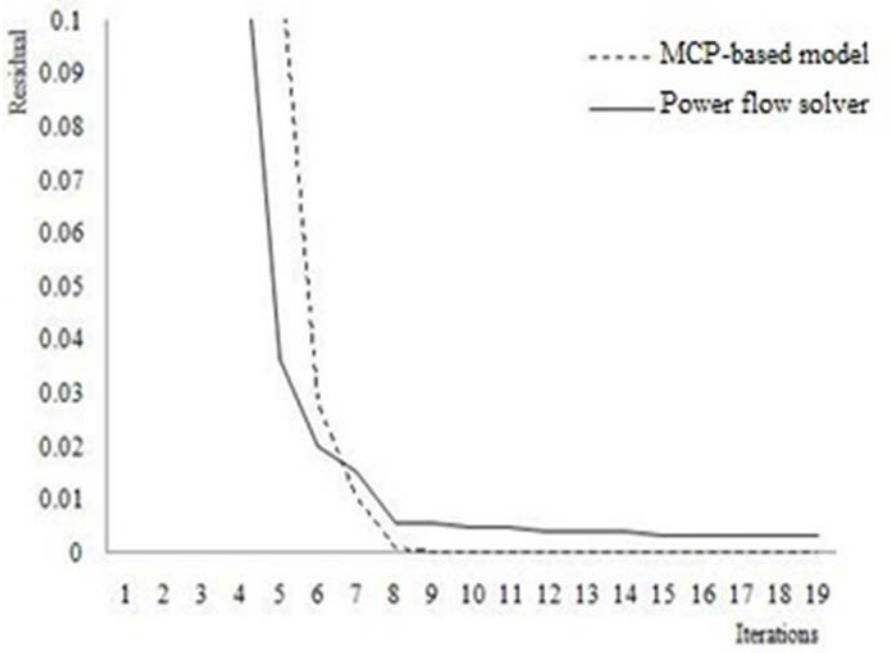

Figure 1: Convergence performance of proposed MCP formulation compared to a robust NR-based solver for the 1211-bus system

3.5 Summary

In this Chapter, a novel MCP model has been proposed to solve the power flow problem. This model is used to demonstrate that the NR-based iteration procedure is basically a step of the GRG method applied to the solution of the proposed MCP model. The optimization is shown to have numerous benefits such as, ease of implementation, flexibility and more importantly, robustness. Thus numerical results show that the proposed optimization method converges when a robust NR-based power flow solver fails to converge for large systems. The proposed model is now applied to power flow studies of systems with uncertain parameters, based on the AA techniques.

CHAPTER 4

AN AFFINE ARITHMETIC APPROACH TO THE POWER FLOW PROBLEM USING MCP FORMULATION

4.1 Introduction

In this chapter, the optimization framework, proposed in Chapter 3 is applied to a power flow problem under uncertainty using the AA-based approach in order to obtain the operational ranges for power flow variables. The associated uncertainties could be internal such as approximation error or external such as forecasting error (e.g., demand, generation and weather forecast). The proposed AA algorithm is tested on a 14-bus test system and its results are then compared with the MCS results. The AA method shows slightly more conservative bounds, however it is faster and does not need any information for statistical distributions of random variables.

4.2 AA Forms of Power Flow Variables in AA Form

All the state variables associated with the proposed optimization based power flow model (e.g., the bus voltage magnitude and the voltage angle in polar form or real and imaginary components of bus voltage in rectangular form) are stated in affine form with a center value and noise magnitudes. Center values represent the value of a variable considering the given deterministic case, i.e., when uncertainties are neglected; and noise magnitudes represent deviations of the power flow variables due to the uncertainties. There is also a noise error (ε) associated with each noise magnitude.

4.2.1 Calculating Affine Real and Imaginary Bus Voltage Components

If the sources of uncertainties are assumed to be the real and reactive power injections, the affine forms of the real and imaginary components of the bus voltage magnitude ($\tilde{e}_i$ and $\tilde{f}_i$) can be presented as follows:

$$\tilde{e}_i = e_{i,0} + \sum_{j \epsilon N} e_{i,j}^{P}\, \varepsilon_{P_j^D} + \sum_{j \epsilon N} e_{i,j}^{Q}\, \varepsilon_{Q_j^D} \qquad \forall i \in N \quad (105)$$

$$\tilde{f}_i = f_{i,0} + \sum_{j \epsilon N} f_{i,j}^{P} \, \varepsilon_{P_j^D} + \sum_{j \epsilon N} f_{i,j}^{Q} \, \varepsilon_{Q_j^D} \qquad \forall i \in N \quad (106)$$

where:

$e_{i,0}$ is the center value of the real component of bus voltage at bus *i*;

$f_{i,0}$ is the center value of the imaginary component of bus voltage at bus *i*;

$e_{i,j}^{P}$ is the partial deviation of the real component of bus voltage at bus *i* due to the active power injection at bus *j*

$f_{i,j}^{P}$ is the partial deviation of the imaginary component of bus voltage at bus *i* due to the active power injection at bus *j*

$e_{i,j}^{Q}$ is the partial deviation of the real component of bus voltage at bus *i* due to the reactive power injection at bus *j*

$f_{i,j}^{Q}$ is the partial deviation of the imaginary component of bus voltage at bus *i* due to the reactive power injection at bus *j*

$\varepsilon_{P_j^D}$ is the uncertainty associated with the active power injection at bus *j*

$\varepsilon_{Q_j^D}$ is the uncertainty associated with the reactive power injection at bus *j*

Center values of the power flow variables are calculated by the proposed MCP, where active power demand (P_i^D) and reactive power demand (Q_i^D) parameters at each bus *i* are specified by considering the center of the given intervals for lower and upper bounds of P_i^D and Q_i^D as follows:

$$P_i^D = \left(\overline{P}_i^D + \underline{P}_i^D\right)\Big/_2 \qquad \forall i \in nP \quad (107)$$

$$Q_i^D = \left(\overline{Q}_i^D + \underline{Q}_i^D\right)\Big/_2 \qquad \forall i \in nQ \quad (108)$$

In order to find the partial deviations, a sensitivity analysis technique is used in which P_j^D is perturbed at buses with sources of uncertainty, while it is fixed at its initial values at the other buses. Solving the power flow model (80)-(88) with the modified parameter P_j^D, the new values for real and imaginary components of bus voltage magnitudes e_i^N and f_i^N are obtained. Subtracting the new values from the ones obtained from solving the deterministic power flow problem provides the partial deviation of variables due to changes in real power demand at bus *j* as follows:

$$e_{i,j}^{P} = e_{i}^{N} - e_{i,0} \qquad \forall i,j \in N \qquad (109)$$

$$f_{i,j}^{P} = f_{i}^{N} - f_{i,0} \qquad \forall i,j \in N \qquad (110)$$

4.2.2 Affine Real and Reactive Power Calculations

Affine real power injection $\tilde{P}$ is obtained using the affine real and imaginary bus voltage and current components and affine operations. Two different methods are used to calculate the affine reactive power injection $\tilde{Q}$ in the proposed affine power flow problem. One calculates the affine reactive power injection, using the obtained $\tilde{e}_i$ and $\tilde{f}_i$ from the MCP model and affine and non-affine operations, explained in Chapter 2. The other method calculates the affine reactive power injection as the by-product of the MCP model, the same way that $\tilde{e}_i$ and $\tilde{f}_i$ are calculated. Both methods take into consideration the reactive power generation limits by not violating them because they employ the MCP model in their solution method, which inherently consider the given limits by considering the complementarity conditions. However, the former method has the advantage of calculating the internal errors associated with non-affine operations.

1) Affine real and reactive power calculation using affine operations

In order to find the affine form of the real and reactive power, affine representation of the real and imaginary components of bus currents have to be found. Calculating the affine form of the real and imaginary components of bus voltage in (109) and (110), the affine form of the bus current is obtained by knowing the followings:

$$\tilde{I} = Y\,\tilde{V} \qquad (111)$$

$$\tilde{I} = (G + jB)(\tilde{e} + j\tilde{f}) \qquad (112)$$

Therefore the real and imaginary values for bus current are calculated as follows:

$$\tilde{I}_r = G\tilde{e} - B\tilde{f} \qquad (113)$$

$$\tilde{I}_{im} = G\tilde{f} + B\tilde{e} \qquad (114)$$

where $\tilde{I}_r$ and $\tilde{I}_{im}$ have the affine forms as shown in (115) and (116).

$$\tilde{I}_{r_i} = I_{r_{i,0}} + \sum_{j \epsilon N} I_{r_{i,j}}^{P}\,\varepsilon_{P_j^D} + \sum_{j \epsilon N} I_{r_{i,j}}^{Q}\,\varepsilon_{Q_j^D} \qquad \forall i \in N \quad (115)$$

$$\tilde{I}_{im_i} = I_{im,0} + \sum_{j \epsilon N} I_{im_{i,j}}^{P}\,\varepsilon_{P_j^D} + \sum_{j \epsilon N} I_{r_{i,j}}^{Q}\,\varepsilon_{Q_j^D} \qquad \forall i \in N \quad (116)$$

Note that the real and imaginary components of current share the same sources of uncertainties, i.e., real and reactive power injection.

Furthermore, using the affine and non-affine operations, and the affine forms $\tilde{e}_i$, $\tilde{f}_i$, $\tilde{I}_{r_i}$ and $\tilde{I}_{im_i}$, the real and reactive power $\tilde{P}_i$and $\tilde{Q}_i$ are calculated as presented in (117) and (118):

$$\tilde{P} = \tilde{e}\,\tilde{I}_r + \tilde{f}\,\tilde{I}_{im} \tag{117}$$

$$\tilde{Q} = \tilde{f}\,\tilde{I}_r - \tilde{e}\,\tilde{I}_{im} \tag{118}$$

where $\tilde{P}_i$ and $\tilde{Q}_i$ have the following affine forms, with center value and associated partial deviations:

$$\tilde{P}_i = P_{i,0} + \sum_{j\epsilon N} P_{i,j}^P\,\varepsilon_{P_j^D} + \sum_{j\epsilon N} P_{i,j}^Q\,\varepsilon_{Q_j^D} + P_i^T\varepsilon_{T_i} \qquad \forall i \in N \tag{119}$$

$$\tilde{Q}_i = Q_{i,0} + \sum_{j\epsilon N} Q_{i,j}^P\,\varepsilon_{P_j^D} + \sum_{j\epsilon N} Q_{i,j}^Q\,\varepsilon_{Q_j^D} + Q_i^T\varepsilon_{T_i} \qquad \forall i \in N \tag{120}$$

The center values, $P_{i,0}$ and $Q_{i,0}$; partial deviations, $P_{i,j}^P$ and $Q_{i,j}^P$; and truncation errors P_i^T and Q_i^T are calculated as follows:

$$P_{i,0} = e_{i,0}\,I_{r_{i,0}} + f_{i,0}\,I_{im_{i,0}} \qquad \forall i \in N \tag{121}$$

$$Q_{i,0} = f_{i,0}\,I_{r_{i,0}} - e_{i,0}\,I_{im_{i,0}} \qquad \forall i \in N \tag{122}$$

$$P_{i,j}^P = e_{i,0}\,I_{r_{i,j}}^P + I_{r_{i,0}}\,e_{i,j}^P + f_{i,0}\,I_{im_{i,j}}^P + I_{im_{i,0}}\,f_{i,j}^P \qquad \forall i,j \in N \tag{123}$$

$$Q_{i,j}^P = f_{i,0}\,I_{r_{i,j}}^P + I_{r_{i,0}}\,f_{i,j}^P - e_{i,0}\,I_{im_{i,j}}^P - I_{im_{i,0}}\,e_{i,j}^P \qquad \forall i,j \in N \tag{124}$$

$$P_i^T = \sum_j \left|e_{i,j}^P\right| \sum_j \left|I_{r_{i,j}}^P\right| + \sum_j \left|f_{i,j}^P\right| \sum_j \left|I_{im_{i,j}}^P\right| \qquad \forall i \in N \tag{125}$$

$$Q_i^T = \sum_j \left|f_{i,j}^P\right| \sum_j \left|I_{r_{i,j}}^P\right| - \sum_j \left|e_{i,j}^P\right| \sum_j \left|I_{im_{i,j}}^P\right| \qquad \forall i \in N \tag{126}$$

In the above equations, the noise magnitudes related to reactive power deviations $P_{i,k}^Q$ and $Q_{i,k}^Q$ are ignored, as the reactive power generation is assumed to be zero, and therefore the associated noise magnitudes are zero. The formulation presented in (125) and (126) is the most conservative and computationally efficient method to calculate the magnitude of the internal errors P_i^T and Q_i^T, related to non-affine calculations. This method simply uses the product of the absolute value of the external noise magnitudes. There are other methods to calculate the magnitude of internal error in which the obtained range could be smaller; however they need more computational effort.

In order to find the minimum amount of the noise variables and therefore obtaining narrower AA-based solution intervals, a noise contraction algorithm is used [5]. For this purpose, the obtained affine form (119) and (120) is rearranged in matrix-vector form as follows:

$$\begin{bmatrix} \tilde{P}_1 \\ \dots \\ \tilde{P}_N \\ \tilde{Q}_1 \\ \dots \\ \tilde{Q}_N \end{bmatrix} = \begin{bmatrix} P_{1,0} \\ \dots \\ P_{N,0} \\ Q_{1,0} \\ \dots \\ Q_{N,0} \end{bmatrix} + \begin{bmatrix} P_{1,1}^P & P_{1,2}^P & \cdots & P_{1,N}^P \\ \dots & \dots & \dots & \dots \\ P_{N,1}^P & P_{N,2}^P & \cdots & P_{N,N}^P \\ Q_{1,1}^P & Q_{1,2}^P & \cdots & Q_{1,N}^P \\ \dots & \dots & \dots & \dots \\ Q_{N,1}^P & Q_{N,2}^P & \cdots & Q_{N,N}^P \end{bmatrix} \begin{bmatrix} \varepsilon_{P_1^D} \\ \dots \\ \varepsilon_{P_N^D} \end{bmatrix} + \begin{bmatrix} P_{1,1}^Q & P_{1,2}^Q & \cdots & P_{1,N}^Q \\ \dots & \dots & \dots & \dots \\ P_{N,1}^Q & P_{N,2}^Q & \cdots & P_{N,N}^Q \\ Q_{1,1}^Q & Q_{1,2}^Q & \cdots & Q_{1,nPQ}^Q \\ \dots & \dots & \dots & \dots \\ Q_{nPQ,1}^Q & Q_{nPQ,2}^Q & \cdots & Q_{nPQ,nPQ}^Q \end{bmatrix} \begin{bmatrix} \varepsilon_{Q_1^D} \\ \dots \\ \varepsilon_{Q_N^D} \end{bmatrix} + \begin{bmatrix} P_1^T \\ \dots \\ P_N^T \\ Q_1^T \\ \dots \\ Q_N^T \end{bmatrix} \cdot \begin{bmatrix} \varepsilon_{T_1} \\ \dots \\ \varepsilon_{T_N} \\ \varepsilon_{T_{N+1}} \\ \dots \\ \varepsilon_{T_{2N}} \end{bmatrix} \tag{127}$$

The above equation is represented in the following general form:

$$\tilde{f}(x) = A_0 + Ax_\varepsilon + B_T.x_T \tag{128}$$

where:

$\tilde{f}(x)$ is the power flow equations in affine form.

A_0 is the vector of center values.

A is the matrix of partial deviations.

x_ε is the vector of external uncertainties.

B_T is the vector of internal noise magnitude associated with non-affine operations.

x_T is the vector of noise variables associated with non-affine operations.

In (128), x_T varies in the interval [-1,1], and since it represents the noises associated with non-affine operations, it cannot be contracted, therefore the largest value and the smallest value of the range, i.e., 1.00 and -1.00 are considered for $\varepsilon_{T_i}^{Max}$and $\varepsilon_{T_i}^{Min}$ accordingly. Hence the affine

equation (128) is converted to an interval form with the upper bound $\overline{f}(x)$ and lower bound $\underline{f}(x)$ as follows:

$$\overline{f}(x) = Ax^{Max} + B1 \quad (129)$$

$$\underline{f}(x) = Ax^{Min} + B2 \quad (130$$

where:

x^{Max} is the vector of maximum noise variables associated with the real and reactive power injection.

x^{Min} is the vector of minimum noise variables associated with the real and reactive power injection.

$\overline{f}(x)$ is the vector of maximum value of real and reactive power injections

$\underline{f}(x)$ is the vector of minimum value of real and reactive power injections

$B1$ is the vector of center values plus the noise magnitude value for the affine operation error as shown (131).

$B2$ is the vector of center values minus the noise magnitude for the affine operation error as shown in (131).

$$B1 = \begin{bmatrix} P_{1,0} \\ \cdots \\ P_{N,0} \\ Q_{1,0} \\ \cdots \\ Q_{nPQ,0} \end{bmatrix} + \begin{bmatrix} P_1^T \\ \cdots \\ P_N^T \\ Q_1^T \\ \cdots \\ Q_{nPQ}^T \end{bmatrix} \quad \& \quad B2 = \begin{bmatrix} P_{1,0} \\ \cdots \\ P_{N,0} \\ Q_{1,0} \\ \cdots \\ Q_{nPQ,0} \end{bmatrix} - \begin{bmatrix} P_1^T \\ \cdots \\ P_N^T \\ Q_1^T \\ \cdots \\ Q_{nPQ}^T \end{bmatrix} \quad (131)$$

The above equations (129) and (130) are as follows for the real and reactive power upper and lower bounds:

$$\overline{P}_i = P_{i,0} + \sum_j P_{i,j}^P \, \varepsilon_{P_j}^{Max} + \sum_j P_{i,j}^Q \, \varepsilon_{Q_j}^{Max} + P_i^T \qquad \forall i \in N \quad (132)$$

$$\underline{P}_i = P_{i,0} + \sum_j P_{i,j}^P \, \varepsilon_{P_j}^{Min} + \sum_j P_{i,j}^Q \, \varepsilon_{Q_j}^{Min} - P_i^T \qquad \forall i \in N \quad (133)$$

$$\overline{Q}_i = Q_{i,0} + \sum_j Q_{i,j}^P \, \varepsilon_{P_j}^{Max} + \sum_j Q_{i,j}^Q \, \varepsilon_{Q_j}^{Max} + Q_i^T \qquad \forall i \in N \quad (134)$$

$$\underline{Q_i} = Q_{i,0} + \sum_j Q_{i,j}^P \, \varepsilon_{P_j}^{Min} + \sum_j Q_{i,j}^Q \, \varepsilon_{Q_j}^{Min} - Q_i^T \qquad \forall i \in N \quad (135)$$

where:

$\overline{P}_i$ and $\overline{Q}_i$ are the maximum values of real and reactive power at bus i;

$\underline{P_i}$ and $\underline{Q_i}$ are the minimum values of real and reactive power at bus i;

$\varepsilon_{P_j}^{Min}$ is the minimum uncertainty associated with the real power injection at bus j

$\varepsilon_{Q_j}^{Min}$ is the minimum uncertainty associated with the reactive power injection at bus j

$\varepsilon_{P_j}^{Max}$ is the maximum uncertainty due to real power injection at bus j

$\varepsilon_{Q_j}^{Max}$ is the maximum uncertainty due to reactive power injection at bus j

In (129) and (130), $\overline{f}(x)$ and $\underline{f}(x)$ are already known, as they are the input intervals to the power flow problem. The matrix A is calculated by the sensitivity analysis technique and $B1$ and $B2$ vectors are known by calculating the center values and internal error noise magnitude. Hence the only variables are x^{Max} and x^{Min} which are found by the following LP models:

$$\begin{aligned} \min \quad & \sum_i \varepsilon_{P_i}^{Min} \\ \text{s.t.} \quad & -1 \le \varepsilon_P^{Min} \le 1 \\ & \underline{f}(x) \le A \, \varepsilon_P^{Min} + B2 \end{aligned} \qquad (136)$$

$$\begin{aligned} \max \quad & \sum_i \varepsilon_{P_i}^{Max} \\ \text{s.t.} \quad & -1 \le \varepsilon_P^{Max} \le 1 \\ & A \, \varepsilon_P^{Max} + B1 \le \overline{f}(x) \end{aligned} \qquad (137)$$

LP models (136) and (137) can be easily solved using the available LP solvers, such as CPLEX. Furthermore, ε_P^{Max} and ε_P^{Min} are used to find the real and reactive power intervals as formulated in (132), (133), (134) and (135) and also real and imaginary components of bus voltage as shown in (105) and (106).

2) Affine reactive power calculation as the by-product of the MCP model

Another method to calculate the affine reactive power injection (120) is using the MCP model directly. This approach calculates $\tilde{Q}$ with the same method proposed for calculating $\tilde{e}$ and $\tilde{f}$. It uses the MCP model with the given values for demand to find the center values and then employs

the sensitivity analysis technique to calculate the partial deviations. In order to find the intervals the contraction method is used as previously was explained.

4.3 Numerical Results

In this section, the AA and the MCS methods are both tested on a power flow analysis problem using the IEEE 14-bus system, shown in Figure 2. The uncertainties are assumed to be real and reactive power injection, because of real and reactive power demand variations, caused by "forecast error". A constant power factor is assumed to consider the same proportion of changes in real and reactive power demand. The proposed model is simulated in General Algebraic Modeling System (GAMS).

The implemented MCS method has 3000 iterations, and uses uniform distribution, which is assumed to yield a reliable solution interval [5]. The real and reactive power demands are randomly selected from the input interval, which is in the 10% range of the given demand. The proposed MCP problem is solved to obtain the power flow variables, such as bus voltage magnitude, in each MCS iteration and then the maximum value amongst all the iterations is considered to be the upper bound and the minimum value is considered to be the lower bound. It is noted that increasing the number of iterations in the MCS method does not improve the associated bounds.

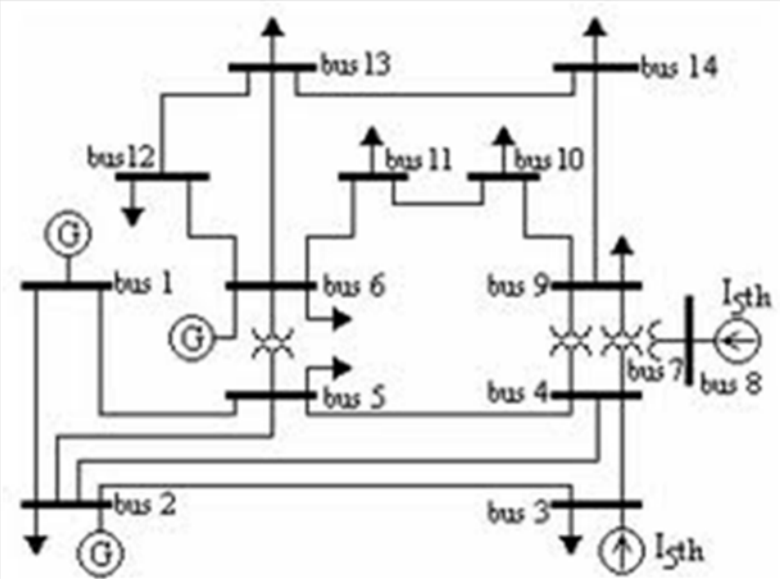

Figure 2: IEEE 14 bus test system [112]

The proposed AA-based method is applied to the IEEE 14-bus system [112] with the same conditions and the same input intervals (10% deviation of the given real and reactive power demands). The center values are obtained by running the MCP model with the deterministic data; and the noise magnitudes are obtained from a sensitivity analysis technique, perturbing active and reactive power demands by 10%. As suggested in [5], an amplification factor can be used to force the AA-based intervals to be beyond the MCS-based ones. However, the obtained AA-based intervals for real and imaginary bus voltage components, in this numerical example are all outside of the MCS-based bounds and therefore there is no need to use an amplification factor to increase the noise magnitudes.

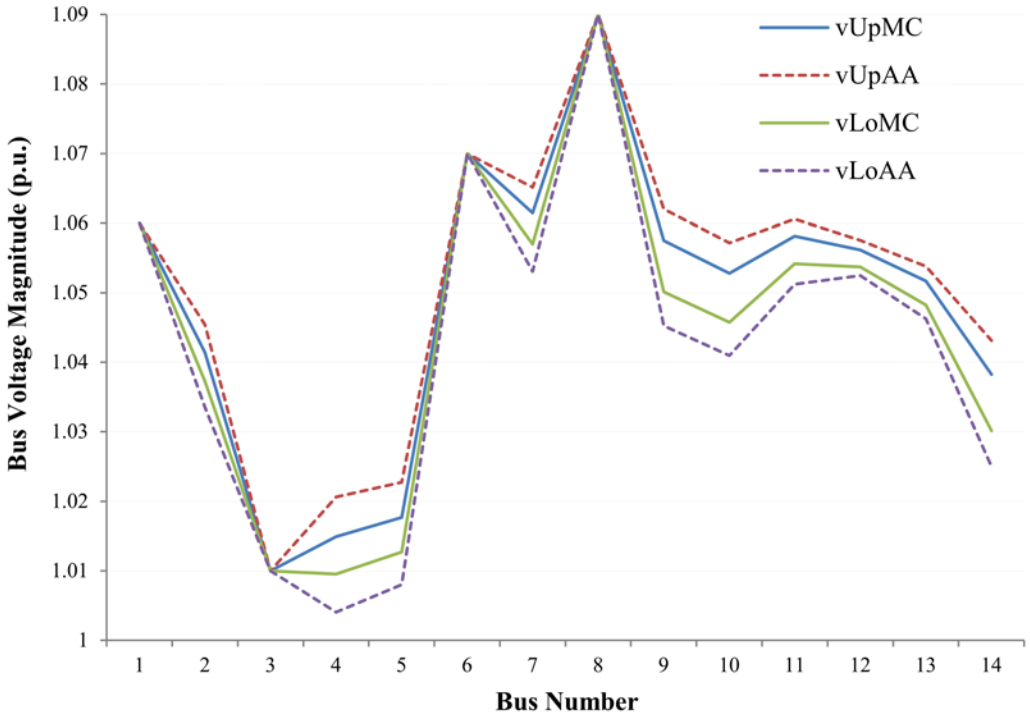

Figure 3: Bus voltage magnitude bounds

The intervals obtained by the MCS method are used as reference to check the validity of the AA-based intervals. As presented in Figure 3 to Figure 5, the AA intervals associated with the bus voltage magnitudes (vUpAA and vLoAA), the real component of bus voltage magnitude (eUpAA and eLoAA) and the imaginary component of bus voltage magnitude (fUpAA and fLoAA) are outside the corresponding MCS intervals. Most of the generator bus voltage magnitudes (bus 1, bus 3, bus 6 and bus 8) are at their set-point values, because their reactive power generation is not

at the limits, and hence the voltage magnitudes do not deviate from their corresponding set-point values. However the reactive power generation at bus 2 is at its maximum limit and hence the voltage magnitude at this bus deviates from its set-point according to the range, shown in Figure 3. The contraction method proposed in [5] is used to find the value of the noise variables. Figure 6 illustrates the substantial improvement in the bus voltage magnitude intervals from their initial values, i.e., the noise variables are 1 and (-1), after the first iteration of the contraction method. However as presented in Figure 7, for this specific example, there is no significant improvement in the intervals after the first iteration of the contraction method, therefore the obtained noise values after the first iteration are considered to be satisfactory. Figure 7 presents the interval improvement in bus voltage magnitudes after the first and the 5^{th} iterations of the contraction method.

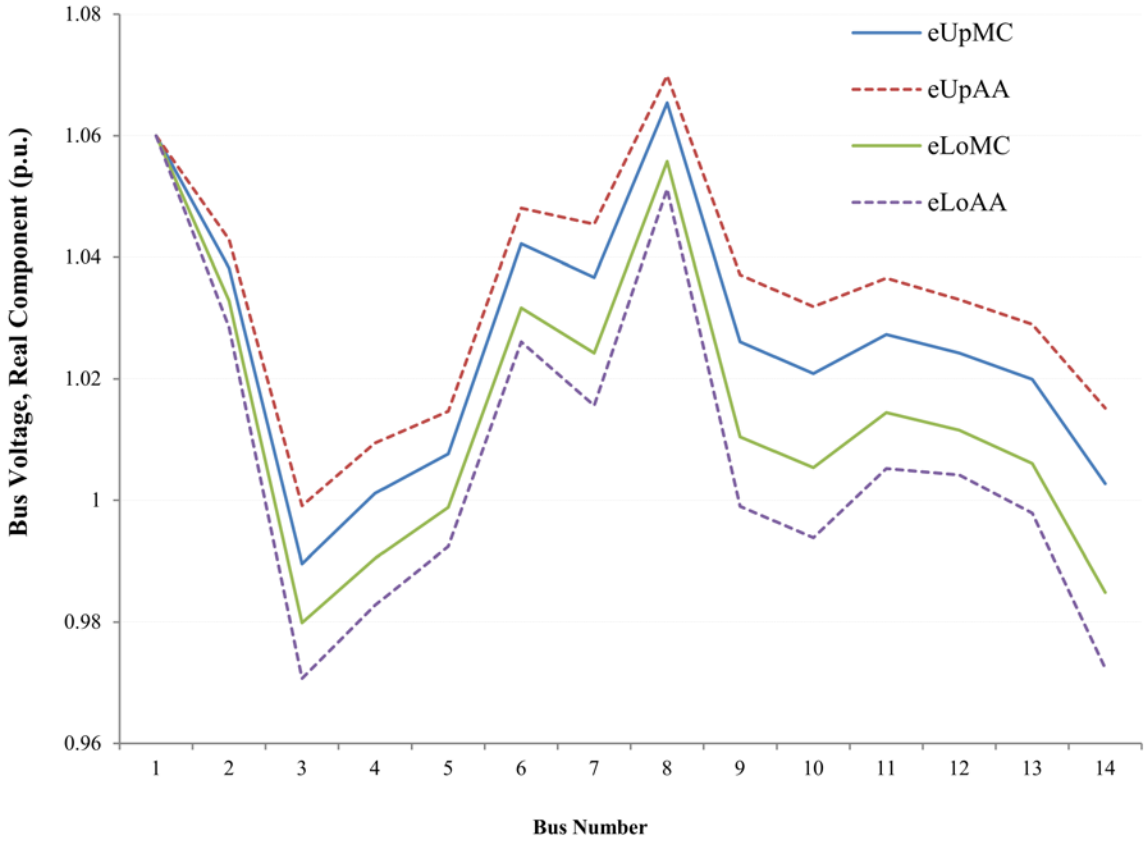

Figure 4: Bus voltage real component bounds

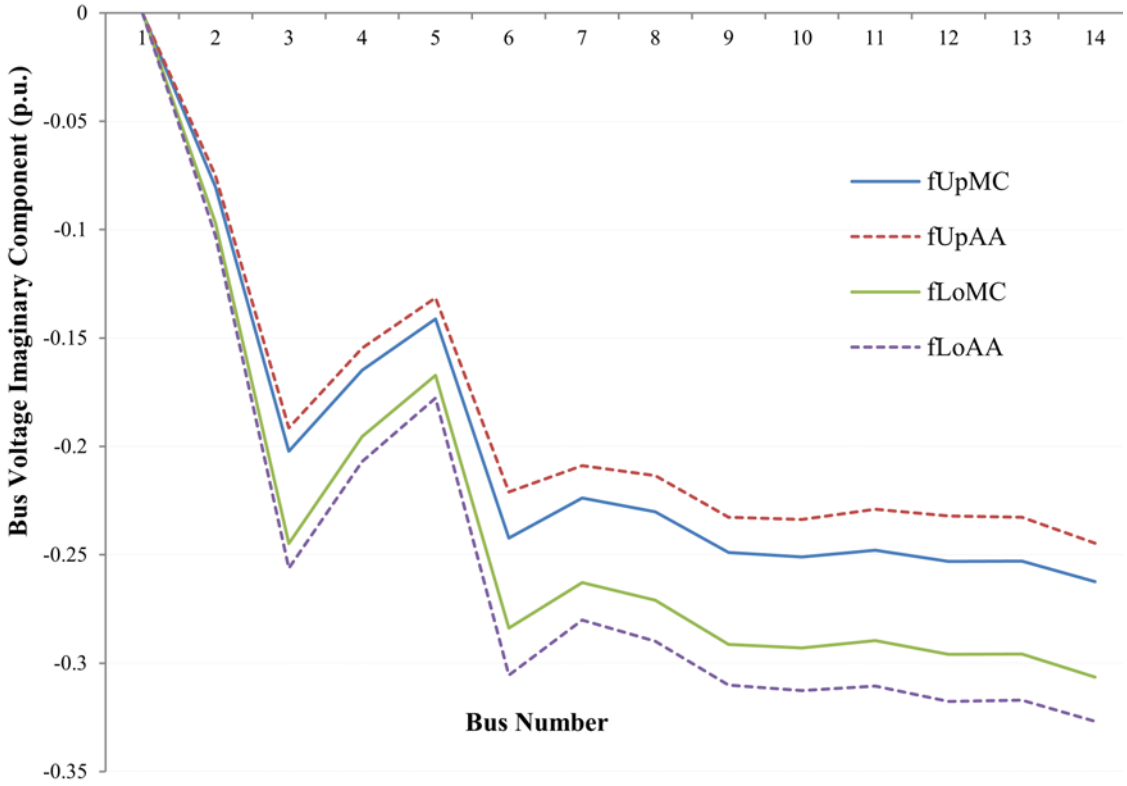

Figure 5: Bus voltage imaginary component

Using the proposed power flow MCP model, there is no need to perform the standard PV- and PQ-bus switching to find the center value of affine reactive power generation, as the complementarity conditions inherently take care of the situation when reactive power generation is at its limits. Thus the center value of the affine reactive power generation does not violate the reactive power generation limits. The intervals associated with the reactive power generation also respect the given limits, as the AA-based upper and lower bounds are obtained by adding the noise magnitudes, calculated by (123) and (124), and when the center value is already at the limits the partial deviations would be zero or negligible.

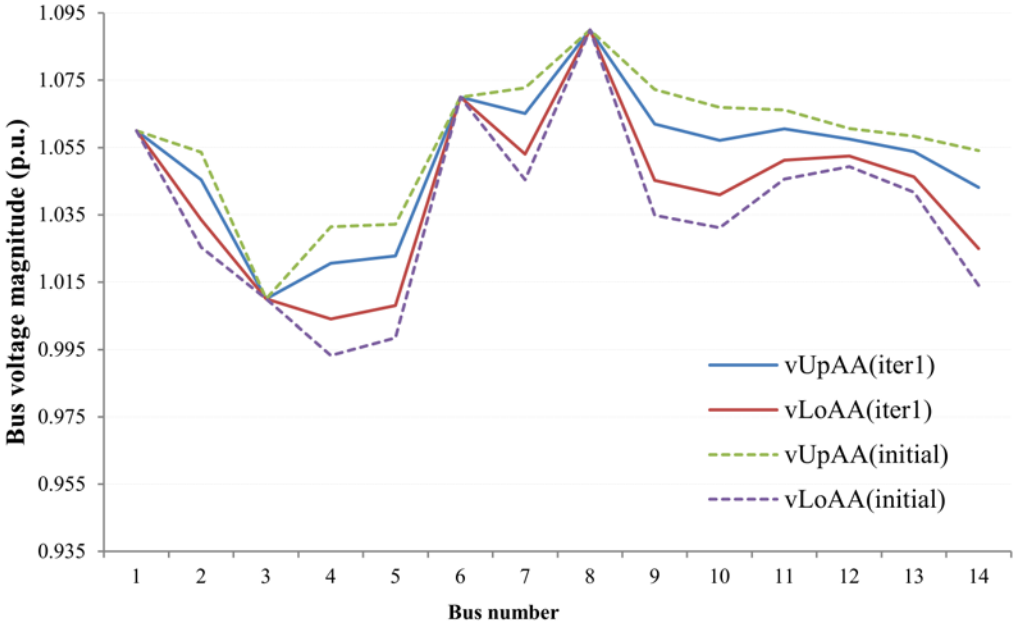

Figure 6: Contraction Method performance after first iteration

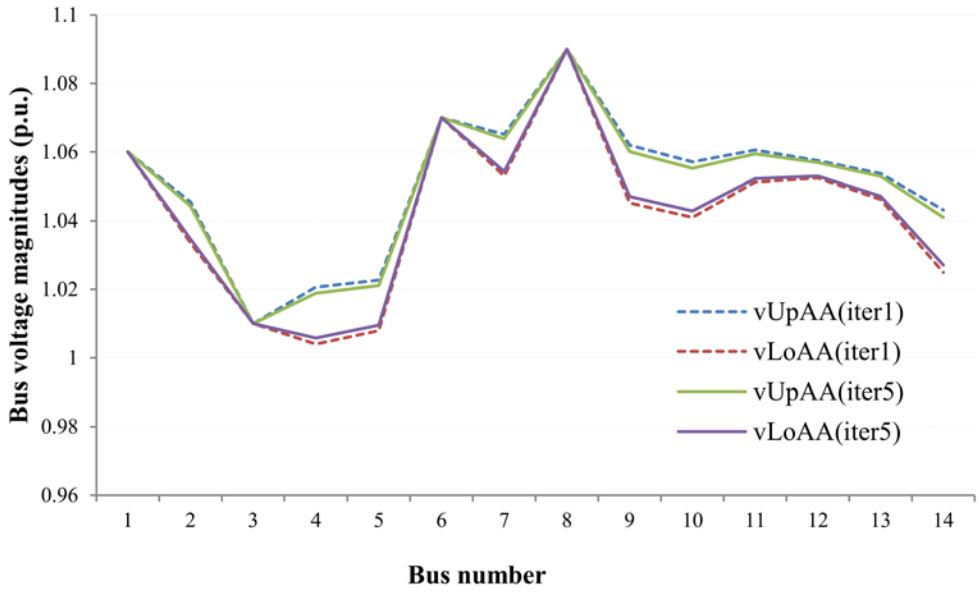

Figure 7: Contraction method performance improvement

Figure 8 illustrates the AA-based reactive power generation interval (AA-qGUp and AA-qGLo) and its center value (AA-qGCtr) and compares them with the given limits. As shown in Figure 8, reactive power generation at the Bus-2 is at the maximum limit and therefore the AA-based upper and lower bounds do not deviate from the center values as all the corresponding partial deviations are zero.

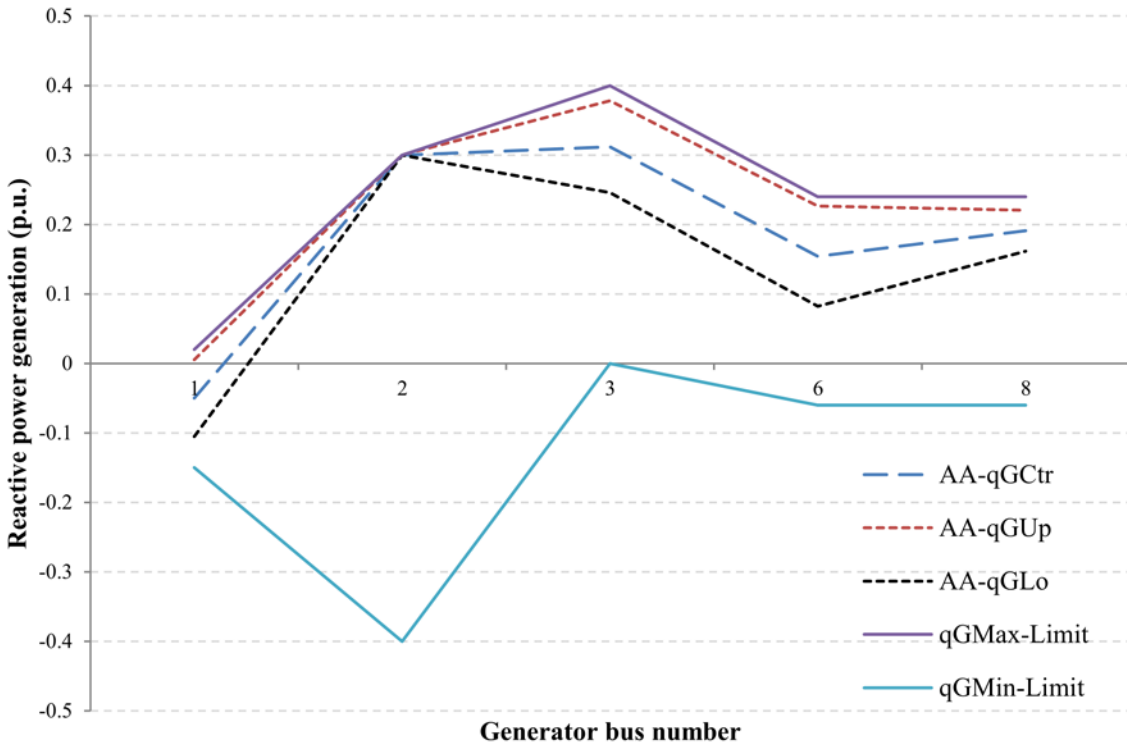

Figure 8: Reactive power generation AA-based limits

Another method to calculate the AA-based reactive power generation interval is to use the MCP model directly by generating the affine form of the reactive power generation as a by-product of the model. Figure 9 demonstrates the results, obtained using this method:

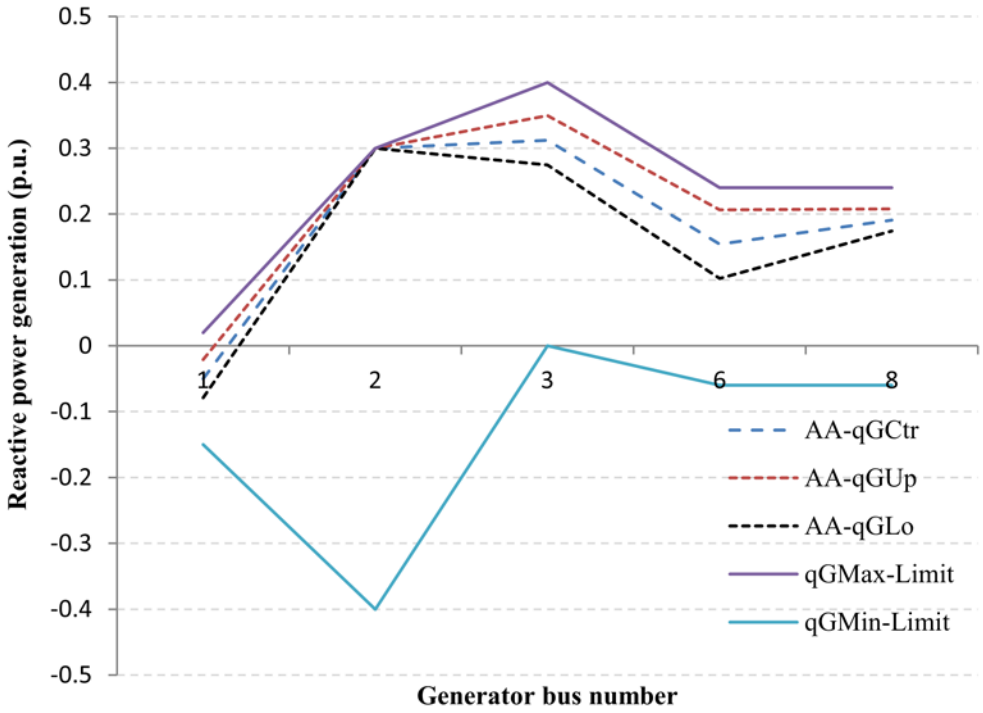

Figure 9: AA-based reactive power generation limits as the by-product of the MCP model

As shown in Figure 9, the obtained interval does not violate the given reactive power generation interval. Also it is much narrower than the interval obtained in Figure 8, as it does not take into consideration the internal errors associated with the calculations.

Figure 10 presents a comparison between the real power injection intervals using the AA and the MCS method. As shown in Figure 10, the real power injection intervals for all buses but the slack bus are almost the same for both the AA and the MCS method, as the real power generation is fixed at these buses and the demand is changing considering the perturbation in the AA method and the pdf in the MCS method. The slack bus real power injection interval is slightly different between the two methods as the real power generation is a variable at the slack bus.

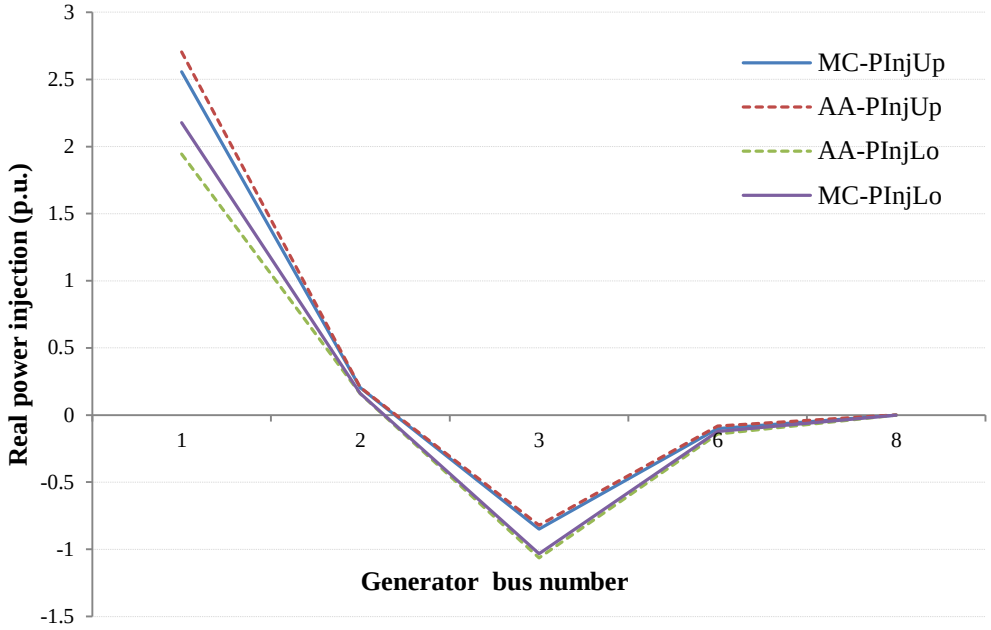

Figure 10: Real power injection

4.4 Summary

In this chapter, an AA-based method is used to solve the power flow problem under uncertainty. The MCP model, proposed in the previous chapter is used to calculate the affine form of real and imaginary components of bus voltage magnitudes in the uncertain power flow problem. The calculated affine forms of real and imaginary components of the bus voltage magnitude are then used to calculate the affine forms of real and reactive power injections. Then the AA form is converted to IA form in order to compare the obtained intervals with the MCS intervals. The proposed method is tested on IEEE 14-bus test system. The results show that the AA intervals are more conservative than the MCS ones, as they consider the worst cases and also the internal errors such as truncation error. The main advantage of the AA method is that it does not need the pdf of the uncertain variables.

CHAPTER 5

AN AFFINE ARITHMETIC METHOD TO SOLVE OPTIMAL POWER FLOW PROBLEMS WITH UNCERTAINTIES

5.1 Introduction

The increased focus on renewable generation has brought forth several concerns pertaining to planning and operation of modern power systems, because of their inherent characteristic of intermittency. In order to fulfill the requirements of the evolving smart power grid, the intermittency need be taken into account in traditional UC, ELD, and OPF models, as well as in long-term planning models of transmission and generation systems.

An AA method is proposed in this chapter to solve the OPF problem with uncertain generation sources. In the AA-based OPF problem, all the state and control variables are treated in affine form, comprising a center value and the corresponding noise magnitudes, to represent forecast, model error, and other sources of uncertainty without the need to assume a pdf. The proposed AA-based OPF problem is used to determine the operating margins of the thermal generators in systems with uncertain wind and solar generation dispatch. The AA-based approach is benchmarked against MCS intervals in order to determine its effectiveness. The proposed technique is tested and demonstrated on the IEEE 30-bus system and also a real 1211-bus European system. Some of the mathematical formulations to obtain the affine form of the state variables associated with the power flow analysis problem are re-stated in this chapter, for the sake of continuity in reading.

Obtaining the margins of operations for thermal generators in the presence of uncertain generation (e.g., wind and solar) and load [113] helps significantly in determining the required reserve capacities, so that the system operates reliably and economically. System operators provide such ancillary services to maintain system reliability [114] and [115]. The Electric Reliability Council of Texas (ERCOT) has faced resource adequacy issues, since less thermal capacity has been added as compared to wind, since 2003, and the additional wind capacity has not contributed to the peak load carrying capability, as wind blows more during off-peak periods [116].

5.2 AA-Based Optimal Power Flow

As demonstrated in Chapter 4, all the variables associated with the proposed AA-based OPF problem (e.g., the bus voltage magnitude and the voltage angle, or real and imaginary components of bus voltages in rectangular form) can be stated in affine form consisting of a center value and noise magnitudes. Center values represent the value of a variable under deterministic assumptions, i.e., when uncertainties are neglected, and noise magnitudes represent deviations of the OPF variables due to the uncertainties.

5.2.1 AA-based Mathematical Model

The proposed AA-based OPF model uses a cost minimization objective function, with all the uncertain variables, such as real and reactive power generation $\tilde{P}_i^G$ and $\tilde{Q}_i^G$, real and reactive power demand $\tilde{P}_i^D$ and $\tilde{Q}_i^D$, bus voltage magnitude $|\tilde{V}_i|$, real and imaginary components of bus voltages $\tilde{e}_i$ and $\tilde{f}_i$, real and imaginary components of bus currents $\tilde{I}_{r_i}$ and $\tilde{I}_{im_i}$, and line currents $\tilde{I}_{ij}$ in affine form. The following equations correspond to the rectangular form of the AA-based cost minimizing OPF problem:

$$\min \quad F(\tilde{P}^G) = \sum_{i \in Th} \alpha_i \tilde{P}_i^{G\,2} + \beta_i \tilde{P}_i^G + c_i \tag{144}$$

$$\text{s.t.:} \quad \Delta\tilde{P}_i\left(\tilde{e}_i, \tilde{f}_i, \tilde{I}_{r_i}, \tilde{I}_{im_i}, \tilde{P}_i^G, \tilde{P}_i^D\right) = 0 \qquad \forall i \in N \tag{145}$$

$$\Delta\tilde{Q}_i\left(\tilde{e}_i, \tilde{f}_i, \tilde{I}_{r_i}, \tilde{I}_{im_i}, \tilde{Q}_i^G, \tilde{Q}_i^D\right) = 0 \qquad \forall i \in N \tag{146}$$

$$|\tilde{V}_i|^2 = \tilde{e}_i^2 + \tilde{f}_i^2 \qquad \forall i \in N \tag{147}$$

$$P_i^{min} \le \tilde{P}_i^G \le P_i^{max} \qquad \forall i \in gen \tag{148}$$

$$Q_i^{min} \le \tilde{Q}_i^G \le Q_i^{max} \qquad \forall i \in gen \tag{149}$$

$$I_{ij}^{min} \le \tilde{I}_{ij} \le I_{ij}^{max} \qquad \forall ij \in L \tag{150}$$

$$V_i^{min\,2} \le \left|\tilde{V}_i\right|^2 \le V_i^{max\,2} \qquad \forall i \in N \tag{151}$$

where N is the set of all buses, nPG is the set of all generator buses, and L is the set of all lines. Furthermore, $\Delta\tilde{P}_i(.)$ and $\Delta\tilde{Q}_i(.)$ are affine real and reactive power mismatch functions, and P_i^{min}, P_i^{max}, Q_i^{min}, Q_i^{max}, I_{ij}^{min}, I_{ij}^{max}, V_i^{min} and V_i^{max} are minimum and maximum limits for real power, reactive power, line currents, and bus voltage magnitudes, respectively, at bus i. All the state and control variables in these equations are in affine form, comprising a center value and the corresponding noise magnitudes. The center values are obtained by solving a deterministic OPF,

in which the mean of the given intervals for upper and lower bounds of real and reactive power demand $\overline{P}_i^D$ and $\underline{P}_i^D$, and $\overline{Q}_i^D$ and $\underline{Q}_i^D$ are considered deterministic demands as follows:

$$P_i^D = \frac{\overline{P}_i^D + \underline{P}_i^D}{2} \qquad \forall i \in nP \quad (152)$$

$$Q_i^D = \frac{\overline{Q}_i^D + \underline{Q}_i^D}{2} \qquad \forall i \in nQ \quad (153)$$

In this paper, uncertain wind and solar generation sources are treated as interval negative loads with a constant power factor, and are hence represented using (152) and (153) in the deterministic OPF.

To obtain the noise magnitudes of real and imaginary components of bus voltages, a sensitivity analysis is carried out, where the generation and demand are perturbed by a small magnitude (e.g., ±1%) at each node. A deterministic OPF is solved for each of these variations, thus solving as many OPFs as the number of uncertain inputs in the system, which corresponds to the number of renewable generators being studied. Therefore, the noise magnitudes can be obtained as follows [5]:

$$e_{i,j}^P = \left.\frac{\partial e_i}{\partial P_j^D}\right|_0 \approx \frac{e_i^N - e_i^0}{\Delta P_j^D} \qquad \forall i,j \in N \quad (154)$$

$$e_{i,j}^Q = \left.\frac{\partial e_i}{\partial Q_j^D}\right|_0 \approx \frac{e_i^N - e_i^0}{\Delta Q_j^D} \qquad \forall i,j \in N \quad (155)$$

$$f_{i,j}^P = \left.\frac{\partial f_i}{\partial P_j^D}\right|_0 \approx \frac{f_i^N - f_i^0}{\Delta P_j^D} \qquad \forall i,j \in N \quad (156)$$

$$f_{i,j}^Q = \left.\frac{\partial f_i}{\partial Q_j^D}\right|_0 \approx \frac{f_i^N - f_i^0}{\Delta Q_j^D} \qquad \forall i,j \in N \quad (157)$$

where $e_{i,j}^P$ and $f_{i,j}^P$ are partial deviations of real and imaginary components of bus voltages due to changes in real power injection, and $e_{i,j}^Q$ and $f_{i,j}^Q$ are partial deviations of real and imaginary components of bus voltages at bus i due to changes in reactive power injection at bus j. The parameters e_i^N and f_i^N are the new real and imaginary components of the bus voltages when the real and reactive power injections are perturbed; e_i^0 and f_i^0 are the initial values of real and imaginary components of bus voltages obtained from the deterministic model; and ΔP_j^D and ΔQ_j^D are the amount of perturbation in real and reactive power injections at bus j.

Note that since the power flow equations are nonlinear, the suggested calculations in (154)-(157) may result in the underestimation of the solution and, therefore, not include the "exact" solutions. In order to avoid underestimation of the solution, an "affine extension" technique suggested in [5] and [117] is used here to increase each noise magnitude using an independent magnification coefficient. Also, it is assumed that an OPF solution for the center value can be obtained as the starting point; hence, the derivatives (154)-(157), which can be obtained by inverting Jacobians of the center-value OPF solution, exist. In the case that a center-value OPF solution cannot be obtained, the proposed technique cannot be applied; this may be resolved by redefining the intervals. It should be noted that, since the classical OPF problem is highly non-convex, using NLP solution methods such as the Interior Point (IP), do not guarantee a global optimal solution. To prevent widely different solutions during the perturbation method used in the sensitivity analysis, at each run, the initial values for each variable are set at the values obtained from solving the center-value OPF. Since these perturbations are small, this procedure guarantees in practice obtaining local maxima close to the center-value OPF solutions.

The affine forms of the real and imaginary components of the bus voltage magnitude $\tilde{e}_i$ and $\tilde{f}_i$, which are linear functions of noise variables $\varepsilon_{P_j^D}$ and $\varepsilon_{Q_j^D}$ representing the uncertainties of active power and reactive power injections at bus j, can then be presented as follows:

$$\tilde{e}_i = e_{i0} + \sum_{j \epsilon N} e_{i,j}^P \, \varepsilon_{P_j^D} + \sum_{j \epsilon N} e_{i,j}^Q \, \varepsilon_{Q_j^D} \qquad \forall i \in N \quad (158)$$

$$\tilde{f}_i = f_{i0} + \sum_{j \epsilon N} f_{i,j}^P \, \varepsilon_{P_j^D} + \sum_{j \epsilon N} f_{i,j}^Q \, \varepsilon_{Q_j^D} \qquad \forall i \in N \quad (159)$$

where e_{i0} and f_{i0} are the center values for real and imaginary components of bus voltages at bus i, respectively, and $e_{i,j}^P$, $f_{i,j}^P$, $e_{i,j}^Q$, and $f_{i,j}^Q$ are defined in (154) to (157).

The affine forms of real and imaginary components of bus voltages, $\tilde{e}_i$ and $\tilde{f}_i$ can be used to calculate, from (58), the square of bus voltage magnitude, using the following relationship:

$$|\tilde{V}_i|^2 = \tilde{e}_i^2 + \tilde{f}_i^2 \qquad \forall i \in N \quad (160)$$

Thus, $|\tilde{V}_i|^2$ has the following form:

$$|\tilde{V}_i|^2 = \left(e_{i0}^2 + f_{i0}^2\right) + 2\sum_{j \epsilon N}\left(e_{i0} e_{i,j}^P + f_{i0} f_{i,j}^P\right) \varepsilon_{P_j^D} + 2\sum_{j \epsilon N}\left(e_{i0} e_{i,j}^Q + f_{i0} f_{i,j}^Q\right) \varepsilon_{Q_j^D} + \left(e_i^T + f_i^T\right) \qquad \forall i \in N \quad (161)$$

Here e_i^T and f_i^T are linear approximation errors due to non-affine operations. Furthermore, knowing the affine forms of the real and imaginary components of the bus voltage magnitude, the real and reactive power can be calculated using the following affine operations:

$$\tilde{I}_i = \sum_{j \epsilon N} \left(\mathrm{G}_{ij} + \hat{\jmath}\mathrm{B}_{ij}\right)\left(\tilde{e}_j + \hat{\jmath}\tilde{f}_j\right) \qquad \forall i \in N \quad 162)$$

where $\hat{\jmath} = \sqrt{-1}$, and G_{ij} and B_{ij} are the real and imaginary components of the Y-bus matrix, respectively. Therefore, the linear affine forms of real and imaginary bus currents $\tilde{I}_{r_i}$ and $\tilde{I}_{im_i}$ can be calculated as follows:

$$\tilde{I}_{r_i} = \sum_{j \epsilon N} \left\{\mathrm{G}_{ij}\left(\tilde{e}_i - \tilde{e}_j\right) - \mathrm{B}_{ij}\left(\tilde{f}_i - \tilde{f}_j\right)\right\} \qquad \forall i \in N \quad 163)$$

$$\tilde{I}_{im_i} = \sum_{j \epsilon N} \left\{\mathrm{G}_{ij}\left(\tilde{f}_i - \tilde{f}_j\right) + \mathrm{B}_{ij}\left(\tilde{e}_i - \tilde{e}_j\right)\right\} \qquad \forall i \in N \quad 164)$$

where $\tilde{I}_{r_i}$ and $\tilde{I}_{im_i}$ have the following general forms after affine operations:

$$\tilde{I}_{r_i} = I_{r_{i0}} + \sum_{j \epsilon N} I_{r_{i,j}}^{P}\, \varepsilon_{P_j^D} + \sum_{j \epsilon N} I_{r_{i,j}}^{Q}\, \varepsilon_{Q_j^D} \qquad \forall i \in N \quad (165)$$

$$\tilde{I}_{im_i} = I_{im_{i0}} + \sum_{j \epsilon N} I_{im_{i,j}}^{P}\, \varepsilon_{P_j^D} + \sum_{j \epsilon N} I_{im_{i,j}}^{Q}\, \varepsilon_{Q_j^D} \qquad \forall i \in N \quad (166)$$

Here, $I_{r_{i0}}$ and $I_{im_{i0}}$ are the center values for real and imaginary components of current magnitudes. $I_{r_{i,j}}^{P}$ and $I_{r_{i,j}}^{Q}$ are partial deviations of the real component of current at bus i for deviation in real and reactive power injection at a bus j, respectively; and $I_{im_{i,j}}^{P}$ and $I_{im_{i,j}}^{Q}$ are partial deviations of imaginary component of current at bus i for deviation in real and reactive power injection at bus j, respectively. Note that the real and imaginary components of the current share the same sources of uncertainties, i.e., real and reactive power injections $\varepsilon_{P_j^D}$ and $\varepsilon_{Q_j^D}$. Furthermore, using affine and non-affine operations and $\tilde{e}_i$, $\tilde{f}_i$, $\tilde{I}_{r_i}$, and $\tilde{I}_{im_i}$, the real and reactive power mismatch $\Delta\tilde{P}_i(.)$and $\Delta\tilde{Q}_i(.)$ in (145) and (146), respectively, can be calculated as follows:

$$\Delta\tilde{P}_i\left(\tilde{e}_i, \tilde{f}_i, \tilde{I}_{r_i}, \tilde{I}_{im_i}, \tilde{P}_i^G, \tilde{P}_i^D\right) = \tilde{P}_i - \tilde{e}_i\, \tilde{I}_{r_i} - \tilde{f}_i\, \tilde{I}_{im_i} = 0 \qquad \forall i \in N \quad (167)$$

$$\Delta\tilde{Q}_i\left(\tilde{e}_i, \tilde{f}_i, \tilde{I}_{r_i}, \tilde{I}_{im_i}, \tilde{Q}_i^G, \tilde{Q}_i^D\right) = \tilde{Q}_i - \tilde{f}_i\tilde{I}_{r_i} + \tilde{e}_i\, \tilde{I}_{im_i} = 0 \qquad \forall i \in N \quad (168)$$

Where $\tilde{P}_i$ and $\tilde{Q}_i$ represent the affine real and reactive power injections, and have the following affine forms, with center value and associated partial deviations:

$$\tilde{P}_i = P_{i0} + \sum_{j\epsilon N} P_{i,j}^P \, \varepsilon_{P_j^D} + \sum_{j\epsilon N} P_{i,j}^Q \varepsilon_{Q_j^D} + P_i^T \qquad \forall i \in N \quad (169)$$

$$\tilde{Q}_i = Q_{i0} + \sum_{j\epsilon N} Q_{i,j}^P \varepsilon_{P_j^D} + \sum_{j\epsilon N} Q_{i,j}^Q \, \varepsilon_{Q_j^D} + Q_i^T \qquad \forall i \in N \quad (170)$$

Where P_{i0} and Q_{i0} are the center values of affine real and reactive power injections; $P_{i,j}^P$ and $Q_{i,j}^P$ are the partial deviations of real and reactive power injections due to changes in real power injections at a bus *j*, respectively; $P_{i,j}^Q$ and $Q_{i,j}^Q$ are the partial deviations of real and reactive power injections due to changes in reactive power injections at bus *j*, respectively; and P_i^T and Q_i^T are real and reactive power injection truncation errors, based on (58). The above affine forms can be calculated as follows:

$$P_{i0} = e_{i0} \, I_{r_{i0}} + \, f_{i0} \, I_{im_{i0}} \qquad \forall i \in N \quad (171)$$

$$Q_{i0} = f_{i0} I_{r_{i0}} - \, e_{i0} \, I_{im_{i0}} \qquad \forall i \in N \quad (172)$$

$$P_{i,j}^P = e_{i0} \, I_{r_{i,j}}^{\,P} + \, I_{r_{i0}} \, e_{i,j}^P + f_{i,0} \, I_{im_{i,j}}^{\,P} + I_{im_{i0}} \, f_{i,j}^P \qquad \forall i,j \in N \quad (173)$$

$$Q_{i,j}^P = f_{i0} \, I_{r_{i,j}}^{\,P} + \, I_{r_{i0}} \, f_{i,j}^P - e_{i,0} \, I_{im_{i,j}}^{\,P} - I_{im_{i0}} \, e_{i,j}^P \qquad \forall i,j \in N \quad (174)$$

$$P_{i,j}^Q = e_{i0} \, I_{r_{i,j}}^{\,Q} + \, I_{r_{i0}} \, e_{i,j}^Q + f_{i,0} \, I_{im_{i,j}}^{\,Q} + I_{im_{i0}} \, f_{i,j}^Q \qquad \forall i,j \in N \quad (175)$$

$$Q_{i,j}^Q = f_{i0} \, I_{r_{i,j}}^{\,Q} + \, I_{r_{i0}} \, f_{i,j}^Q - e_{i,0} \, I_{im_{i,j}}^{\,Q} - I_{im_{i0}} \, e_{i,j}^Q \qquad \forall i,j \in N \quad (176)$$

$$\begin{aligned} P_i^T = & \sum_{j\epsilon N} \left\{ \left| e_{i,j}^P \right| + \left| e_{i,j}^Q \right| \right\} \sum_{j\epsilon N} \left\{ \left| I_{r_{i,j}}^{\,P} \right| + \left| I_{r_{i,j}}^{\,Q} \right| \right\} \\ & + \sum_{j\epsilon N} \left\{ \left| f_{i,j}^P \right| + \left| f_{i,j}^Q \right| \right\} \sum_{j\epsilon N} \left\{ \left| I_{im_{i,j}}^{\,P} \right| + \left| I_{im_{i,j}}^{\,Q} \right| \right\} \end{aligned} \qquad \forall i \in N \quad (177)$$

$$\begin{aligned} Q_i^T = & \sum_{j\epsilon N} \left\{ \left| f_{i,j}^P \right| + \left| f_{i,j}^Q \right| \right\} \sum_{j\epsilon N} \left\{ \left| I_{r_{i,j}}^{\,P} \right| + \left| I_{r_{i,j}}^{\,Q} \right| \right\} \\ & - \sum_{j\epsilon N} \left\{ \left| e_{i,j}^P \right| + \left| e_{i,j}^Q \right| \right\} \sum_{j\epsilon N} \left\{ \left| I_{im_{i,j}}^{\,P} \right| + \left| I_{im_{i,j}}^{\,Q} \right| \right\} \end{aligned} \qquad \forall i \in N \quad (178)$$

This formulation, as previously mentioned, is the most conservative but computationally efficient for calculating the magnitude of the internal errors P_i^T and Q_i^T. The affine forms (169)

and (170) for real and reactive powers can be represented in interval forms $\left[\underline{P_i}, \overline{P_i}\right]$ and $\left[\underline{Q_i}, \overline{Q_i}\right]$, where:

$$\overline{P_i} = P_{i0} + radP_i\left(\varepsilon_{P_j^D}, \varepsilon_{Q_j^D}\right) \qquad \forall i \in N \quad (179)$$

$$\underline{P_i} = P_{i0} - radP_i\left(\varepsilon_{P_j^D}, \varepsilon_{Q_j^D}\right) \qquad \forall i \in N \quad (180)$$

$$\overline{Q_i} = Q_{i0} + radQ_i\left(\varepsilon_{P_j^D}, \varepsilon_{Q_j^D}\right) \qquad \forall i \in N \quad (181)$$

$$\underline{Q_i} = Q_{i0} - radQ_i\left(\varepsilon_{P_j^D}, \varepsilon_{Q_j^D}\right) \qquad \forall i \in N \quad (182)$$

Here, $radP_i\left(\varepsilon_{P_j^D}, \varepsilon_{Q_j^D}\right)$ and $radQ_i\left(\varepsilon_{P_j^D}, \varepsilon_{Q_j^D}\right)$ are the following functions of noise variables $\varepsilon_{P_j^D}$ and $\varepsilon_{Q_j^D}$, with the most conservative values when they are equal to 1 or -1, and represent the total amount of deviation from the center value:

$$radP_i\left(\varepsilon_{P_j^D}, \varepsilon_{Q_j^D}\right) = \sum_{j \epsilon N} P_{i,j}^P \varepsilon_{P_j^D} + \sum_{j \epsilon N} P_{i,j}^Q \varepsilon_{Q_j^D} + P_i^T \qquad \forall i \in N \quad (183)$$

$$radQ_i\left(\varepsilon_{P_j^D}, \varepsilon_{Q_j^D}\right) = \sum_{j \epsilon N} Q_{i,j}^P \varepsilon_{P_j^D} + \sum_{j \epsilon N} Q_{i,j}^Q \, \varepsilon_{Q_j^D} + Q_i^T \qquad \forall i \in N \quad (184)$$

These intervals can be used to determine the operational range of generation for dispatchable generators (e.g., thermal, hydro), when there are sources of uncertainty such as renewable generation in the system.

A. Contraction Method

The intervals obtained from (179)-(182) are dependent on the value of the noise variables $\varepsilon_{P_j^D}$ and $\varepsilon_{Q_j^D}$, which are between -1 and 1. The most conservative intervals are obtained by fixing these variables at their maximum values; however, this results in large intervals. Hence, based on the method presented in [118] and [119], a contraction method is used to reduce the bounds. In order to reasonably contract the intervals, while respecting the physical characteristics of the system (e.g. voltage and generation limits), the discussed next LP is solved to obtain the minimum values of noise variables; the suggested optimization problem is linear since all the affine variables are constructed using linear affine operations. Thus, by replacing in the AA-based OPF model (144)-(151), all uncertain variables with their AA forms defined in (158)-(170), one obtains the following representation of the OPF model:

$$\min \quad \tilde{F}\left(\varepsilon_{P_j^D}, \varepsilon_{Q_j^D}\right) \tag{185}$$

$$\Delta\tilde{P}_i\left(\varepsilon_{P_j^D}, \varepsilon_{Q_j^D}\right) = 0 \qquad \forall i \in N \tag{186}$$

$$\Delta\tilde{Q}_i\left(\varepsilon_{P_j^D}, \varepsilon_{Q_j^D}\right) = 0 \qquad \forall i \in N \tag{187}$$

$$P_i^{min} \le P_i\left(\varepsilon_{P_j^D}, \varepsilon_{Q_j^D}\right) \le P_i^{max} \qquad \forall i \in NPG \tag{188}$$

$$Q_i^{min} \le Q_i\left(\varepsilon_{P_j^D}, \varepsilon_{Q_j^D}\right) \le Q_i^{max} \qquad \forall i \in NPG \tag{189}$$

$$I_{ij}^{min^2} \le \tilde{I}_{r_{ij}}{}^2\left(\varepsilon_{P_j^D}, \varepsilon_{Q_j^D}\right) + \tilde{I}_{im_{ij}}{}^2\left(\varepsilon_{P_j^D}, \varepsilon_{Q_j^D}\right) \le I_{ij}^{max^2} \qquad \forall ij \in L \tag{190}$$

$$V_i^{min^2} \le \tilde{V}_i^2\left(\varepsilon_{P_j^D}, \varepsilon_{Q_j^D}\right) \le V_i^{max^2} \qquad \forall i \in N \tag{191}$$

$$-1 \le \varepsilon_{P_j^D} \le 1 \qquad \forall j \in rnw \tag{192}$$

$$-1 \le \varepsilon_{Q_j^D} \le 1 \qquad \forall j \in rnw \tag{193}$$

where the objective function $\tilde{F}(.)$ is the affine linear expansion of (144), as follows:

$$\begin{aligned}\tilde{F}\left(\varepsilon_{P_j^D}, \varepsilon_{Q_j^D}\right) = \sum_{i\epsilon N}\Bigg[\alpha_i\left\{{P_{i0}}^2 + \sum_{j\epsilon N} 2P_{i0}\,P_{i,j}^P\varepsilon_{P_j^D} + \sum_{j\epsilon N} 2P_{i0}P_{i,j}^Q\varepsilon_{Q_j^D} + 2P_{i0}P_i^T + P_i^{T'}\right\} \\ + \beta_i\left\{\sum_{j\epsilon N} P_{i0} + P_{i,j}^P\,\varepsilon_{P_j^D} + \sum_{j\epsilon N} P_{i,j}^Q\varepsilon_{Q_j^D} + P_i^T\right\} + c_i\Bigg]\end{aligned} \tag{194}$$

Note that in the above equation, due to an affine product, a new error magnitude $P_i^{T'}$ is introduced. The line currents $\tilde{I}_{r_{ij}}$ and $\tilde{I}_{im_{ij}}$ in (190) are calculated as follows:

$$\tilde{I}_{r_{ij}} = \mathrm{G}_{ij}\left(\tilde{e}_i - \tilde{e}_j\right) - \mathrm{B}_{ij}\left(\tilde{f}_i - \tilde{f}_j\right) \qquad \forall ij \in L \tag{195}$$

$$\tilde{I}_{im_{ij}} = \mathrm{G}_{ij}\left(\tilde{f}_i - \tilde{f}_j\right) + \mathrm{B}_{ij}\left(\tilde{e}_i - \tilde{e}_j\right) \qquad \forall ij \in L \tag{196}$$

Observe that the OPF model (185)-(191) is an LP problem, since all affine forms are linear functions of the noise variables $\varepsilon_{P_j^D}$ and $\varepsilon_{Q_j^D}$. This linear noise contraction model can be easily solved using available LP solvers, such as CPLEX [120].

Figure 11 depicts the procedure used to calculate the intervals for the affine variables and hence arrive at the solution intervals to the OPF with uncertainties. Note that the demand intervals at each bus are the input of the model. These intervals consider the uncertainties associated with both demand and renewable generation by considering the latter as negative loads. Then affine

variables $\tilde{e}_i$ and $\tilde{f}_i$ are constructed using both a deterministic OPF model to obtain center values, and a sensitivity analysis based on several perturbed OPFs to obtain the noise magnitudes. Affine operations are then applied on these affine variables in order to calculate other affine variables, such as $\tilde{P}_i$ and $\tilde{Q}_i$. To minimize the size of the intervals, a contraction method is used to minimize the noise magnitudes associated with each of these variables.

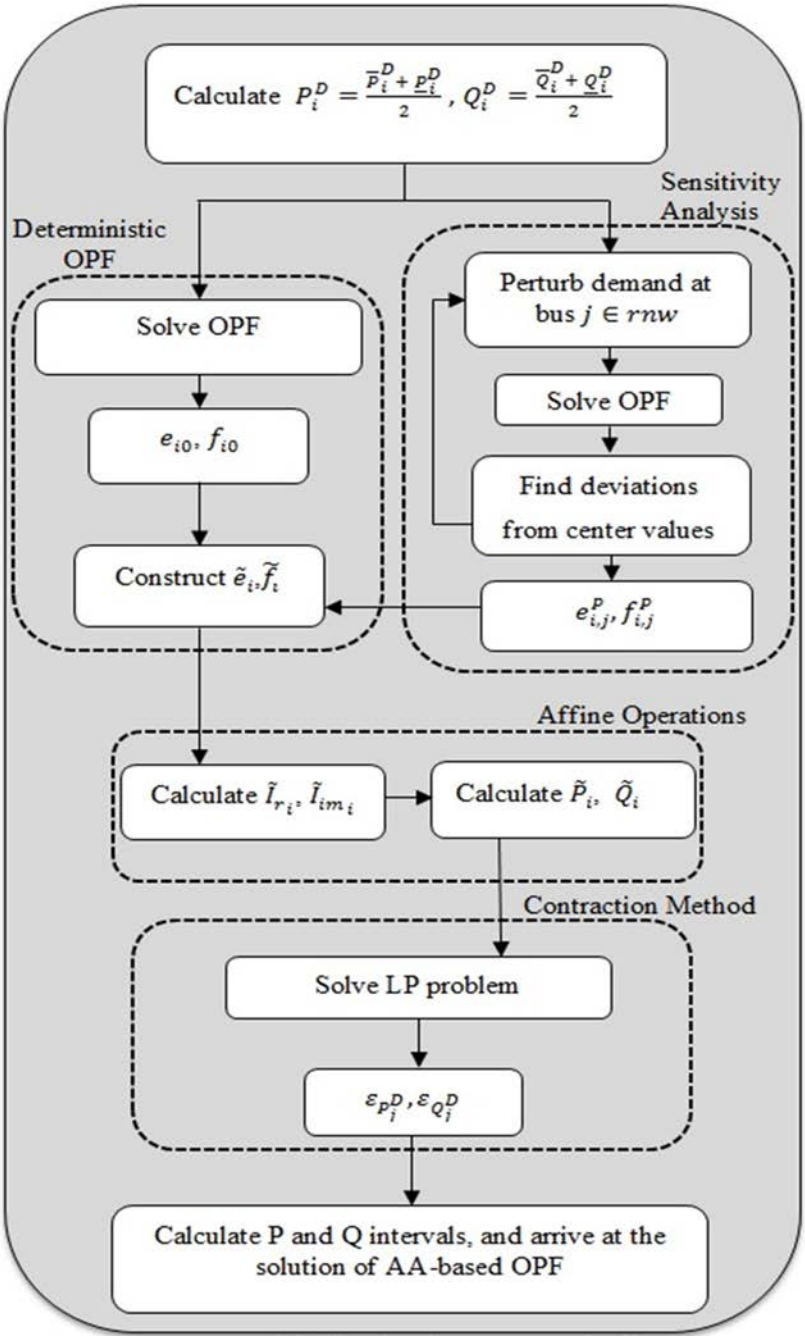

Figure 11: Proposed AA-based OPF

5.3 Results and Discussions

In this section, the proposed AA-based OPF is tested using the IEEE 30-bus system [112] and a real European 1211-bus system, and compared with the MCS solution. The IA method has not been used as a means for comparison in this thesis, since the bounds provided by the IA approach are too conservative or simply cannot be obtained and therefore is not a feasible method. The IA wider bounds are simply because of not considering the correlation amongst the variables which leads to error explosion. In fact, the application of the IA method to the OPF problem has been studied by researchers and observed that the IA-based OPF diverges for realistic systems with a reasonable number of uncertainties due to too wide intervals. This resulted in singularities of the Jacobian of the Lagrangian function, even after preconditioning, and hence it could not be used for the types of studies presented in the current work.

In the 30-bus system, one of the generators is replaced with a wind turbine to study the effects of uncertainty arising from the renewable sources in the system. The 1211-bus real European system has 160 generators (thermal, hydro, wind, and solar), 58 are solar and 8 are wind generators, for a total renewable capacity of 11678 MW; considering that the total generation capacity of the system, including imports, is 183 GW, this corresponds to 6.4% of the generation capacity of the system. The total system demand is 153 GW, including exports. The transmission system comprises 1567 lines and 122 fixed transformers. The intermittency in wind and solar generation is assumed to be compensated by thermal generation in both of the test systems, and thus the proposed AA-based method is used to determine the power output intervals of these generators, hence calculating the generation reserve needed to reliably and optimally supply the demand. The proposed model is simulated in the General Algebraic Modeling System (GAMS) [121]. The solvers used, i.e., COINIPOPT for the OPF solution [122], and CPLEX for the LP contraction problem, have their parameters set at their respective default, off-the-shelf settings, so as not to bias their "standard" performance. Major settings such as tolerance level or maximum number of iterations of the solver are by default the same for all solvers (e.g., feasibility tolerance is 10^{-6}). The implemented MCS method converges after 3000 iterations for both test systems, assuming that the uncertain parameters have uniform distribution within the bounds defined for the assumed variable generation.

A. 30-bus System

In the IEEE 30-bus test system, a wind turbine is assumed to be located at Bus 2. It is considered that this generator power output varies in a ±30% range of its forecasted center value, $P_{20}^{D} = -1.283\ p.u.$, since this is treated as a negative injection with unity power factor.

All the center values are obtained by executing the nonlinear OPF model with the deterministic data, and the noise magnitudes are obtained from the sensitivity analysis technique described in Section IV. The intervals obtained by the MCS method are used as the benchmark to check the validity of the obtained AA-based intervals. Figure 12 compares the bus voltage magnitude bounds using both AA (VupAA and VloAA) and MCS (VupMC and VloMC) methods. Note that there is no significant difference between the two approaches. The bounds obtained by the MCS method lie slightly inside the AA-based ones, because the MCS method provides the "exact" intervals, whereas the AA-based approach provides more conservative margins, as expected.

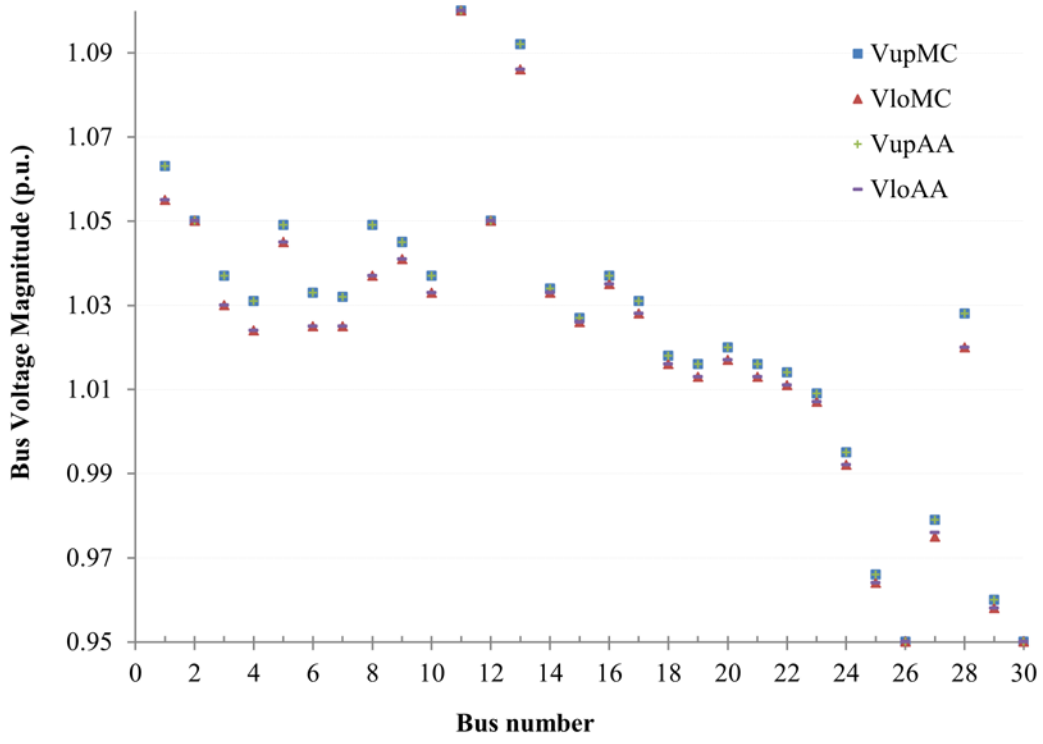

Figure 12: Bus voltage magnitude bounds.

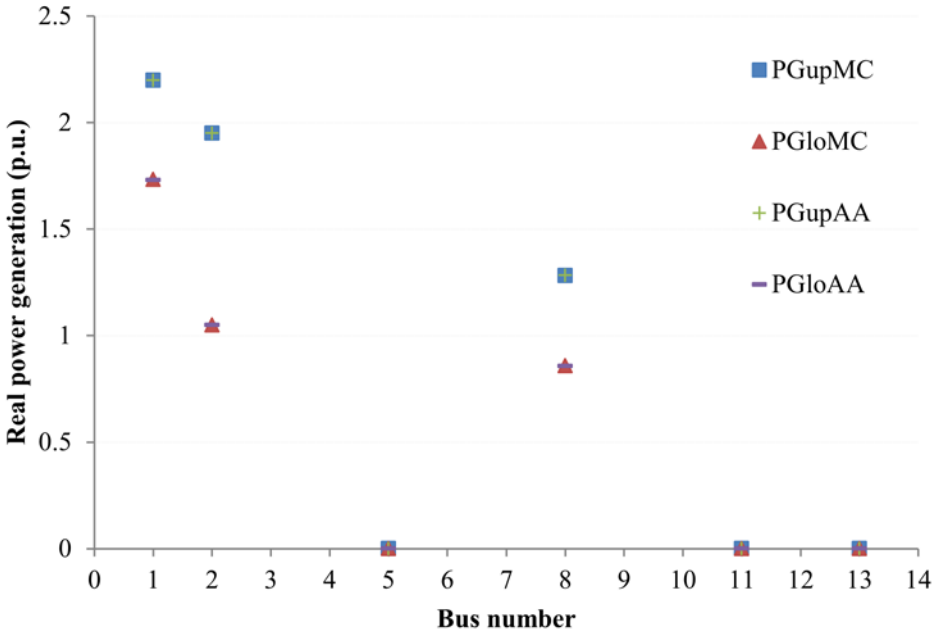

Figure 13: Real power generation intervals.

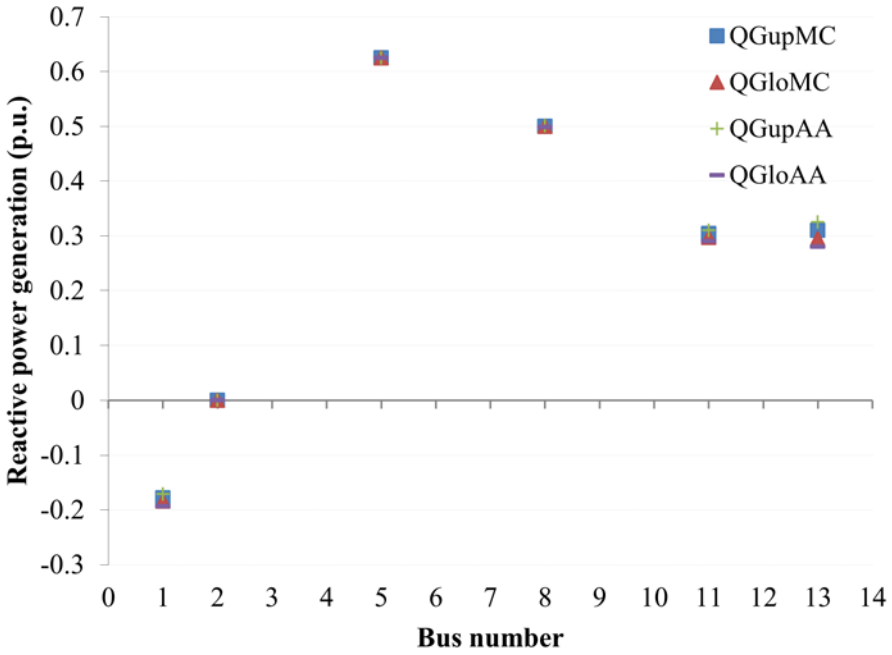

Figure 14: Reactive power generation intervals.

Observe that the difference between the AA-based and MCS-based methods is very small. The real power intervals, shown in Figure 13, depict the interval output for thermal generators at Bus 1 and Bus 8, when the wind turbine output varies in the given interval at Bus 2; all other generators are synchronous condensers and hence have zero real power output.

Figure 14 demonstrates the recative power generation inervals. As shown, the resulted AA-based margins of reactive power generation closely match the ones obtained from the MCS method. Note that the differnce between the upper and lower bounds of the illustrated intervals in Figure 14 is very small

B. 1211-bus System

The AA method is also applied to a real European 1211-bus system. Figure 15 and Figure 16 show the real and reactive power deviations of the thermal generators, and Figure 17 shows the deviation of bus voltage magnitudes at all buses with respect to the center value, in percentage, obtained from both the AA-based approach and MCS. In this case, a ±10% deviation active power injection for wind and solar with unity power factor is assumed.

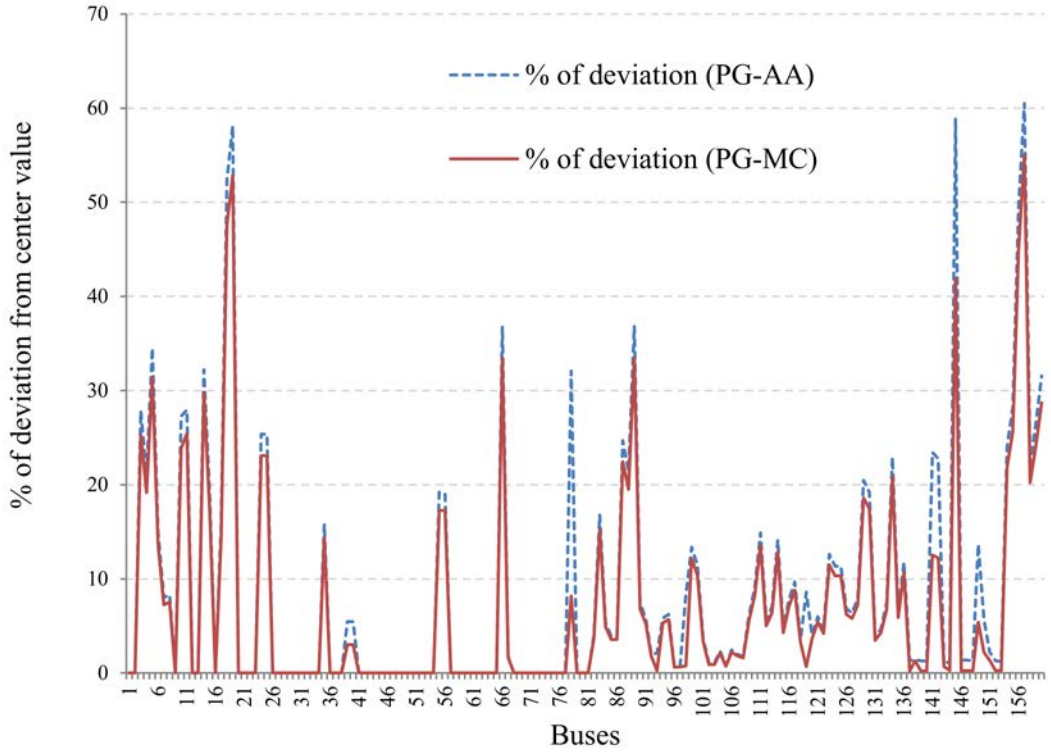

Figure 15: Percentage of real power deviation for thermal generators.

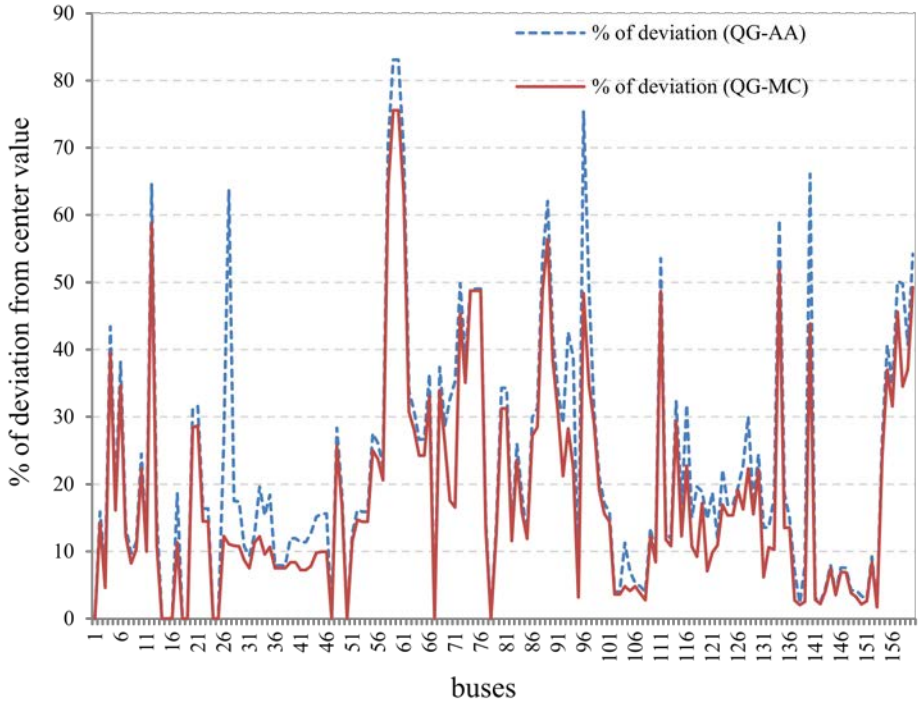

Figure 16: Percentage of reactive power deviation for thermal generators.

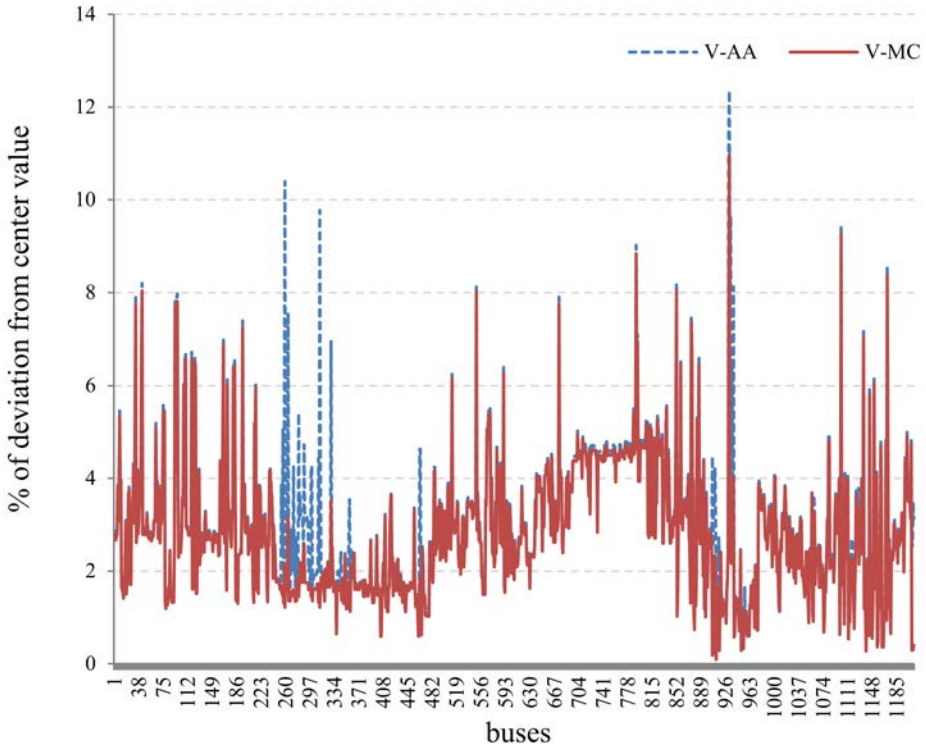

Figure 17: Percentage of deviation for bus voltage magnitudes.

The deviations are obtained as follows:

$$\%\ \text{deviation for}\ \tilde{x} = \frac{\overline{X} - \underline{X}}{X_0} * 100 \tag{197}$$

Observe that the errors in this case are significantly large for some generators than those obtained for the smaller IEEE 30-bus system, as expected, since the number of uncertainties is much larger, i.e., 1 in the small system versus 66 in the real system. Table I illustrates the error of the proposed AA-method in the maximum total thermal generation required to compensate for the wind and solar power generation uncertainties. Note that the 1.015% total error in table I is only 1231 MW in the real European system.

Table VI: THERMAL CAPACITIES, USING MCS AND AA-BASED APPROACHES

Total Thermal Reserve	AA-based Method (GW)	MCS Method (GW)	% of Error
Maximum	144.04	142.57	1.02%
Minimum	131.1	128.2	2.21

The AA method is faster than the MCS approach, as the MCS method needs 3000 iterations for convergence, while the AA method requires as many iterations as the number of uncertain variables, i.e., one iteration for the IEEE 30-bus test system and 66 iterations for the real 1211-bus system. Furthermore, the additional OPFs are based on small perturbations of the center-value OPF, and hence convergence can quickly be attained by using the center-value OPF solution as starting point.

5.4 Summary

A novel AA-based model has been proposed to solve the OPF problem with intervals to represent system uncertainty, such as variable wind and solar power generation. The AA-based method has significant advantages over exiting methods to study the uncertainties in OPF problems, which can be summarized as follows:

- The method does not rely on the pdf approximation of the uncertain variables, such as demand and generation.
- In the AA approach, the correlation among the variables is considered and, therefore, the output intervals are not as conservative as in IA.

- The proposed method takes into account the internal errors caused by truncations and approximations.
- The method is accurate, as it yields results close to the “exact” intervals.
- The proposed approach is efficient, as it does not require many iterations to converge, and hence it is much faster than other existing methods such as MCS.

The intervals obtained from the proposed technique can be used to approximate the margins of operation for dispatchable generators needed to properly account for system uncertainties. In order to test the efficiency and accuracy of the AA-based OPF, the method was tested on the IEEE 30-bus test system and a real 1211-bus European system, and benchmarked against the MCS method. The AA-based approach was shown to efficiently yield intervals close to the MCS bounds. This method can be used to also study the impact of demand variations in power systems, and other similar applications where intervals could be used to represent uncertainties, without the need to assume pdfs.

CHAPTER 6

SUMMARY AND FUTURE WORK

6.1 Summary of the Thesis

Chapter-1 presents an introduction to this thesis, and lays out the motivation behind the research. A comprehensive review of the literature, focusing on the deterministic and probabilistic power flow analysis problem, the deterministic and probabilistic OPF problem and DG impacts on the operation and planning of power systems is presented. Thereafter, the main research objectives are outlined.

In Chapter-2 a background to the mathematical tools which are used throughout the thesis is presented. First, the formulation of power system operations, i.e., power flow analysis problem and OPF are discussed, and then their solution methodologies for both deterministic and probabilistic problems are laid out. The discussed NLP methods are NR and gradient methods; and the probabilistic methods are SVC-based approaches such as AA and IA, and finally MCS. It is argued that the AA method has significant advantages in solution accuracy over other presented methods. Finally, the Chapter presents a brief review on DGs, their advantages and shortcomings in the context of power system operation and planning.

In Chapter-3, a novel MCP model is proposed to solve the power flow problem. This method is shown to be more flexible, accurate and robust than the classical power flow solution methods, such as NR. Various features of power flow analysis problem such as PV-PQ bus switching are embedded in this formulation, as new optimization constraints. The proposed model is used to demonstrate that the NR-based iteration procedure is basically a step of the GRG method which is applied to the solution of the proposed MCP model. Furthermore, the numerical results demonstrate that the proposed model converges while a robust NR-based power flow solver fails to converge for large systems.

In Chapter-4, the MCP model is used to calculate the affine form of real and imaginary components of bus voltage magnitudes in the stochastic power flow problem. The calculated affine forms of real and imaginary components of the bus voltage magnitude are then used to calculate the affine forms of real and reactive power injections. Then the AA form is converted to

IA form in order to compare the obtained intervals with the MCS intervals. The proposed method is tested on the IEEE 14-Bus Test System. The results show that the AA intervals are more conservative than the MCS intervals, as they consider the worst cases and also the internal errors such as truncation error.

Finally, in Chapter-5, the probabilistic OPF problem is solved using the AA method. In the AA-based OPF problem, all the state and control variables are treated in affine form, comprising a center value and the corresponding noise magnitudes, to represent forecast, model error, and other sources of uncertainty without the need to assume a pdf. The proposed AA-based OPF problem is used to determine the operating margins of the thermal generators in systems with uncertain wind and solar generation dispatch. The AA-based approach is benchmarked against MCS intervals in order to determine its effectiveness. The proposed technique is tested and demonstrated on the IEEE 30-bus system and also a real 1211-bus European system.

6.2 Main Contributions

The major contributions of the research presented in this thesis are as follows:

1. Reformulating the Power Flow Problem as an MCP

   A novel formulation of the power flow problem is proposed within an optimization framework that includes complementarity constraints. The proposed formulation can take advantage of state-of-the-art solvers for NLP and complementarity problems. The proposed MCP-based power flow model, which by design always has a theoretical solution, is shown to have increased robustness and flexibility with respect to the existent power flow methods. Based on the proposed MCP formulation, it is also formally demonstrated that the NR solution of the power flow problem is essentially a step of the traditional GRG algorithm.
2. Solving the Probabilistic Power Flow Problem Under Uncertainty Using an AA-based Approach

   The MCP-based power flow model is used in an AA-based power flow problem, in order to obtain the operational ranges for the power flow variables under uncertainty. The associated uncertainties could be internal such as rounding error or external such as forecasting error (e.g., demand, generation and weather forecast). The proposed AA algorithm is tested on a 14-bus test system and its results are then compared with the MCS results. The AA method shows slightly more conservative bounds, however it is

faster and does not need any information for statistical distributions of random variables.

3. Solving the Probabilistic OPF Problem Using an AA-based Approach

   An AA method is proposed to solve the OPF problem with uncertain generation sources. In the AA-based OPF problem, all the state and control variables are treated in affine form, comprising a center value and the corresponding noise magnitudes, to represent forecast, model error, and other sources of uncertainty without the need to assume a pdf. The AA-based approach is benchmarked against MCS intervals in order to determine its effectiveness. The proposed technique is tested and demonstrated on the IEEE 30-bus system and also a real 1211-bus European system.

4. Obtaining the Margins of Thermal Generators to Estimate the reserve requirements
   The proposed AA-based OPF problem is used to determine the operating margins of the thermal generators in systems with uncertain wind and solar generation dispatch. Obtaining the margins of operations for thermal generators in the presence of uncertain generation (e.g., wind and solar) and load helps significantly in determining the required reserve capacities, so that the system operates reliably and economically.

6.3 Scope for Future Work

The following directions for future research are suggested, based on the research carried out and presented in this thesis:

1. AA-Based Market Clearing UC Model with Uncertainty

   This research can be extended to solve the UC problem in the presence of data uncertainty, based on the AA approach. The market clearing UC models determine a generation commitment and production schedule for the participating generators and a procurement schedule for customers in a day-ahead energy market. These problems are influenced significantly by uncertainties in power generation and demand. Uncertainties in generation may arise from the presence of intermittent sources of energy such as wind and solar; while that in demand, from load forecast errors. Because the UC problem has binary variables, the AA method could be implemented in the second stage of a multi-stage UC problem, after the binary variables are fixed in the first stage of the solution method.

2. AA-Based Method to Determine Spinning Reserve Requirements in Microgrids

The AA method can serve as an effective tool to estimate the spinning reserve requirements in microgrids with renewable sources of generation. By incorporating the spinning reserve requirements in the AA-based OPF model, proposed in Chapter 4, the operator is able to provide enough spinning reserve capacity, while minimizing the cost of providing it.

The provision of spinning reserves enables the power system operators to provide enough capacity, when there is an imbalance between demand and generation due to the unpredictable incidents such as generator outage, demand forecast errors and unexpected generation deviations from supply sources.

This research proposes to apply the AA-based method to estimate spinning reserve requirements considering renewable generation intermittency and demand forecast errors as well as possible contingencies that may arise prior to dispatch. Calculating the AA-based generation bounds, the operator knows the expected range of electricity production from the available renewable sources, and therefore can estimate how much spinning reserve is needed to maintain the system operation within specified regions.

It is expected that the AA-based method provides more conservative bounds than the MCS method, as it considers the worst cases and also it take into consideration the internal errors associated with calculations. This method is much more computationally efficient than the MCS method, since it does not need many iterations as the MCS method requires.

3. Stochastic Optimal Transmission Switching

Transmission line switching problems are often formulated as MINLP or MIP models to optimize the topology of the transmission system in order to reduce the dispatch cost. Since 2005, a few papers have proposed optimization models based on a modified OPF model along with N-1 contingency analysis to find the binary state of the transmission lines while preserving the reliability of the system and minimizing the cost of supplying electricity. Finding the new topology, the generator is then capable of co-optimizing the generation dispatch without jeopardizing system reliability. Therefore, instead of considering transmission assets as static assets in OPF problems, they are treated as controllable variables. Optimal transmission line switching can play a significant role in the economics of smart grids, moreover it improves voltage profiles and increase transfer capacity. Optimal transmission switching solution is based on the existing transmission system and does not address transmission expansion planning aspects.

None of the proposed models consider the uncertainties within the power system operation such as demand forecast error or generation intermittency. These uncertainties are not captured by performing N-1 contingency analysis. Furthermore, the high penetration of DG sources such as wind farms can significantly impact transmission system operations, and therefore a stochastic optimal transmission switching model is vital to consider all the associated uncertainties.

This research seeks to apply the AA-based method on stochastic optimal switching to find the intervals associated with state and control variables when the model obtains an optimal transmission topology.

REFERENCES

[1] A. Zervos and C. Kjaer, "Pure power-wind energy scenarios up to 2030," European Wind Energy Association, 2008.

[2] Canadian Wind Energy Association, "Wind Facts," October 2012. [Online]. Available: http://www.canwea.ca/.

[3] IESO, "A review on global wind energy policy," Independent electricity system operator, 2013. [Online]. Available: www.ieso.com.

[4] Renewable Energy and Distributed Generation Force, "Canada's action on climate change," 12 07 2010. [Online]. Available: http://www.climatechange.gc.ca.

[5] A. Vaccaro, C. Canizares and D. Villacci, "An affine arithmetic-based methodology for reliable power flow analysis in the presence of data uncertainty," *IEEE Transactions on Power Systems,* vol. 25, no. 2, pp. 624-632, 2010.

[6] B. Stott, "Review of load-flow calculation methods," *Proceedings of the IEEE,* vol. 62, no. 7, pp. 916-929, July 1974.

[7] B. Scott, "Effective starting process for Newton-Raphson load flows," *Proceedings of the Institution of Electrical Engineers,* vol. 118, no. 8, pp. 983-987, Aug 1971.

[8] W. Tinney and C. E. Hart, "Power flow solution by Newton's method," *IEEE Transactions on Power Apparatus and Systems,* Vols. PAS-86, pp. 1449-1460, Nov 1967.

[9] B. Scott and O. Alsac, "Fast decoupled doad flow," *IEEE Transactions on Power Apparatus and Systems,* Vols. PAS-93, pp. 859-869, Jun 1974.

[10] Y. Chen and C. Shen, "A Jacobian-free Newton-GMRES(m) method with adaptive preconditioner and its application for power flow calculations," *IEEE Transaction on Power Systems,* vol. 21, no. 3, pp. 1096-1103, Aug 2006.

[11] L. Braz, C. Castro and C. Murati, "A critical evaluation of step size optimization based load flow methods," *IEEE Transactions on Power Systems,* vol. 15, no. 1, pp. 202-207, February 2000.

[12] A. Sasson, C. Trevino and F. Aboytes, "Improved Newton's load flow through a minimization technique," *IEEE Transactions on Power Apparatus and Systems,* Vols. PAS-90, no. 5, pp. 1974 - 1981, Sept. 1971.

[13] L. Barboza and R. Salgado, "Corrective solutions of steady state power system via newton optimization method," *Brazilian Journal of Control and Automation,* vol. 11, no. 3, 2000.

[14] M. Schaffer and D. Tylavsky, "A non-diverging polar-form Newton-based power flow," *IEEE Transactions on Industry Applications ,* vol. 24, no. 5, September 1988.

[15] A. Semlyen, "Fundamental concepts of a KRYLOV subspace power flow methodology," *IEEE Transactions on Power Systems,* vol. 11, no. 3, pp. 1528-1537, August 1996.

[16] Y. Saad and M. Schultz, "GMRES: a generalized minimal residual algorithm for solving nonsymmetric linear systems," *SIAM Journal on Scientific and Statistical Computing,* vol. 7, no. 3, pp. 856-869, July 1986.

[17] P. Brown and Y. Saad, "Hybrid Krylov methods for nonlinear systems of equations," *SIAM Journal on Scientific and Statistical Computing,* vol. 11, no. 3, pp. 450-481, May 1990.

[18] H. Dag and A. Semlyen, "A new preconditioned conjugate gradient power flow," *IEEE Transactions on Power Systems,* vol. 18, no. 4, pp. 1248-1256, Nov 2003.

[19] Y. Zhang and H. Chiang, "Fast Newton-FGMRES solver for large-scale power flow study," *IEEE Transactions on Power Systems,* vol. 25, no. 2, pp. 769 - 776, May 2010.

[20] F. Milano, "Continuous Newton's method for power flow analysis," *IEEE Transactions on Power Systems,* vol. 24, no. 1, p. 50, Feb 2009.

[21] J. Carpentier, "Contribution á l'étude du dispatching économique," *Bulletin de la Société Française des Électriciens,* vol. 3, no. 8, pp. 431-447, 1962.

[22] H. Dommel and W. Tinney, "Optimal power flow solutions," *IEEE Transactions on Power Apparatus and Systems,* vol. 10, pp. 1866-1876, 1968.

[23] A. El-Abiad and F. Jaimes, "A method for optimum scheduling of power and voltage magnitude," *IEEE Transactions on Power Apparatus and Systems,* vol. 4, pp. 413-422, 1969.

[24] A. Sasson, "Combined use of the Powell and Fletcher - Powell nonlinear programming methods for optimal load flows," *IEEE Transactions on Power Apparatus and Systems,* vol. 88, no. 10, pp. 1530-1537, 1969.

[25] A. Sasson, F. Viloria and F. Aboytes, "Optimal load flow solution using the hessian matrix," *IEEE Transactions on Power Apparatus and Systems,* Vols. PAS-92, no. 1, pp. 31-41, 1973.

[26] P. Mukherjee and R. Dhar, "Optimal load-flow solution by reduced-gradient method," *Proceedings of the Institution of Electrical Engineers,* vol. 121, no. 6, pp. 481-487, 1974.

[27] R. Shoults and D. Sun, "Optimal power flow based upon P-Q decomposition," *IEEE Transactions on Power Apparatus and Systems,* vol. 2, pp. 397-405, 1982.

[28] D. Sun, B. Ashley, B. Brewer, A. Hughes and W. Tinney, "Optimal Power Flow by Newton Approach," *IEEE Transaction on Power Apparatus and Systems,* Vols. PAS-103, no. 10, pp. 2864-2880, 1984.

[29] G. Reid and L. Hasdorff, "Economic dispatch using quadratic programming," *IEEE Transactions on Power Apparatus and Systems,* Vols. PAS-92, no. 6, pp. 2015-2023, 1973.

[30] R. Burchett, H. Happ and D. Vierath, "Quadratically convergent optimal power flow," *IEEE Transactions on Power Apparatus and Systems,* vol. 11, pp. 3267-3275, 1984.

[31] K. Aoki, A. Nishikori and R. Yokoyama, "Constrained load flow using recursive quadratic programming," *IEEE Transactions on Power Systems,* vol. 2, no. 1, pp. 8-16, 1987.

[32] J. Momoh and J. Zhu, "Improved interior point method for OPF problems," *IEEE Transactions on Power Systems,* vol. 14, no. 3, pp. 1114-1120, 1999.

[33] R. Mota-Palomino and V. Quintana, "Sparse reactive power scheduling by a penalty function - linear programming technique," *IEEE Transactions on Power Systems,* vol. 1, no. 3, pp. 31-39, 1986.

[34] D. Sun, B. Ashley, B. Brewer, A. Hughes and W. Tinney, "Optimal power flow by Newton approach," *IEEE Transactions on Power Apparatus and Systems,* vol. 10, pp. 2864-2880, 1984.

[35] F. Capitanescu, M. Glavic, D. Ernst and L. Wehenkel, "Interior-point based algorithms for the solution of optimal power flow problems," *Electric Power System Research,* vol. 77, no. 5, pp. 508-507, 2007.

[36] Y. Wu, A. Debs and R. Marsten, "A direct nonlinear predictor-corrector primal-dual interior point algorithm for optimal power flows," *IEEE Transactions on Power Systems,* vol. 9, no. 2, pp. 876-883, 1994.

[37] G. Torres and V. Quintana, "On a nonlinear multiple-centrality-corrections interior-point method for optimal power flow," *IEEE Transactions on Power Systems,* vol. 16, no. 2, pp. 222-228, 2001.

[38] L. Lai, J. Ma, R. Yokoyama and M. Zhao, "Improved genetic algorithms for optimal power

flow under both normal and contingent operation states," *International Journal of Electrical Power & Energy Systems,* vol. 19, no. 5, pp. 287-292, 1997.

[39] K. Iba, "Reactive power optimization by genetic algorithm," *IEEE Transactions on Power Systems,* vol. 9, no. 2, pp. 685-692, 1994.

[40] M. Abido, "Optimal power flow using particle swarm optimization," *International Journal of Electrical Power & Energy Systems,* vol. 24, no. 7, pp. 563-571, 2002.

[41] B. Borkowska, "Probabilistic load flow," *IEEE Transactions on Power Apparatus and Systems,* vol. 3, pp. 752-759, 1974.

[42] R. Allan, B. Borkowska and C. Grigg, "Probabilistic analysis of power flows," *Proceedings of the Institution of Electrical Engineers,* vol. 121, no. 12, pp. 1551-1556, 1974.

[43] J. Dopazo, O. Klitin and A. Sasson, "Stochastic load flows," *IEEE Transactions on Power Apparatus and Systems,* vol. 94, no. 2, pp. 299-309, 1975.

[44] R. Allan, C. Grigg, D. Newey and R. Simmons, "Probabilistic power-flow techniques extended and applied to operational decision making," *Proceedings of the Institution of Electrical Engineers,* vol. 123, no. 12, pp. 1317-1324, 1976.

[45] A. Leite da Silva, V. Arienti and R. Allan, "Probabilistic load flow considering dependence between input nodal powers," *IEEE Transactions on Power Apparatus and Systems,* vol. 6, pp. 1524-1530, 1984.

[46] R. Allan and M. Al-Shakarchi, "Probabilistic ac load flow," *Proceedings of the Institution of Electrical Engineers,* vol. 123, no. 6, pp. 531-536, 1976.

[47] R. Allan and M. Al-Shakarchi, "Linear dependence between nodal powers in probabilistic ac load flow," *Proceedings IEE,* vol. 124, no. 6, pp. 529-534, 1977.

[48] R. Allan, A. Leite da Silva and R. Burchett, "Evaluation methods and accuracy in probabilistic load flow solutions," *IEEE Transactions on Power Apparatus and Systems,* vol. 5, pp. 2539-2546, 1981.

[49] R. Allan and A. Leite da Silva, "Probabilistic load flow using multilinearisations," *IEE Proceedings Conference on Generation, Transmission and Distribution,* vol. 128, no. 5, pp. 280-287, 1981.

[50] M. Brucoli, F. Torelli and R. Napoli, "Quadratic probabilistic load flow with linearly modelled dispatch," *International Journal of Electrical Power & Energy Systems,* vol. 7, no. 3, pp. 138-146, 1985.

[51] L. Sanabria and T. Dillon, "Stochastic power flow using cumulants and Von Mises functions," *International Journal of Electrical Power & Energy Systems,* vol. 8, no. 1, pp. 47-60, 1986.

[52] P. Zhang and S. Lee, "Probabilistic load flow computation using the method of combined cumulants and Gram-Charlier expansion," *IEEE Transactions on Power Systems,* vol. 19, no. 1, pp. 676-682, 2004.

[53] D. Villanueva, J. Pazos and A. Feijoo, "Probabilistic load flow including wind power generation," *IEEE Transactions on Power Systems,* vol. 26, no. 3, pp. 1659-1667, 2011.

[54] Z. Wang and F. Alvarado, "Interval arithmetic in power flow analysis," *IEEE Transactions on Power Systems,* vol. 7, no. 3, pp. 1341-1349, 1992.

[55] C. Su, "Probabilistic load-flow computation using point estimate method," *IEEE Transactions on Power Systems,* vol. 20, no. 4, pp. 1843-1851, 2005.

[56] P. Pajan and V. Paucar, "Fuzzy power flow: considerations and application to the planning and operation of a real power system," *Proceedings of International Conference on Power System Technology,* vol. 1, pp. 433-437, 2002.

[57] M. Matos and E. Gouveia, "The fuzzy power flow revisited," *IEEE Transactions on Power Systems,* vol. 23, no. 1, pp. 213-218, 2008.

[58] A. Vaccaro, C. Canizares and D. Villacci, "A simple and reliable algorithm for computing boundaries of power flow solutions due to system uncertainties," in *Proceedings of IEEE PowerTech,* Bucharest, 2009.

[59] A. Leite da Silva, S. Ribeiro, V. Arienti, R. Allan and M. Do Coutto Filho, "Probabilistic load flow techniques applied to power system expansion planning," *IEEE Transactions on Power Systems,* vol. 5, no. 4, pp. 1047-1053, 1990.

[60] A. Leite da Silva, R. Allan, S. Soares and V. Arienti, "Probabilistic load flow considering network outages," *IEE Proceedings-Generation, Transmission and Distribution,* vol. 132, no. 3, pp. 139-145, 1985.

[61] P. Jorgensen, J. Christensen and J. Tande, "Probabilistic load flow calculation using Monte Carlo techniques for distribution network with wind turbines," *Proceedings. 8th International Conference on Harmonics And Quality of Power,* vol. 2, pp. 1146-1151, 1998.

[62] G. Viviani and G. Heydt, "Stochastic optimal energy dispatch," *IEEE Transactions on Power Apparatus and Systems,* vol. 7, pp. 3221-3228, 1981.

[63] M. El-Hawary and G. Mbamalu, "A comparison of probabilistic perturbation and deterministic based optimal power flow solutions," *IEEE Transactions on Power Systems,* vol. 6, no. 3, pp. 1099-1105, 1991.

[64] T. Karakatsanis and N. Hatziargyriou, "Probabilistic constrained load flow based on sensitivity analysis," *IEEE Transactions on Power Systems,* vol. 9, no. 4, pp. 1853-1860, 1994.

[65] P. Zhang and S. Lee, "A new computation method for probabilistic load flow study," *IEEE Power Conference Proceeding,* vol. 4, pp. 2038-2042, 2002.

[66] A. Schellenberg, W. Rosehart and J. Aguado, "Cumulant-based probabilistic optimal power flow (P-OPF) with Gaussian and gamma distributions," *IEEE Transactions on Power Systems,* vol. 20, no. 2, pp. 773-781, 2005.

[67] G. Verbic and C. Canizares, "Probabilistic optimal power flow in electricity markets based on a two-point estimate method," *IEEE Transactions on Power Systems,* vol. 21, no. 4, pp. 1883-1893, 2006.

[68] H. Zhang and P. Li, "Chance constrained programming for optimal power flow under uncertainty," *IEEE Transactions on Power Systems,* vol. 26, no. 4, pp. 2417-2424, November 2011.

[69] J. He, L. Cheng, D. Kirschen and Y. Sun, "Optimising the balance between security and economy on a probabilistic basis," *IET Generation, Transmission & Distribution,* vol. 4, no. 12, pp. 1275-1287, 2010.

[70] T. Ackermann, G. Andersson and L. Söder, "Distribured generation: a definition," *Electrical Power System Research,* vol. 57, no. 3, pp. 195-204, 2001.

[71] P. Dondi, D. Bayoumi, C. Haederli, D. Julian and M. Suter, "Network integration of distributed power generation," *Journal of Power Sources,* vol. 106, pp. 1-9, 2002.

[72] G. Pepermans, J. Driesen, D. Haeseldonckx, R. Belmans and W. D'haeseleer, "Distributed generation: definition, benefits and issues," *Energy Policy,* vol. 33, no. 6, pp. 787-798, 2005.

[73] B. Alderfer, M. Eldridge and T. Starrs, "Making connections: Case studies of interconnection barriers and their impact on distributed power projects," 2000.

[74] L. Johnston and National Renewable Energy Laboratory, "Rate structures for customers with onsite generation: practice and innovation," 2006. [Online]. Available: energy.ca.gov.

[75] M. Pirnia, J. Nathwani and D. Fuller, "Ontario feed-in-tariffs: system planning, implications and impacts on social welfare," *The Electricity Journal*, vol. 24, no. 8, pp. 18-28, 2011.

[76] A. Le, M. Kashem, M. Negnevitsky and G. Ledwich, "Optimal distributed generation parameters for reducing losses with economic consideration," in *IEEE Power Engineering Society General Meeting*, 2007.

[77] J. Zhao, J. Foster, Z. Dong and K. Wong, "Flexible transmission network planning considering distributed generation impacts," *IEEE Transactions on Power Systems*, vol. 26, no. 3, pp. 1-10, 2011.

[78] F. Bouffard and F. Galiana, "Stochastic security for operations planning with significant wind power generation," *IEEE Transactions on Power Systems*, vol. 23, no. 2, pp. 306-316, 2008.

[79] P. Varaiya, F. Wu and J. Bialek, "Smart operation of smart grid: Risk-limiting dispatch," *IEEE General meeting Proceeding*, vol. 99, no. 1, pp. 40-57, 2011.

[80] L. Soder, "Reserve margin planning in a wind-hydro-thermal power system," *IEEE Transactions on Power Systems*, vol. 8, no. 2, pp. 564-571, 1993.

[81] F. Bouffard, F. Galiana and A. Conejo, "Market clearing with stochastic security - Part I: formulation," *IEEE Transactions on Power Systems*, vol. 20, no. 4, pp. 1818-1826, 2005.

[82] F. Bouffard, F. Galiana and A. Conejo, "Market clearing with stochastic security - Part II: case studies," *IEEE Transactions on Power Systems*, vol. 20, no. 4, pp. 18-27-1835, 2005.

[83] M. Ortega-Vazquez and D. Kirschen, "Estimating the spinning reserve requirements in systems with significant wind power generation penetration," *IEEE Transactions on Power Systems*, vol. 24, no. 1, pp. 114-124, 2009.

[84] F. Bouffard and M. Ortega-Vazquez, "The value of operational flexibility in power systems with significant wind power generation," *IEEE Power and Energy Society General Meeting*, pp. 1-5, 2011.

[85] M. L. Crow, Computational methods for electric power systems, 2 ed., CRC Press, 2009.

[86] A. Kulkarni, M. Pai and P. Sauer, "Iterative solver techniques in fast dynamic calculations of power systems," *International Journal of Electrical Power & Energy Systems*, vol. 23, no. 3, pp. 237-244, March 2001.

[87] S. Conti and S. Raiti, "Probabilistic load flow using Monte Carlo techniques for distribution networks with photovoltaic generators," *Solar Energy*, vol. 81, no. 12, pp. 1473-1481, 2007.

[88] Z. Jizhong, Optimization of power system operation, Wiley-IEEE Press, 2009.

[89] J. Momoh, Electric power system applications of optimization, CRC, 2011.

[90] R. Baldick, Applied optimization: formulation and algorithms for engineering systems, Cambridge University Press, 2006.

[91] M. Ferris and T. Munson, "GAMS/PATH user guide, Version 4.3," 2000.

[92] A. Ben-Israel, "A Newton-Raphson method for the solution of systems of equations," *Journal of Mathematical Analysis and Aplications*, vol. 15, no. 2, p. 243, August 1996.

[93] A. Antoniou and W. Lu, Practical optimization: algorithms and engineering applications, illustrated ed., New York : Springer, 2007.

[94] A. Gómez-Expósito, A. Conejo and C. Canizares, Electric energy systems: analysis and operation, CRC Press, 2008.

[95] J. Stolfi and L. De Figueiredo, "Self-validated numerical methods and applications," Citeseer, 1997.

[96] G. Anders, Probability concepts in electric power systems, New York, NY: John Wiley and Sons Inc., 1989.

[97] J. Lopes, N. Hatziargyriou, J. Mutale, P. Djapic and N. Jenkins, "Integrating distributed generation into electric power systems: A review of drivers, challenges and opportunities," *Electr.Power Syst.Res.,* vol. 77, no. 9, pp. 1189-1203, 2007.

[98] T. Ackermann, K. Garner and A. Gardiner, "Embedded wind generation in weak grids—economic optimisation and power quality simulation," *Renewable Energy,* vol. 18, no. 2, pp. 205-221, 1999.

[99] N. Jenkins, J. B. Ekanayake and G. Strbac, Distributed Generation, Inst. of Engineering & Technology (IET), 2009.

[100] I. Blanco and C. Kjaer, "Wind at work," European Wind Energy Association, January 2009.

[101] N. Hadjsaid, J. Canard and F. Dumas, "Dispersed generation impact on distribution networks," *Computer Applications in Power, IEEE,* vol. 12, no. 2, pp. 22-28, 1999.

[102] J. Cardell and R. Tabors, "Operation and control in a competitive market: distributed generation in a restructured industry," *The Energy Journal,* vol. 18, pp. 111-136, 1997.

[103] S. Heier, Grid integration of wind energy conversion systems, 2006.

[104] R. Waltz and T. Plantenga, "KNITRO user's manual," 2010.

[105] B. Murtagh and M. Saunders, "MINOS 5.5 user guide," Stanford, California, 1998.

[106] W. Rosehart, C. Roman and A. Schellenberg, "Optimal power flow with complementarity constraints," *IEEE Transactions on Power Systems,* vol. 20, no. 2, 2005.

[107] Y. Wallach, "Gradient methods for load-flow problems," *IEEE Transactions on Power Apparatus and Systems,* vol. 87, no. 5, pp. 1314 - 1318, May 1968.

[108] C. Canizares, "Calculating optimal system parameters to maximize the distance to saddle-node bifurcations," *Circuits and Systems I: Fundamental Theory and Applications,* vol. 45, no. 3, pp. 225-237, 1998.

[109] R. Rosenthal and A. Brooke, "GAMS, a user's guide," *GAMS Development Corporation,* 2007.

[110] C. Canizares and F. Alvarado, "UWPFLOW: continuation and direct methods to locate fold bifurcations in AC/DC/FACTS power systems," 1999.

[111] Powertech Labs. Inc., "DSATools, dynamic security assessment software," 2005.

[112] University of Washingtom, "UWashington test system archive," 1961. [Online]. Available: http://www.ee.washington.edu/research/pstca/pf30/pg_tca30bus.htm.

[113] PJM, "PJM reserve requirement study," October 2012. [Online]. Available: http://www.pjm.com/~/media/committees-groups/subcommittees/raas/20110929/20110929-2011-pjm-reserve-requirement-study.ashx.

[114] K. Cheung, P. Shamsollahi, D. Sun, J. Milligan and M. Potishnak, "Energy and ancillary service dispatch for the interim ISO New England," *IEEE Transactions on Power Systems,* vol. 15, no. 3, pp. 968-974, 2000.

[115] K. Cheung, "Anscillary service market design and implementation in North America: From theory to practice," in *Electric Utility Deregulation and Restructuring and Power Technologies,* Redmond, WA, 2008.

[116] R. Baldick, "Wind and energy markets: A case study of Texas," *IEEE Systems Journal,* vol. 6, no. 1, pp. 27-35, 2012.

[117] D. Grabowski, M. Olbrich and E. Barke, "Analog circuit simulation using range arithmetics," in *Design Automation Conference 2008 Asia and South Pacific*, Seoul, 2008.

[118] H. Sherali and W. Adams, A reformulation-ninearization technique for solving discrete and continuous nonconvex problems, Springer, 1999.

[119] J. Ninin, P. Hansen and F. Messine, "A reliable affine relaxation method for global optimization," *Groupe D'études et de Recherche en Analyse des Décisions,* 2010.

[120] CPLEX, "10.0 user's manual," ILOG, SA, 2006.

[121] R. Rosenthal, "GAMS- A user's guide," Washington, DC., 2013.

[122] M. Saltzman, in *COIN-OR: an open-source library for optimization*, Boston, Kluwer Academic Publishers, 2002.